Interior Exploration Using Seismic Investigations, Geodesy, and Heat Transport (InSight) Summary

November, 2015

Note: Sections that deal with the Participating Scientist program have been removed

Contributors:
Sue Smrekar, Jet Propulsion Laboratory, California Institute of Technology
Elizabeth Barrett, Jet Propulsion Laboratory, California Institute of Technology
Don Banfield, Cornell University
Catherine Johnson, University of British Columbia
Bill Folkner, Jet Propulsion Laboratory, California Institute of Technology
Matt Golombek, Jet Propulsion Laboratory, California Institute of Technology
Matthias Grott, DLR Institute of Planetary Research
Philippe Lognonné*, Institut de Physique du Globe de Paris*
Justin Maki, Jet Propulsion Laboratory, California Institute of Technology
Nils Mueller, Jet Propulsion Laboratory, California Institute of Technology
Kathryn Rowe, University of California Los Angeles
Chris Russell, University of California Los Angeles
Miles Smith, Jet Propulsion Laboratory, California Institute of Technology
Tilman Spohn, DLR Institute of Planetary Research

Compiled by:
The InSight Project Science Office

DISCLAIMER: Although every effort will be made to implement the designs and plans described in this package, budgetary, programmatic, schedule, or technical issues may result in changes in these plans.

1 Table of Contents

Additional Documents
Appendix A: InSight Archive Generation, Validation, and Transfer Plan

2 Overview

2.1 Document Overview

This article describes the InSight lander, payload and mission operations.   Appendix A is the current InSight Archive Generation, Validation, and Transfer Plan.

2.2 InSight Mission Summary

InSight is part of NASA's Discovery Program. InSight is a mission dedicated to NASA's efforts to understand the fundamental processes of terrestrial-planet formation and evolution by performing a comprehensive surface-based geophysical investigation of Mars. InSight will provide key information on the composition and structure of an Earth-like planet that has gone through most of the evolutionary stages of the Earth up to, but not including, plate tectonics. Thus, the traces of this history are still contained in the basic parameters of Mars: the size, state and composition of the core, the composition and layering of the mantle, the thickness and layering of the crust, and the thermal flux from the interior. These science objectives could be accomplished by landing nearly anywhere on the surface of Mars. The engineering rationale for landing in Elysium Planitia is described in Section 2.5.

InSight will launch on March 4, 2016 with a 23-day launch period duration, on an Atlas V-401 from the Vandenberg Air Force Base (VAFB) launch facility on a Type 1 trajectory to Mars. After a 7-month cruise, InSight will land on the surface of Mars on September 28, 2016. Following landing there is a period of approximate 69 sols for the deployment and characterization of the instruments. After successful deployment of the instruments, InSight will perform science surface monitoring operations for one Mars year (two Earth years—September 2016 to September 2018).

InSight will address the mission science objectives by focusing on three scientific investigations: seismology, precision-tracking and heat-flow measurements. In order to obtain this information, InSight will use two scientific instruments: a seismometer and a self-penetrating mole trailing an instrumented tether for determining heat flux. In addition, InSight uses an X-band transponder (part of the Spacecraft Telecom Subsystem) to enable two-way precision Doppler tracking of the planet's rotation. A suite of auxiliary sensors and payload elements, described below, support these measurements.

2.3 InSight Science Objectives

The overall goal of the InSight mission is to improve our understanding of terrestrial planet formation and evolution by understanding the origin and evolution of Mars. InSight investigates Mars' interior structure, thermal and chemical evolution, and geologic processes. It also determines Mars' present level of geologic activity and impact flux. InSight reveals the processes of formation and differentiation of the Martian core and crust, and illuminates the evolution of its interior by constraining the following parameters:

- Determine the depth of the crustal-mantle boundary to within ±10 km
- Detect any regional-scale crustal layering with velocity contrast ≥0.5 km/s over a depth interval ≥5 km
- Determine the seismic velocities in the upper 600 km of mantle to within ±0.25 km/s
- Determine whether the outer core is liquid or solid to a 90% confidence level
- Determine the core radius to within ±200 km
- Determine the core density to within ±450 kg/m^3
- Determine the heat flux at the landing site to within ±5 mW/m^2
- Determine the rate of seismic activity to within a factor of 2 for rates greater than 2×10^{18} Nm/yr
- Determine epicenter distance to ±25% and epicenter azimuth to ±20°
- Determine the rate of meteorite impacts to within a factor of 2

The Lander will place two instrument packages on the surface of Mars with the aid of the Instrument Deployment System (IDS):

- The **IDS** is composed of a robotic arm called the Instrument Deployment Arm (IDA), an Instrument Deployment Camera (IDC) located in the forearm of the IDS, and an Instrument Context Camera (ICC) located under the Lander's deck right underneath the IDA's base. All the components of the IDS are built and operated by the Jet Propulsion Laboratory (JPL).
- The **SEIS** (Seismic Experiment for Interior Structure) is a seismometer that monitors seismic activity and tidal displacements and is built and operated by the French space agency CNES (Centre National d'Études Spatiales) and their partners[1]. It also includes the APSS (Auxiliary Payload Sensor Suite), which consist of the Temperature and Wind Sensor (TWINS), Pressure Sensor (PS), and the InSight Flux Gate (IFG -- a magnetometer).
- The **HP³** (Heat-Flow and Physical Properties Package) determines the geothermal heat flux by penetrating down into the surface of Mars by at least 3 meters and is built and operated by the German aerospace agency (Deutsches Zentrum für Luft- und Raumfahrt, DLR). The HP³ also includes a radiometer (RAD).

Over the course of a Martian year (~23 Earth months) the SEIS and HP³ instruments, in conjunction with an X-band radio Doppler tracking science investigation that measures rotational variations (Rotation and Interior Structure Experiment [**RISE**]), will achieve InSight's science primary objectives. The IDC, APSS, and RAD support the deployment and data reduction for SEIS and HP³. Additionally, this sensor suite will enable a wide range of ancillary science. Figure 2.3-1 depicts the InSight instruments in a landed configuration.
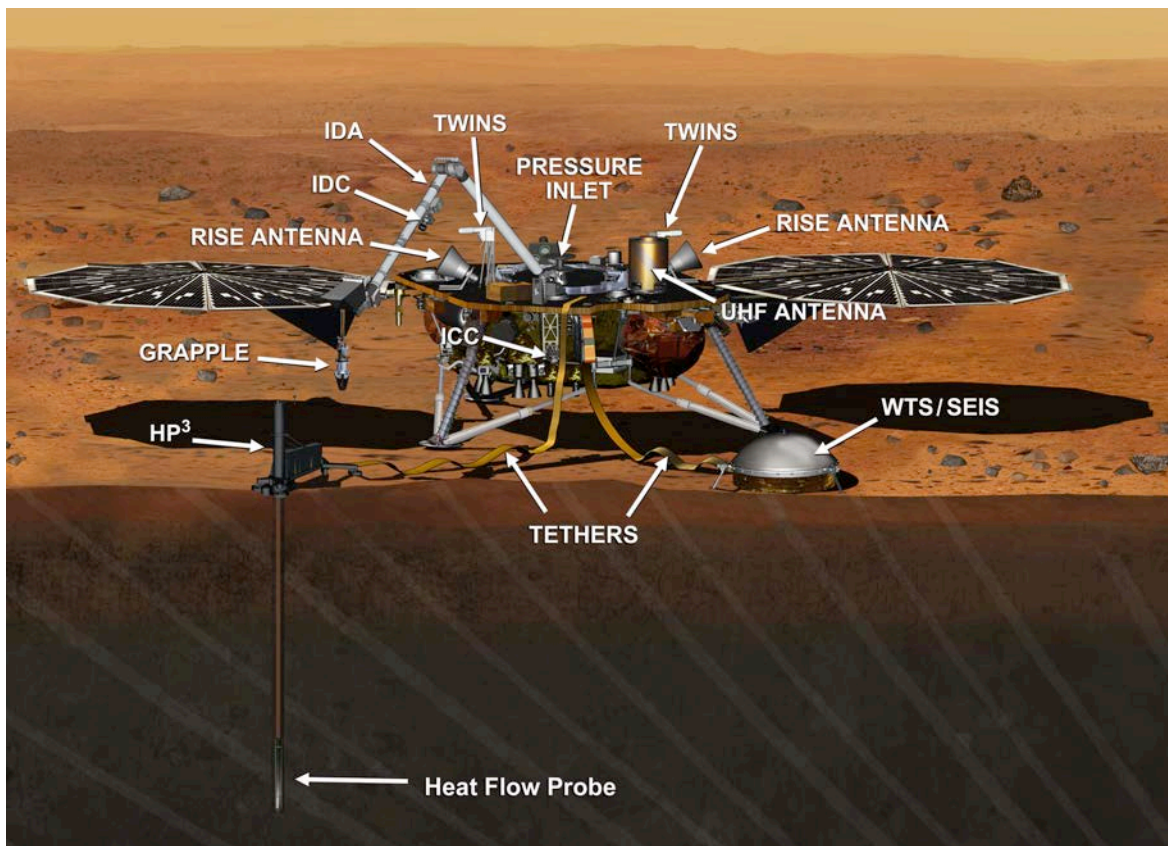

Figure 2.3-1: InSight Lander with payload instruments deployed.

---

[1] Institut de Physique du Globe de Paris (IPGP); Institut Superieur de l'Aeronautique et de l'Espace (ISAE); Eidgenössische Technische Hochschule (ETH); Max-Planck-Institut für Sonnensystemforschung (MPS); Imperial College, London

2.4   InSight Science Team

The InSight Science Team currently consists of the Principle Investigator, Bruce Banerdt, the Deputy PI/Project Scientist, Suzanne Smrekar, the Program Scientist, Robert Fogel, the instrument PIs, Philippe Logonné for SEIS, Tilman Spohn for HP³, and William Folkner for RISE, other co-Is and Collaborators. The full list of Co-Is is given below (Table 2.4-1). The list of collaborators is given in the Rules of Road (Appendix B). This document also provides the ground rules and polices that govern InSight science investigations, including data access, rights, release, and publication. Any updates to the Rules of the Road document will apply to the entire Science Team. The role of the science team is to advise the project on optimization of the science return, including selecting the deployment locations for SEIS and HP³, and on the prioritization of data for downlink.

The InSight Science Team is organized into Science Working Groups. These groups serve to prepare the team for a variety operations, data analysis and interpretation objectives.

Table 2.4-1: InSight Science Team Members

Name	Institute
Sami Asmar	Jet Propulsion Laboratory (JPL)
Don Banfield	Cornell University
Ulrich Christensen	Max Planck Institute for Solar System Research (MPS)
Véronique Dehant	Royal Observatory of Belgium (ROB)
Bill Folkner	Jet Propulsion Laboratory (JPL)
Raphael Garcia	Institut Supérieur de l'Aéronautique et de l'Espace (ISAE)
Domenico Giardini	Swiss Federal Institute of Technology (ETHZ)
Matt Golombek	Jet Propulsion Laboratory (JPL)
Matthias Grott	DLR Institute of Planetary Research
Troy Hudson	Jet Propulsion Laboratory (JPL)
Catherine Johnson	University of British Columbia (UBC) Planetary Science Institute (PSI)
Günter Kargl	Austrian Academy of Sciences (ÖAW)
Brigitte Knapmeyer-Endrun	Max Planck Institute for Solar System Research (MPS)
Naoki Kobayashi	University Tokyo/Japanese Space Agency (JAXA)
Philippe Lognonné	Institut de Physique du Globe de Paris (IPGP)
Justin Maki	Jet Propulsion Laboratory (JPL)
David Mimoun	Institut Supérieur de l'Aéronautique et de l'Espace (ISAE)
Antoine Mocquet	Université de Nantes
Paul Morgan	Colorado School of Mines
Mark Panning	University Florida
Tom Pike	Imperial College, London (ICL)
Tilman Spohn	DLR Institute of Planetary Research
Jeroen Tromp	Princeton University
Renee Weber	NASA-Marshall Space Flight Center (MSFC)
Mark Wieczorek	Institut de Physique du Globe de Paris (IPGP)

2.5   Landing Site Selection

InSight will land in western Elysium Planitia on Hesperian plains just north of the dichotomy boundary. The 130 km by 27 km ellipse (E9) is located on smooth plains with Noachian highlands to the south and west, a ridge of Medussae Fossae Formation to the southeast and very young lavas from Athabasca Valles to the east. The E9 ellipse is located at 4.4°N, 135.8°E about 540 km north of the Curiosity landing site (Figure 2.5-1).
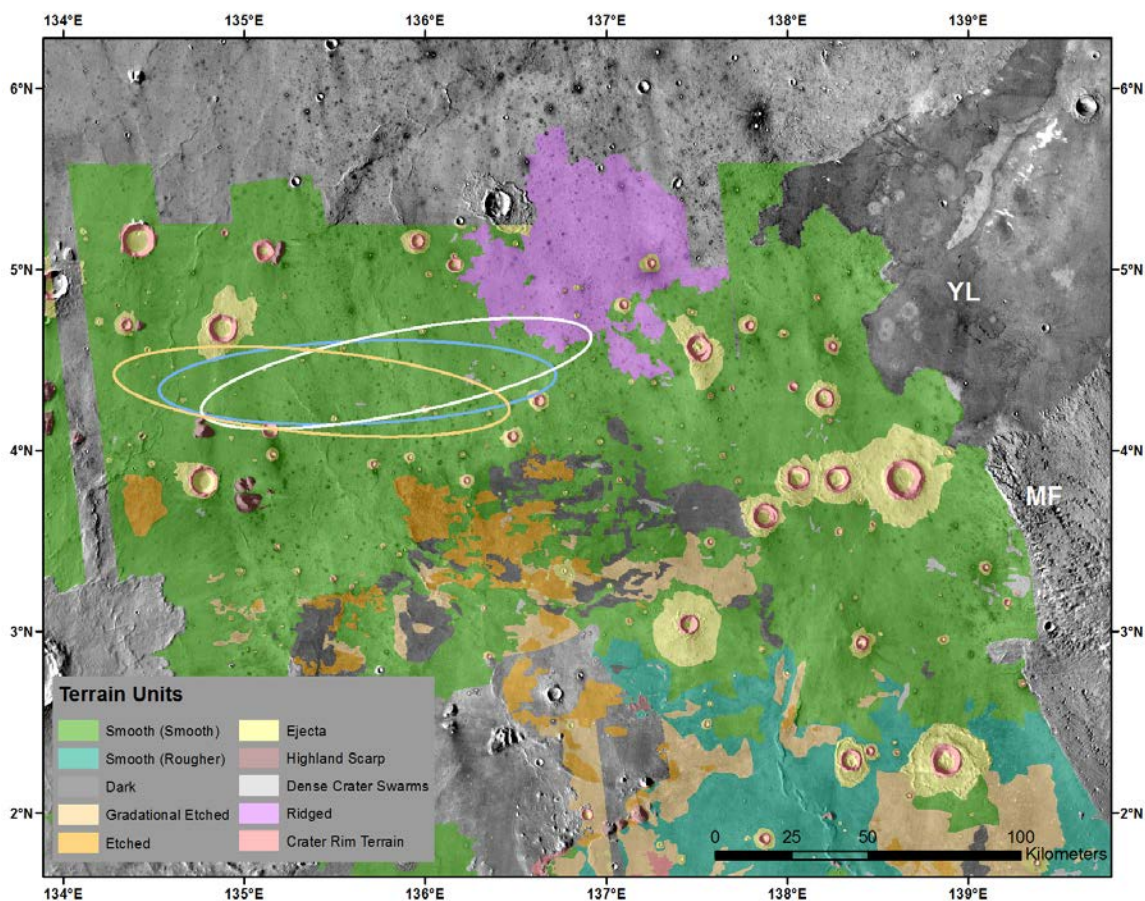
Figure 2.5-1: Map of the InSight landing ellipse E9, showing the ellipses (130 km by 27 km) for launch at the opening (white), middle (blue) and close (orange) of the launch opportunity. Terrain units as defined in Wigton et al. [2014], with the ellipse located dominantly on the smooth terrain (green), which is smooth, flat and has few rocks. The ellipse is about 600 km north of the dichotomy boundary and is likely underlain by Early Hesperian basalts superposed by a 5-13 m surficial unit of impact-generated regolith. Noachian highlands are to the south and west (with remnant massifs rising through the plains), a ridge of Medussae Fossae Formation to the southeast (marked MF) and very young lavas from Athabasca Valles to the east (marked YL). Base map is THEMIS daytime thermal image mosaic, so cooler areas are darker and have higher thermal inertia due to more rocks or higher cohesion (note dark young lavas). Note dark, rocky ejecta craters on the plains are limited in size to less than roughly 2 km diameter and greater than around 50-200 m diameter indicating a strong layer between 5-20 m and 200 m depth (and weaker sediments above and below) [Golombek et al., 2013a; Warner et al., 2014; Pivarunas et al., 2015].

The plains surface on which the InSight ellipse is located is mapped as an Early Hesperian transition unit (eHt) by Tanaka et al. (2014), which could be sedimentary or volcanic. A volcanic interpretation of the plains in the area of the InSight ellipses is supported by: 1) the presence of rocks in the ejecta of fresh craters ~0.2-20 km diameter arguing for a strong competent layer ~20-200 m deep [e.g., Golombek et al., 2013a; Catling et al., 2011, 2012], 2) exposures of strong, jointed bedrock overlain by ~10 m of fine grained regolith in nearby Hephaestus Fossae in southern Utopia Planitia at 21.9°N, 122.0°E [Golombek et al., 2013a], and 3) the presence of wrinkle ridges, which have been interpreted to be fault-propagation folds, in which slip on thrust faults at depth is accommodated by asymmetric folding in strong, but weakly bonded layered material (aka basalt flows) near the surface [e.g., Mueller and Golombek, 2004].

The primary landing safety engineering requirements for InSight landing site selection are [Golombek et al., 2013b]:

a) MOLA elevation below -2.5 km for sufficient atmosphere to slow the spacecraft during entry, descent, and landing
b) Latitude 3°N to 5°N for solar-power margins
c) Ellipse size 130 km × 27 km for ~99% landing accuracy
d) Smooth, flat, radar-reflective surface
e) Thermal inertia >100–140 J m^{-2} K^{-1} $s^{-1/2}$ for a load-bearing surface without substantial fine-grained dust
f) Rock abundance ≤10% for a ~<1% probability of impacting a rock that could damage the base of the lander or impede opening the solar panels
g) Regional (84 m length scale) and local terrain slopes (2-5 m length scale) <15° for radar tracking and touchdown stability

The instrument deployment requirements include: Rock abundance <10% and slopes <15° (same as for landing safely) and a broken up regolith >5 m thick to allow full penetration of the HP^3 mole. There are no science requirements on the landing site. All of these requirements are met by ellipse E9.

Landing site selection for InSight has taken about three years. The original Discovery Mission proposal included a reference ellipse in Elysium Planitia that appeared to meet the engineering constraints. At the end of phase A (5/12), the project had identified 16 ellipses and began requesting HiRISE and CTX images [Golombek et al., 2013b]. Within about 1 year CTX had acquired about 90% coverage of these ellipses, that together with HiRISE images, allowed the mapping of terrains. These ellipses included both a smooth terrain that appeared exceptionally benign (very smooth with few rocks) and etched terrain (rougher with higher rock abundance) as well as transitional units [Golombek et al., 2013a; Wigton et al., 2014]. Additional HiRISE images revealed a substantial number of secondary craters that extend in rays ~1400 km to the south of Corinto crater, a fresh crater about 1000 km to the north of prospective landing sites [Golombek et al., 2014a; Bloom et al., 2014]. The project downselected to 4 ellipses in July 2013 that are located dominantly on the smooth terrain [Golombek et al., 2014b].

The Council of Terrains and Council of Atmospheres were established in February 2014 to create data products to assist in surface characterization (e.g., digital elevation, slope and rock maps) and reference atmospheres for entry and descent simulations. During landing site evaluation, HiRISE, CTX and HRSC images were processed into digital elevation maps, MOLA data were examined to identify steep slopes at 100 m length scale, HiRISE data were used to create photoclinometry slope maps and rock maps, radar and SHARAD data were analyzed to understand reflectivity and subsurface layering, thermal data were examined to understand the physical properties of surface materials, terrain units were mapped in CTX and HiRISE images, and rocky ejecta craters were mapped and fracture and fragmentation theory applied to the Elysium plains to understand regolith thickness. The second project down selection occurred in January 2015, which provisionally selected ellipse E9. Project certification of the ellipse will occur in the fall of 2015.

Thermophysical properties of the landing ellipse in remote sensing data and comparison to existing landing sites [e.g., Golombek et al., 2008] suggests the InSight surfaces are composed of cohesionless sand or low cohesion soils [Golombek et al., 2013a]. The albedo and dust cover index are similar to dusty and low-rock abundance portions of the Gusev cratered plains [Golombek et al., 2006] and dust devil tracks are common in HiRISE images. Mapping of rocky ejecta craters in extensive HiRISE images of the ellipses indicates a broken up regolith produced by cratering since the Hesperian that is 5-13 m thick [Warner et al., 2014; Pivarunas et al., 2015], likely similar to the impact generated regolith at the Gusev cratered plains [e.g., Golombek et al., 2006] and thus conducive for full penetration of the HP^3 mole.

3 The Lander

3.1 Basic Description

The InSight lander has a high level of heritage from the Phoenix spacecraft with upgrades due to parts obsolescence, payload accommodations, and extended operations. InSight is a highly centralized flight

system designed around a core lander that controls all functions throughout all the mission phases. The lander contains the avionics (computer and telecommunications hardware) and power electronics. Figure 3.1-1 shows the location of some of the major components of the lander in an immediate post-landing configuration where the payloads are all still located on the deck.   Figure 2.3-1 shows the configuration of the lander and location of the instruments after the payloads have been deployed.

The overall characteristics of the lander include a total mass of about 390 kg, a lander deck size of approximately 1.5m x 1.9m and height of ~0.5m to the top of the lander deck. The robotic arm can extend an additional 1.86 m above the lander deck. The lander supports the science instrument payload investigations, provides high-speed computational capability and substantial data storage, and provides X-band Direct-to-Earth (DTE) and Direct-from-Earth (DFE) telecommunications as well as the ability to communicate via UHF with Mars Reconnaissance Orbiter and Mars Odyssey (which will store and relay the data to Earth).

3.2   Energy

Power is supplied to the lander by two solar arrays with a total surface area of 5.16 m^2 that are deployed immediately after landing. The final orientation and tilt of the lander, array dust covering, and local atmospheric tau measurements all affect the power available from the arrays. The maximum expected energy collected with the solar arrays over one Martian sol in an ideal situation is ~3600 W-hr. Under worst-case atmospheric dust conditions and with conservative tilt and dust accumulation on the solar arrays, the energy collected could be as little as ~750 W-hr; however the combined conditions that would result in this little energy are relatively unlikely. The arrays are supported by two lithium ion batteries (total expected storage capacity of 48 A-hr at the start of the surface mission) that are expected to cycle through a charge/discharge cycle on a per sol basis, with a maximum allowed depth of discharge of 60%. Due to energy limitations the lander is expected to sleep the majority of the time, waking up every 3 hours to perform fault protection diagnostics as well as twice per sol for scheduled full wakeups for communications and transferring science data from the payloads. While the lander sleeps, the payloads are expected to nominally remain continuously powered and collecting data. In circumstances in which, due to dust storms or heater loads during the cold season, energy consumption must be reduced, payloads will be powered off as required to maintain essential operations and lander energy balance. It is expected that under worst-observed atmospheric dust conditions and with conservative tilt and dust accumulation on the solar arrays, the number of sols spent with reduced instrument activity to conserve energy (including dust storm survival, with all instruments off) will total fewer than 180 sols.

3.3   Telecom

The surface telecommunications system uses three antennae, an east and a west medium-gain X-band antenna for Direct-to/from-Earth communications and a UHF helix antenna for relay communications with an orbiter. The nominal mission plan during the deployment phase is to utilize the east X-band antenna to uplink directly from Earth to the lander, whereas the plan during the science monitoring phase is to uplink via relay orbiters. Downlink from the lander to Earth throughout the mission will nominally be accomplished via relay through either Mars Reconnaissance Orbiter or Mars Odyssey with two passes a day. If for any reason the UHF return link is not available, data can be downlinked via the X-band assets but at a much slower rate. The average downlink via orbiter relays is expected to be >90 Mbits/sol and the average uplink via relays will be several hundred Mbits/sol.
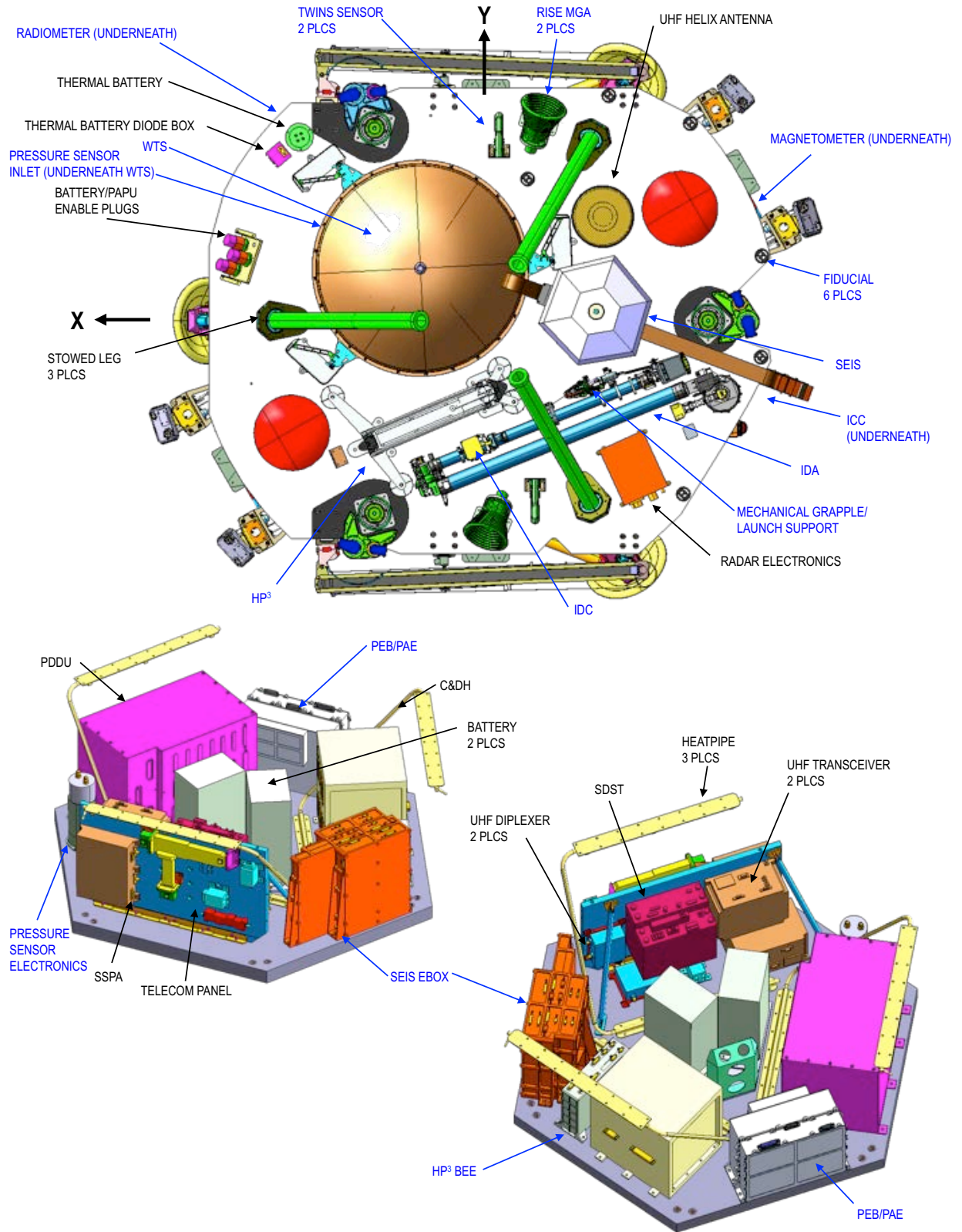
Figure 3.1-1: InSight lander deck (prior to payload deployment) and avionics compartment (thermal enclosure) components. Lander components are labeled in black with payload components in blue.

4 Science Instrument Investigations

There are two main categories of science instruments on InSight – those that remain on the lander throughout the mission and those that are deployed to the surface post-landing. The Instrument Deployment System (IDS) is utilized to place the Seismic Experiment for Interior Structure (SEIS) and associated Wind and Thermal Shield (WTS) as well as the support structure of the Heat Flow and Physical Properties Probe (HP³) onto the surface. The HP³ radiometer (RAD), and the Auxiliary Payload Sensor Suite (APSS) remain attached to the lander along with the Rotation and Interior Structure Experiment (RISE) that utilizes the X-band antennae. Figure 3.1-1 shows the configuration of the payloads prior to deployment. Figure 2.3-1 shows the post-deployment configuration. Additional detail about each payload is available below.

4.1 Seismic Experiment for Interior Structure (SEIS)

4.1.1 Description

The purpose of the SEIS instrument is to measure the surface ground velocity by a set of seismometers covering the 0.01-10 Hz frequency bandwidth for the 3 axis Very Broad Band (VBB) sensors and 0.1-50 Hz for the 3 axis Short Period (SP) sensors. These measurements are augmented by a gravity output of the VBBs (down to 50 mHz, the Phobos tide frequency), an overlap of the VBB and SP seismic sensors bandwidth outside their nominal bandwidth and by additional measurements enabling a better characterization and possibly mitigation of the lander and atmospheric generated noises.

The SEIS sensors will be deployed on the Mars surface by a robotic arm and will then operate almost continuously until end of mission. In summary, the instrument consists of the following functional subunits:

- *SEIS Acquisition and Control Electronics (SEIS-AC)*, located in the lander warm electronics box
- *Sensor Assembly (SA)* (including the Leveling System (LVL), the VBBs, the SPs, a set of temperature and tilt sensors and the Thermal Blanket (TBK). The SA will be deployed onto the surface.
- *SEIS Tether system,* which connects the SEIS-AC and the SA and is made of a tether, a tether box, and of a service loop and associated release shunt.
- *A SEIS cradle*, staying on the lander and locking the SA prior its deployment to the lander
- *A Wind and Thermal Shield (WTS),* deployed over the SA and providing thermal and wind protection.

In addition, SEIS will be supported by the Auxiliary Payload Support System (APSS), which will provide additional measurements of the magnetic field using the 3-axis InSight Flux Gate (IFG) magnetometer, of the pressure field with a micro barometer sensor, and Temperature and Winds for InSight (TWINS) sensors.

A functional block diagram of the instrument is shown in Figure 4.1-2 where the different subsystems are indicated by colors. The three VBB axes are fully independent one from each other while the 3 SPs share a common feedback card. All feedback cards are located in the lander SEIS-AC and will therefore have their temperature controlled by the lander warm box. Note that the SEIS-AC is fully redundant. The LVL control electronics is not redundant, but the three legs of the Leveling Platform are motorized while only two are needed to achieve the VBBs leveling with a resolution better than 0.1°.
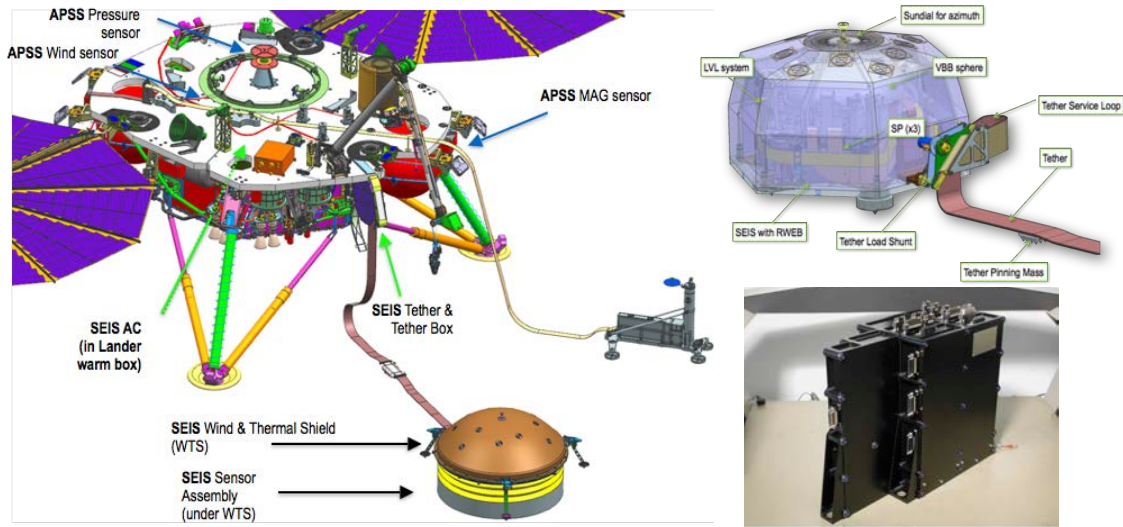
Figure 4.1.1-1: Different subsystems of the SEIS experiment when deployed on the ground by the robotic arm. On the left, the WTS covering the Sensor assembly (1a). On the Right: top (1b), Sensor Assembly (SA) and bottom (1c), SEIS acquisition and control electronics (SEIS-AC)
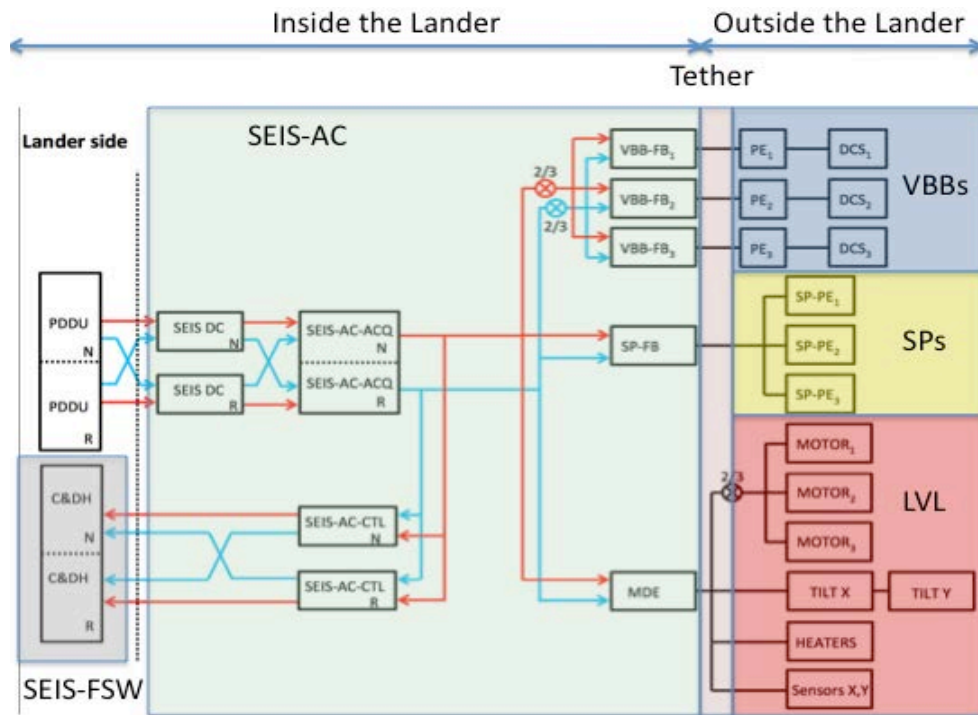
Figure 4.1.1-2: Functional block diagram of the SEIS instrument indicating the lander mounted SEIS-AC, the tether connecting the SEIS-AC to the deployed element and the subsystems of the Sensor Assembly, including the 3 VBBs, the three SPs and the motors and two different tiltmeters of the LVL (coarse tiltmeter for platform leveling and fine tiltmeters for precise calibration). Several temperature sensors are complementing the block diagram and monitor the various boards of SEIS-AC, Sensors heads and sensor proximity electronics (PE) plus a scientific temperature sensor located on the ring of the LVL structure. Not indicated in the block diagram as disconnected electrically from SEIS are the Wind and Thermal Shield (WTS), and the cradle supporting the SA during launch, cruise, and entry, descent, and landing.

4.1.2 Science Objectives

4.1.2.1   Threshold Science Objectives

Eight out of the ten Level 1 requirements of the InSight mission are associated with the SEIS science objectives. These are listed in Table 4.1.2.1-1 together with references illustrating possible data processing techniques that have been used or proposed for seismological studies of Mars or the Moon. Many other techniques have of course been developed for Earth, but are typically used for seismic network data processing.

Both structure and activity related science data products will be integrated into a structure model catalogue and an activity catalogue, which will be delivered by the SEIS team at the end of the nominal mission.

Table 4.1.2.1-1: Threshold (Structure related) and baseline (Activity related) science goals of the SEIS Experiment

L1 Requirement	Associated SEIS measures	Selected References for Mars or Moon seismology
Mars Structure L1 requirements		
Determine the depth of the crust-mantle boundary to within ±10 km	Rayleigh group or phase velocity from R1, R2, R3 wavetrains; Receiver functions; Regional located impacts; Crustal phases	Vinnick et al., 2001, Khan et al. 2000, 2002, 2007, Lognonné et al., 2003, Gagnepain-Beyneix et al., 2006, Chenet et al., 2006, Panning et al., 2015
Detect velocity contrast > 0.5 km/sec over depth interval > 5m within the crust, if it exists	Receiver functions, H/V spectrum analysis, Local located impact	Cooper et al., 1974, Dainty et al., 1974, Nakamura et al., 1975, Horvath et al., 1980, Vinnick et al., 2001, Dal Moro et al., 2015
Determine seismic velocities in the upper 600 km of the mantle to within ±0.25 km	Body waves and Rayleigh group or phase velocity from R1, R2, R3 wavetrain, Normal modes, Secondary body waves phases analysis	Nakamura, 1983, Lognonné et al., 2003, Gagnepain-Beyneix et al., 2006, Khan et al., 2000, 2002, 2007, Panning et al., 2015, Rivoldini et al., 2011, Verhoeven et al., 2005
Positively distinguish between liquid and solid outer core	ScS phases, Tidal Love Numbers	Van Hoolst et al., 2003, Weber et al., 2011; Garcia et al., 2011, Rivoldini et al., 2011
Determine the radius of core to within ±200 km	ScS phases, Tidal Love Numbers	Weber et al., 2011, Garcia et al., 2011, Van Hoolst et al., 2003, Rivoldini et al., 2011
Mars Seismic Activity L1 requirements		
Determine the rate of seismic activity to within a factor of 2	Seismic Arrival time and Seismic amplitude analysis	Nakamura et al., 1981, Philipps et al., 1991, Golombek et al., 1992, Knapmeyer et al., 2006, Panning et al., 2015
Determine epicenter distance to ±25% and azimuth to ±20°	Seismic Arrival time and Seismic amplitude analysis	
Determine the rate of meteorite impacts to within a factor of 2	Seismic Arrival time and Seismic amplitude analysis	Davis, 1993, Lognonné et al., 2009, Gudkova et al., 2011, 2015, Lognonné & Johnson, 2007, 2015, Teanby and Wookey, 2011, 2015, Teanby, 2015

4.1.3 Science Goal Implementation and Sensor Performances

4.1.3.1   Sensor Performances

With only one lander and an expected relatively low Mars seismic activity, the InSight SEIS requires a low instrument noise level (10^{-9} ms^{-2}/Hz$^{1/2}$ in the bandwidth 0.01 to 1 Hz and 10^{-8} ms^{-2}/Hz$^{1/2}$ in the bandwidth 1 Hz- 10 Hz). The performance and installation quality of the InSight seismometer will therefore be critical parameters to ensure success with a sensitivity higher than previous Mars seismometers (see Anderson et al., 1977 and Lognonné et al., 1998). SEIS also can expect a much better deployment because of the robotic installation of SEIS from the deck of the lander down to the ground followed by the lowering of a wind and thermal shield (WTS) on the SA. Figure 4.1.3.1-1 illustrates the packaging and configurations of the VBBs, including the evacuated titanium sphere in which VBB sensors are located. A thermal blanket is wrapped around both the VBB sphere and SPs (Figure 4.1.1-1) and the WTS (Figure 4.1.1-1) will provide additional shielding. All together, these three thermal barriers produce an effective two level thermal filter with time constants of 2 hr and 5.5 hr. It is likely that SEIS will be close to the best deployment and sensitivity that can be achieved by a robotic installation on the surface of Mars.

The SEIS VBB (see Figure 4.1.3.1-1) is based around three inverted oblique pendulums, with gravity acting against the spring to lower the pendulum natural frequency to about 0.45Hz for a proof mass of 190 g. It uses a highly sensitive capacitive transducer to drive a feedback designed to provide a response that is relatively flat in ground velocity to within 10 dB from 50 to 0.5 s, with an expected noise below 10^{-9} m s^{-2} Hz$^{-1/2}$ between 0.02 and 2 Hz on the vertical (VEL) output (Figure 4.1.3.1-1). The output is digitized at 24 bits, giving 10 dB headroom over the instrument noise floor and a saturation threshold larger than Viking. The VBB has in addition a thermal compensation mechanism, which will be tuned on Mars in order to minimize the amplitudes of thermally driven daily variations, enabling in addition to the VEL output the records of a High Gain Mass position output (POS), flat in ground acceleration from DC to 0.02 Hz and with expected self noise of 10^{-9} m s^{-2} Hz$^{-1/2}$ between 0.005 and 0.02 Hz. All VBB are located in a titanium sphere, which maintains low pressure until end of mission and minimizes the proof mass Brownian noise to <3 x 10^{-10} m s^{-2} Hz$^{-1/2}$. Expected sensor self noise and gains in the range of operating conditions are given in Figure 4.1.3.1-2. Axes in the X,Y, and Z directions are made through recomposition of the three oblique axes.
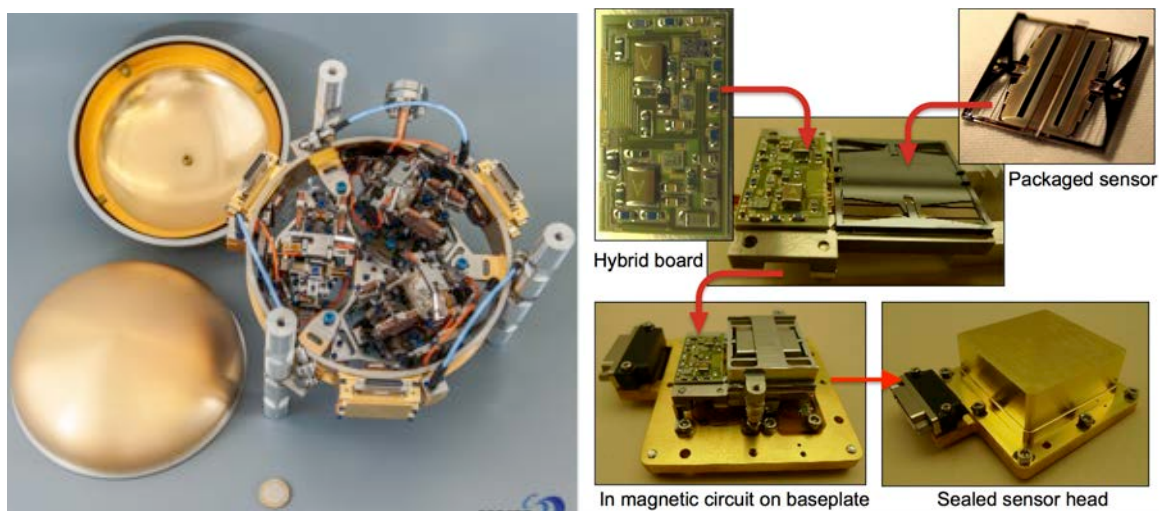
Figure 4.1.3.1-1: (Left) Flight Sphere with the 3 VBBs before sphere closure. (Right) SP QM sensor and its integration scheme in the SP sealed sensor head.

SEIS SP (Figure 4.1.3.1-1) consists of a set of micromachined sensor heads, one vertical and two horizontal axes. The suspension and proof mass of each sensor are etched from single-crystal silicon wafers using deep reactive ion etching to produce a 6 Hz suspension and a 0.5 g proof mass. The motion

of the proof mass is capacitively measured by the change in overlap between an array of electrodes on the proof mass and an opposed fixed array connected to the outer frame of the suspension. A sliding rather than squeeze-film gas damping occurs in the capacitive transducer, a Q of a few hundred can be achieved without evacuation. SEIS SP's feedback produces a flat velocity output over a bandwidth from 40 Hz after anti-alias finite impulse response (FIR) to below 0.05 Hz producing an overlap with the VBB, with a determined acceleration sensitivity of 5×10^{-9} ms^{-2} Hz$^{-1/2}$. The sensor self noise as determined on Earth and gains in the range of operating conditions are given in Figure 4.1.3.1-3.
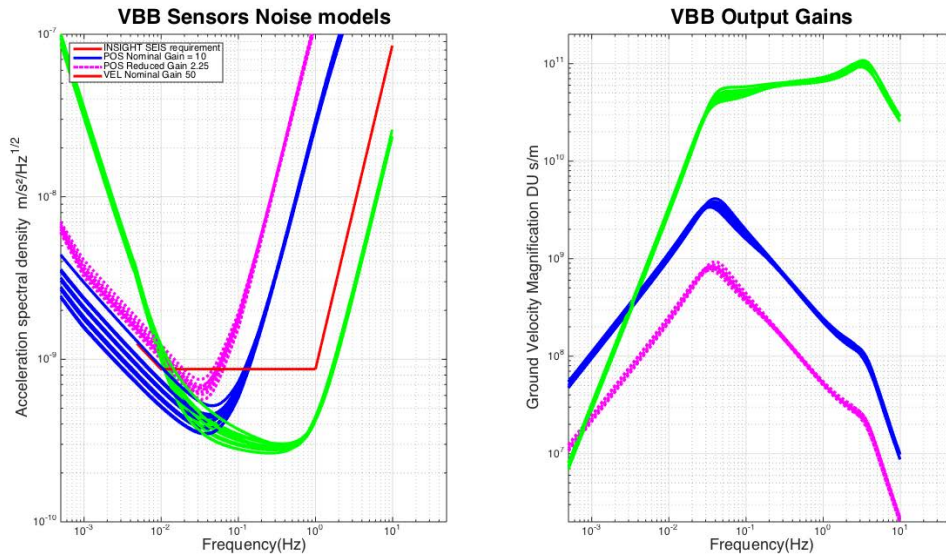
Figure 4.1.3.1-2: Noise models and gains (in Digital Unit (DU) per ground velocity (m/s), e.g. DU s/m) of the 3 flight model VBB sensors, for temperature between -65° and -25°C (corresponding to typical temperature seasonal variations). Nominal velocity and position outputs are the green and blue lines, respectively, while the reduced Gain gravity outputs (POS) are the magenta ones. Red line is the InSight SEIS Vertical requirement projected at the sensor level (Z noise is amplified by about 1.15 while the horizontal noise is reduced by about 0.77, as compared to the oblique VBB noise).
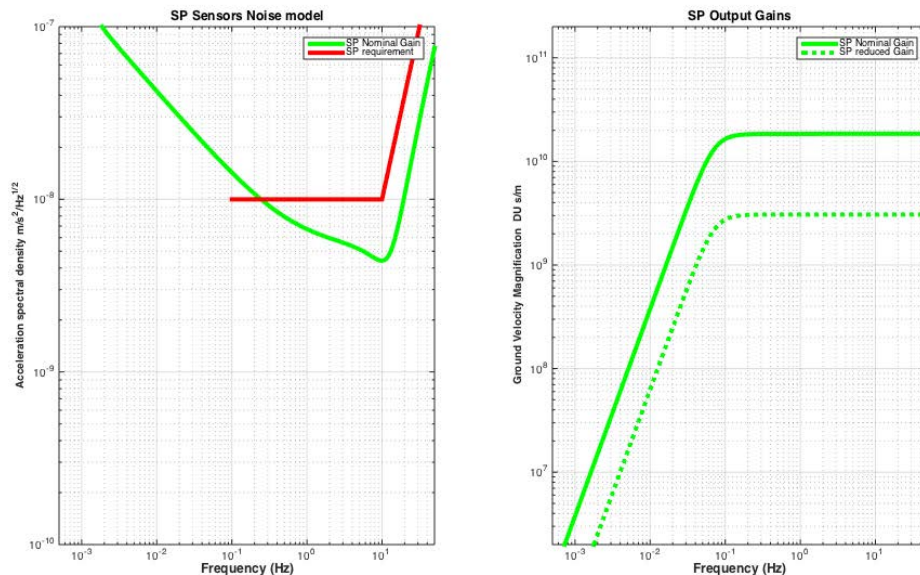
Figure 4.1.3.1-3: Noise models and Gain (in DU s/m) of the flight model SPs. Nominal Velocity Gain and reduced Velocity Gain are the green and blue lines, respectively. Red line is the InSight SEIS Vertical requirement.

4.1.3.2   Installation and A Priori Seismic Noise

It is expected that environmental noise will, especially during the day, be the first source of noise. Part of this noise is associated with temperature variations, partially filtered by the SEIS thermal protection and is related to the surface installation. Typical diurnal temperature variations are however expected to be ~10°C in winter and ~22°C in summer at the VBBs sensor locations with larger temperature variations on the LVL and SPs. Another noise contribution is related to the a priori low rigidity of the Martian upper subsurface, which leads to ground deformations/vibrations generated by pressure fluctuations of the atmosphere or the interaction of the lander and of the WTS with the wind flow. Although considerably smaller than those reported by the Viking experiment (Anderson et al., 1977, Nakamura and Anderson, 1979, Lorenz, 2012), diurnal noise variations will likely be observed in the range of 10^{-9} ms^{-2} Hz$^{-1/2}$ to 10^{-8} ms^{-2} Hz$^{-1/2}$ (see Figure 4.1.3.2-1a,b for the day and night micro-seismic noise prediction of the SEIS noise model). In the short period range, a larger noise is expected to be associated with the lander solar panels and structural wind-excited oscillations (Figure 4.1.3.2-1c). Although part of this noise is expected to be decorrelated by the APSS sensors, the non-seismic origin of that part of the recorded noise will have to be integrated in all noise analysis.
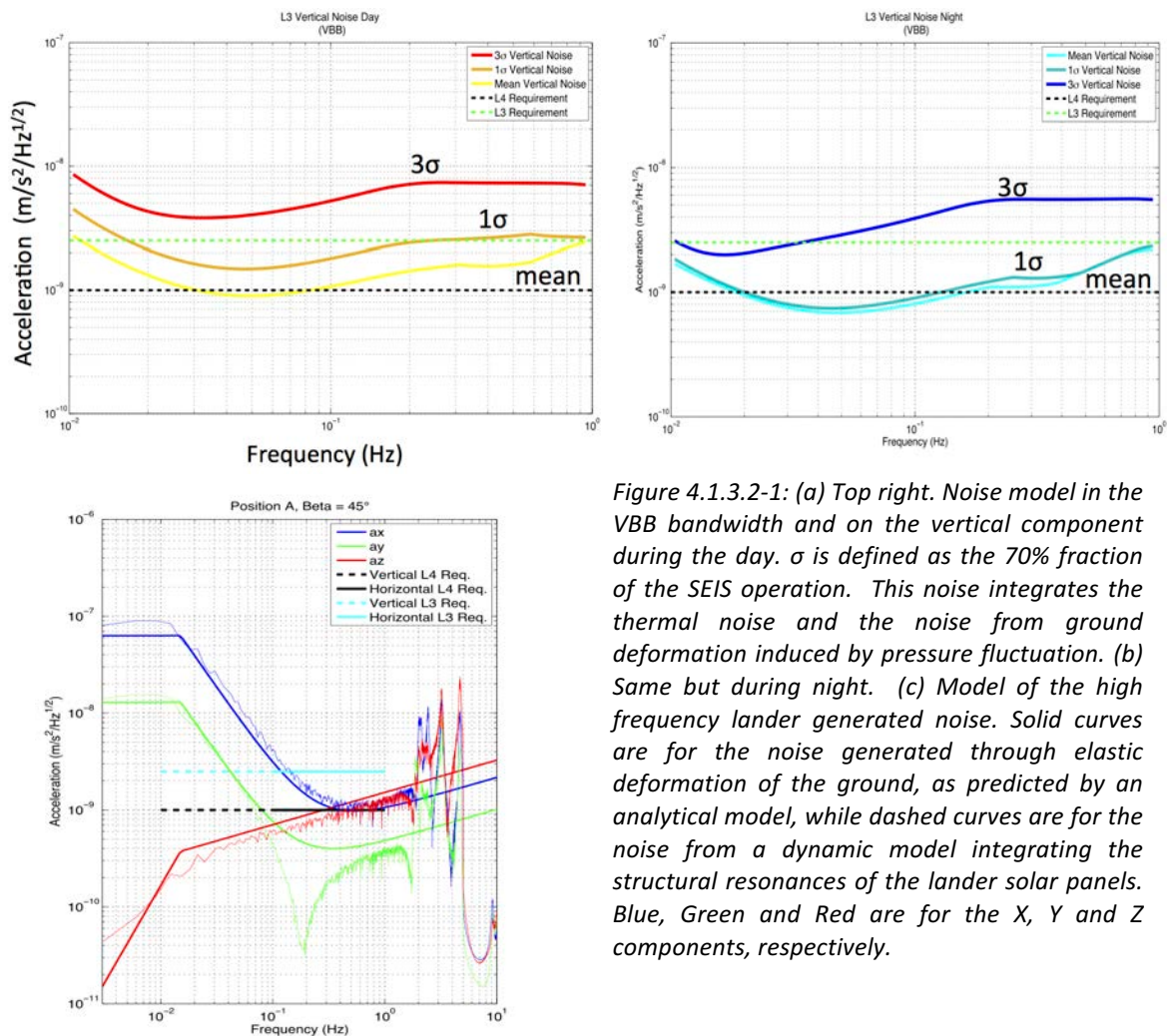
Figure 4.1.3.2-1: (a) Top right. Noise model in the VBB bandwidth and on the vertical component during the day. σ is defined as the 70% fraction of the SEIS operation. This noise integrates the thermal noise and the noise from ground deformation induced by pressure fluctuation. (b) Same but during night. (c) Model of the high frequency lander generated noise. Solid curves are for the noise generated through elastic deformation of the ground, as predicted by an analytical model, while dashed curves are for the noise from a dynamic model integrating the structural resonances of the lander solar panels. Blue, Green and Red are for the X, Y and Z components, respectively.

4.1.3.3   SEIS Auxiliary Sensors

A set of temperature sensors will monitor the temperatures of the subsystems, including all VBB sensors (16 bits 2 wires PT1000, 1/10 sps, 1/100K resolution), the LVL ring system with a SCIentific Temperature (SCIT, 24 bits 4 wires PT1000, 1/200K resolution) and sensor Proximity Electronics (PEs) and Feedback (FB) cards (12 bits 2 wires PT100, 1/10 sps, 1/10 resolution). Accuracy of the SCI Temperature is better than 0.25 K while others are about 1 K.

The LVL is equipped with two types of tiltmeter, each type recording the two axis tilts of the LVL ring coordinate common to the VBB horizontal plane. The first one is a coarse MEMS type tiltmeter while the second one is an electrolytic precise tiltmeter. Both are acquired by a 12 bit analog-to-digital converter (ADC), with an oversampling ratio defined by command. Measured resolution of the flight model MEMS and Electrolitics Tilmeters are around 140 arcsec and < 0.7 arcsec, respectively.

4.1.3.4   SEIS Acquisition Performance

All SEIS high rate seismic data (VBB VEL and SP) are sampled by a dedicated 24 bit ADC at a primary rate of 500 sps and then decimated by FIRs down to the selected output rate (100 sps or 20 sps). Low rate science data (VBB POS, SCI Temperature) are sampled by a dedicated 24 bit ADC at a primary rate of 10 sps. VBB temperatures have also a primary sampling of 10 sps but with a 16 bit ADC. These low rate data are then decimated by FIRs down to the selected output rate (1 sps or 1/10 sps). All FIRs can be remotely updated and are designed with 120 dB attenuation above the Nyquist and less than 3 dB of attenuation at frequencies below 80% of the Nyquist. Other House Keeping data, as briefly described in the Appendix A, are sampled at the selected rate (typically 1/100 sps for nominal conditions).

4.1.4 Instrument Operation

4.1.4.1   SEIS Operations

After deployment of the instrument onto the surface of Mars by the InSight robotic arm, operations of the SEIS instrument are expected to be continuous, with the exception of severe lander power restriction or emergencies. This continuous operation is made possible by the autonomy of the SEIS-AC, which enables the SEIS operation even when the lander is in sleeping mode. Change in SEIS operation modes as well as calibrations and LVL activations are possible only when the lander is awake.

All data will be stored in the SEIS-AC mass memory before being transmitted to the lander mass memory during lander wake-ups. Similarly, APSS data will also be sampled at high rate (20 sps for pressure and 3 axis magnetic field and 1 sps for the wind). Both SEIS and APSS data will generate about 600 Mbits/sol, too high a volume for full transmission. The data are therefore decimated in order to fit in the SEIS data transmission allocation of 30 Mbits/sol. See Section 4.1.6 for details on the decimation and generation of the continuous data flow.

Continuous data will be sent regularly to Earth and processed by the SEIS operation center, SISMOC, located at the Technical Center of the French Space Agency CNES in Toulouse (France). These data will then be processed in order to identify the occurrence of quakes, and event requests will be made to recover the high frequency SP, VBB and when necessary APSS data corresponding to the event period. About 5 Mbits per sol of SEIS event data are planned on average, corresponding to about 15 minutes of SP raw data at 100 sps and 10 mins of VBB raw data at 10 sps, as well as the high rate APSS data of the same periods. 3 additional Mbits per sol are allocated to APSS only events.

4.1.5 Calibration

4.1.5.1   VBB VEL and SP Calibrations

Calibration of the VBB VEL and SP outputs will be performed through built-in calibration coil and digital to analogue generator, calibrating all individual axes. Calibration of these seismic outputs is better than 5% and the calibration signal can be remotely uploaded if requested. Pre-launch calibration of the flight model VBB has been performed at several temperatures within the operating range for better knowledge of the temperature variations of the transfer function and calibration coil efficiency. These calibration data will be used for resolving the 3 axis ground acceleration into X, Y, and Z components. The LVL resonances have also been calibrated and mainly affect the horizontal components. The resonances

are in the range of 30-50 Hz with a structural resonance quality Q<10 on the Z component depending on the length of the LVL feet and deployment geometry.

4.1.5.2   VBB POS Calibrations

Additional calibration of the VBB POS output will be performed on Mars during SEIS commissioning and one sol every month in order to achieve the gravity measurement accuracy requested for tidal analysis. These calibrations will be performed by a series of LVL tilts measured by the electrolytic tiltmeter and used as calibration tilts for the VBBs, in addition to VBB open loop frequency measurements. The calibration goal is to reach in-situ accuracy of 0.2% within 0.1° of LVL tilt.

4.1.5.3   VBB and SP Environment Sensitivity Calibration

APSS sensors will be used to perform on-site decorrelation of pressure and magnetic field sensitivity. Pressure noise will be mainly related to ground deformation driven by the wind supported pressure fluctuations (Sorrels, 1971, Zürn and Widmer, 1995, Beauduin et al., 1996,) while magnetic field is expected to affect the VBB sensor (Forbriger et al., 2010) as the later has no mu-metal shielding. Performances of the APSS sensors are described below..

4.1.6 SEIS Flight Software Operation

In addition to the Instrument operation, the SEIS flight software (SEIS FSW) will play a key role in the on board management of the science data. SEIS FSW will:

- store the raw data acquired at high sampling rate (i.e. 100 sps for SPs , 20 sps for VBBs, APSS Pressure and APSS IFG, 1 sps for APSS TWINS) in the lander mass memory. These data will remains in the lander mass memory for about 6 weeks, depending on the compression of data.
- generate from these data a flow of continuous data adjusted to the SEIS transmission allocation bandwidth. For nominal bandwidth, this is made by down sampling the 3 axis VBB data into three 2 sps continuous time series and by the production of a single 10 sps, vertical like time series from summation of and hybridization of both VBBs and SPs channels (SEISVELZ). Similar decimations are made from the APSS data and in addition, the average high passed seismic energy of the Vertical SP is sent every second (ESTASP) together with the similar high frequency energy of the pressure (ESTAP) and magnetometer (ESTAM). These continuous data are summarized in Table 4.1.6-1 together with those of the APSS sensors for SEIS support and will make a total of about 30 Mbits per sol.
- extract and when requested decimate the event data down to the selected output rate (e.g. 100, 50 or 25 sps for SPs, 20 or 10 sps for VBBs)
- perform sensor replacement in case of any sensor failure. This might be done by generating a replacement 20 sps time series from the 100 sps SPs (in case of one VBB failure), or by decimating the replacement 100 sps VBBs to nominal 20 sps (in case of SP failure).

4.1.7 Ground System Operation

Figure 4.1.7-1 summarizes the ground operations of SEIS, including Project and Science Tactical and Science Non-tactical activities.

Project tactical activities will be performed by the SEIS Operation Center (SISMOC) center at CNES, which will be responsible for the SEIS operation and the generation of the SEIS data in mini-SEED data (SEED is for Standard for the Exchange of Earthquake Data, see Ahern et al., 2012 and Appendix A for a description of SEED and mini-SEED data). Data will then be distributed in SEED by the IPGP Data center (http://centrededonnees.ipgp.fr) and the hosted SEIS data service (in development at this time, http://seis-insight.eu). This SEIS data service will distribute both the proprietary SEIS data to the SEIS team and, together with IRIS Data Management Center and NASA Planetary Data System, the non-proprietary data after the PDS release dates.

Table 4.1.6-1: List of the continuous data transmitted to Earth. All data will be decimated by FIRs and further processed for the ESTA signals, which correspond to the average variance of the high pass filtered signals. See more details in the Data Archiving Plan (Appendix A)

Data Budget
RAW DATA

Acquired datas	Channel Name	Bits per sample	Data Rate (sps)
VBB 1 Velocity	VEL1	24	20
VBB 1 Position	POS1	24	1,00
VBB 1 Temp	TEMP1	16	0,1
VBB 2 Velocity	VEL2	24	20
VBB 2 Position	POS2	24	1
VBB 2 Temp	TEMP2	16	0,1
VBB 3 Velocity	VEL3	24	20
VBB 3 Position	POS3	24	1
VBB 3 Temp	TEMP3	16	0,1
Scientific temperature #1	STEMP1	24	1
Scientific temperature #1	STEMP2	24	0
TWINS#1 raw	TW1	432	1
TWINS#2 raw	TW2	432	0
Space Craft Power bus	SCPB	16	1
Pressure sensor, pressure 3 bytes	PP	24	20
Pressure sensor, temperature 3 bytes	TP	24	20
MAG 12 bytes	MAG1-2-3	96	20
MAG Temperature 3 bytes	MAGT	24	20
SP1	SP1	24	100
SP2	SP2	24	100
SP3	SP3	24	100
HK (assume 72 channels on 16 bits)	HK-n	1152	0,01

Data Budget
CONTINOUS DATA

Acquired datas	Channel Name	Bits per sample	Data Rate (sps)
VBB 1 Velocity	VEL1	24	2
VBB 1 Position	POS1	24	0,5
VBB 1 Temp	TEMP1	16	0,1
VBB 2 Velocity	VEL2	24	2
VBB 2 Position	POS2	24	0,5
VBB 2 Temp	TEMP2	16	0,1
VBB 3 Velocity	VEL3	24	2
VBB 3 Position	POS3	24	0,5
VBB 3 Temp	TEMP3	16	0,1
Scientific temperature	STEMP1	24	0,1
TWINS#1 Continuous	TW1C1	432	0,1
TWINS#2 Continuous	TW2C3	0	0
Space Craft Power bus	SCPB	16	0,1
Pressure sensor, pressure 3 bytes	PP	24	2
Pressure sensor, temperature 3 bytes	TP	24	0,2
MAG 9 bytes	MAG1-2-3	96	0,2
MAG HK 3 bytes	MAGT	24	0,02
SP1	SP1	24	0
SP2	SP2	24	0
SP3	SP3	24	0
SEIS PPS AOBT	TCLK	272	0,000556
HK (assume 72 channels on 16 bits)	HK-n	1152	0,01
Seis processed data			
SEISVELZ	LPZ	24	10
SPZ	SPZ	24	0
POSZ	POSZ	24	0
ESTASP	TRISP	24	1
ESTAVBB	TRIVBB	24	0
ESTAP	TRIP	24	0,5
ESTAM	TRIM	24	0,1

SEIS and APSS science tactical activities will mainly consist of the fast analysis (one week cycle) of the continuous data in order to identify seismic events, to perform first analysis of these events (arrival times, pre-location, etc.) and to format event requests for the downlink of the associated high rate data. This task will be coordinated by the Mars Quake Service, hosted by the Swiss Federal Institute of Technology in Zurich (ETHZ, Zürich, Switzerland) together with the Institut Supérieur de l'Aéronautique et de l'Espace (ISAE, Toulouse/France) and the Jet Propulsion Laboratory (JPL, Pasadena, USA). Event requests may be made by alteam members. Data prioritization will be made weekly at the SEIS-InSight project level. The Mars Structure Service will coordinate research activities associated with the generation of internal models of Mars (and associated Mars Structure catalogue) and will be hosted by the Institut de Physique du Globe de Paris (IPGP) together with University of Florida and University of Nantes.

Educational activities will also be performed through the transmission of the data to a network of several hundred of middle and high schools worldwide, associated with several "seismo at school" programs in the United States (https://www.iris.edu/hq/sis), France (http://www.edusismo.org) Switzerland (http://www.seismoatschool.ethz.ch) and the United Kingdom (http://www.bgs.ac.uk/schoolseismology).
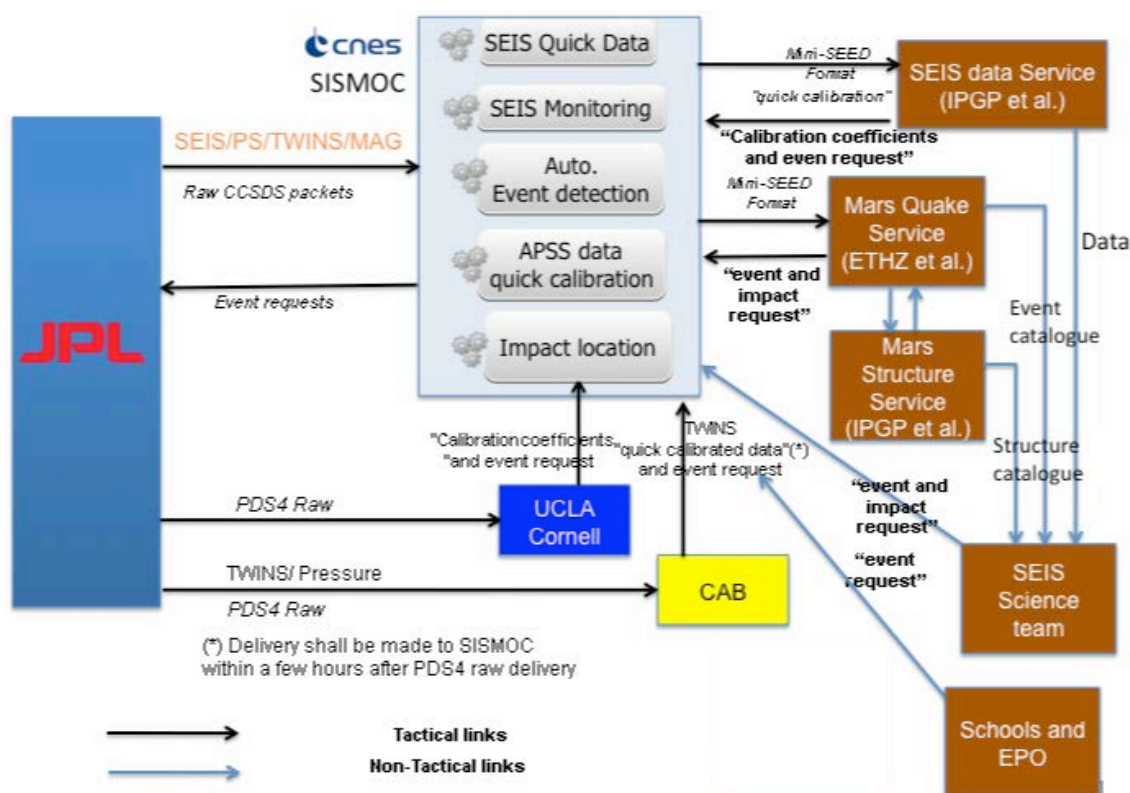

Figure 4.1.7-1: SEIS ground system structure, including the Tactical Operation at SISMOC, Science Tactical and non-Tactical operations and Science team and outreach activities. CAB, UCLA, and Cornell are part of the APSS instruments described in Section 4.2.

4.2 Auxiliary Payload Sensor Suite (APSS)

4.2.1 Introduction

The Auxiliary Payload Sensor Suite (APSS) is a set of sensors consisting of the Pressure Sensor (PS), Temperature and Winds for InSight (TWINS), and the InSight Flux Gate magnetometer (IFG), all controlled by the Payload Auxiliary Electronics (PAE). These sensors provide environmental information that will be used in planning spacecraft operations (including instrument deployment) as well as to support SEIS

(Seismic Experiment for Interior Structure) data analysis, and for their own scientific objectives. Figure 4.2.1-1 shows the locations of the components of the APSS equipment suite.

Like the SEIS instrument, the APSS is designed to run continuously, and to record data without gaps at a high enough sampling rate to aid SEIS data analysis in search of seismic signals. In addition to being the first instance of a magnetometer at the surface of Mars, APSS will also be the first continuous and high frequency record of pressure, air temperature and winds at the surface of Mars.
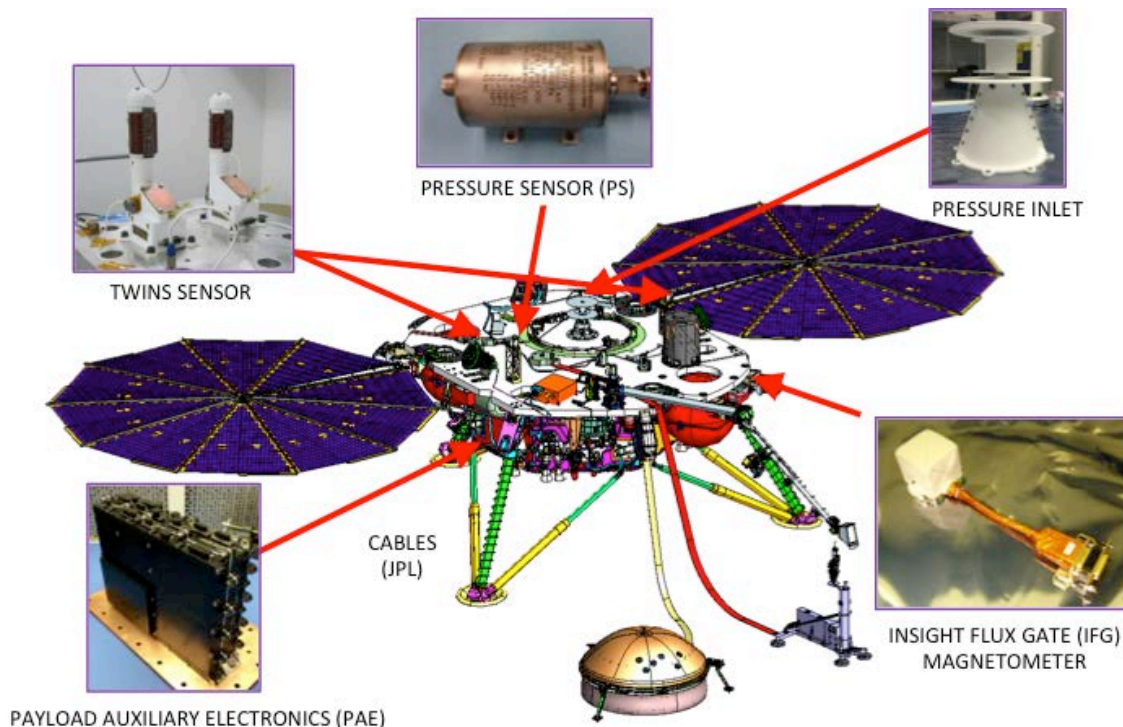

Figure 4.2.1-1: Location of each component in the APSS sensor suite.

4.2.2 Temperature and Winds for InSight (TWINS)

4.2.2.1   Introduction

TWINS is composed of two essentially identical sensor booms placed horizontally and diametrically opposite and parallel to one another on top of the lander deck, along the Y-axis as shown in Figure 4.2.2.1-1. Each boom is a modified Mars Science Laboratory (MSL) Rover Environmental Monitoring Station (REMS) boom, and contains sensors for both 3-D wind and air temperature measurements. The deck placement is intended to minimize the effects of wind-flow perturbations induced by the other elements on the lander top deck by ensuring that at least one of the booms will be windward of the bulk of the lander body for nearly any given wind direction.
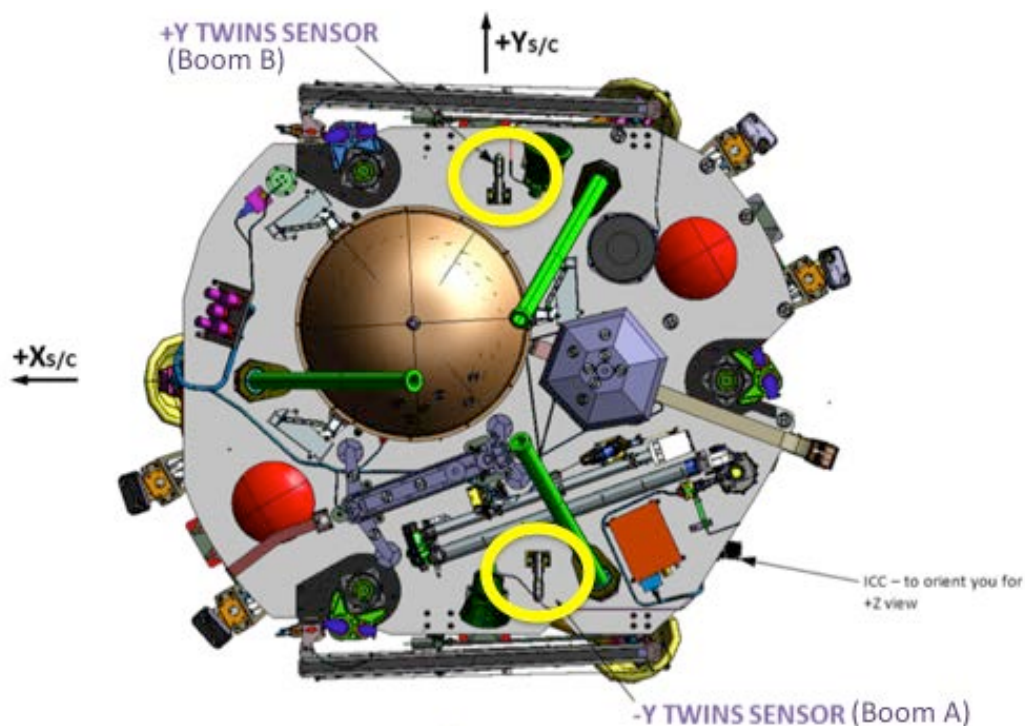
Figure 4.2.2.1-1: A view of the InSight lander deck, showing the location of the TWINS booms (circled in yellow).

4.2.2.2 Science Objectives

TWINS' primary requirement is to support SEIS by indicating when the winds are above 5m/s, representing a state when wind perturbations are likely significantly degrading the signal to noise ratio of the SEIS measurements. However, in addition to this crude indicator of SEIS data quality, TWINS will supply the time-resolved 3-D wind vector in the vicinity of the InSight lander, which can be used to estimate the detailed wind perturbations on the SEIS measurements. Additionally, TWINS will be used to characterize the local wind behavior at the landing site prior to and during the timeframe when the Instrument Deployment Arm (IDA) is moving the SEIS, WTS, and HP[3] (Heat flow and Physical Properties Package) instruments to the surface to choose the best possible conditions and times, and to ensure the safety of that operation.

TWINS data will also be used for other science goals beyond those of SEIS. For example, TWINS data will be key in characterizing the local meteorology of the landing site, including diurnal tides, mesoscale circulations, seasonal variations, slope winds, and perhaps even transient waves. Dust devils are expected to be found at the InSight landing site, and TWINS data will be valuable in characterizing them. Because TWINS will be recording data continuously, it is uniquely valuable in quantifying wind thresholds for aeolian change and solar panel dust removal events. Additionally, simultaneous measurements from REMS at Gale Crater (data available through the Planetary Data System – atmospheric node) and TWINS at InSight's landing site will help validate and improve meteorological models.

4.2.2.3 Instrumentation

Both booms are identical, and each carries a wind speed and direction sensor as well as an air temperature sensor. Wind speed and direction are provided by three sensor boards (2-dimensional hot film anemometers) arrayed around the tip of each boom. Each of these sensor boards consists of 4 hot dice and 1 cold die that sense the local wind speed and direction in the plane of the sensor. The three sensor boards are located 120° apart around the boom axis, as shown in Fig. 4.2.2.3-1. The full wind speed and direction is calculated by differencing measurements between the hot and cold dice, and then between the sensor boards facing in different directions. Readings from all the dice are sent back to Earth,

where a retrieval algorithm is used to combine them with the pressure measurements, engineering data from the front-end electronics and the calibration curves to yield the wind speed and direction for each boom.
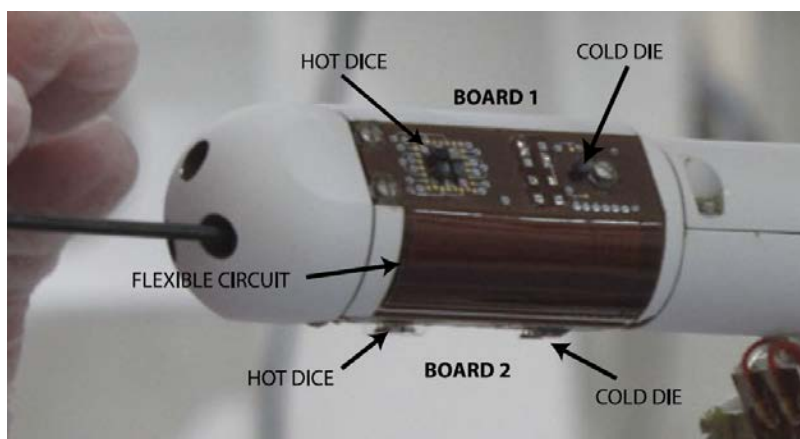

Figure 4.2.2.3-1: TWINS wind sensor detail.

The wind sensor has a response time of roughly 1s to wind perturbations, reducing its sensitivity to fluctuations above about 1Hz. The wind speed measurement has an accuracy such that wind speeds up to about 5.5 m/s will be sensed to within about 1.5 m/s. For wind speeds above this, the error bars increase, for example at 15 m/s the error bars are 2.85 m/s.
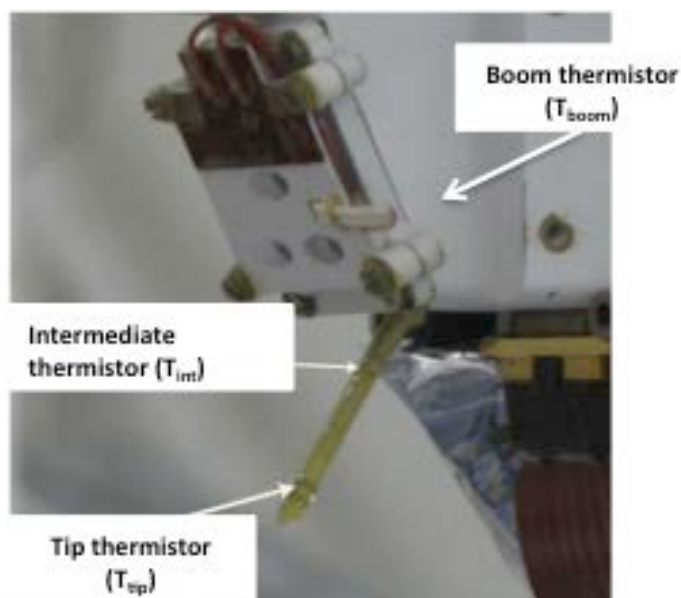
Figure 4.2.2.3-2: TWINS air temperature sensor detail.

The air temperature is sensed using a small low thermal conductivity rod extending below the base of each boom (See Fig. 4.2.2.3-2). This rod has resistance temperature detectors (RTD) at its tip and midway along its length. Using these measured temperatures, as well as that at the base of the rod, the ambient air temperature can be estimated, despite the thermal contamination from the boom and the effects of solar radiation. The air temperature sensors response time depends on the atmospheric turbulence, being on the order of 30s in forced convection, although it will be sampled at 1Hz. It performs over the range of 167K to 277K with an accuracy of about 5K and a resolution of 0.1K.

4.2.2.4   Instrument Operation

In general, only one TWINS boom will be operational at any one time for power considerations. However, to characterize the diurnal wind conditions and in preparation for placing SEIS, WTS and HP[3] on the surface, TWINS may initially be operated using both booms simultaneously. Once the typical diurnal wind direction variations at the landing site are characterized, a boom-switching strategy will be employed to select the windward boom for operation at any particular local time. TWINS data will be recorded continuously, sampled at 1Hz. Under nominal downlink conditions, the full data set will be downlinked at a lower rate, namely 0.1Hz. For TWINS, the wind measurements will simply be sampled at the lower rate, as opposed to any more complex filtering as is done for SEIS and PS. For the air temperature measurements, they will be averaged to produce the downsampled values and a standard deviation over the averaging time will also be reported. As with the SEIS or PS data, selected "events" can be downlinked at the full data rate (within the limits of the downlink budget).

4.2.2.5   Calibration

The TWINS instrument has been calibrated using a low-pressure wind tunnel at the Centro de Astrobiologia (CAB). The wind sensor's calibration curves were estimated for all the angular configurations and a significant number of Reynolds numbers within the expected operational range (pressure and speed). Using the same facility, dedicated calibration campaigns were performed to determine or refine the parameters involved in the end-to-end air temperature sensor numerical models. There are no means of re-calibrating the instrument after launch or on the surface of Mars.

4.2.3 Pressure Sensor (PS)

4.2.3.1   Introduction

The PS is a pressure transducer manufactured by TAVIS Corporation (Figure 4.2.3.1-1a), located in the lander body, and connected to the ambient atmosphere with an inlet on the lander top deck (Figure 4.2.3.1-2). The inlet (Figure 4.2.3.1-1b) is specifically designed to minimize the effects of wind on the pressure measurement, with a design similar to the "Quad-Disc" design developed for single inlet microbarometric measurements terrestrially (Nishiyama & Bedard, 1991). Before deployment, the WTS (Wind & Thermal Shield) will cover the Quad-Disc inlet for the PS (Figure 4.2.3.1-3). The Pressure Sensor's sensitivity to winds may be increased (likely <1Pa for 7m/s winds) until WTS is deployed, but the pressure measurements will likely still be meteorologically useful during this pre-deployment timeframe.

Figure 4.2.3.1-1: a) The Tavis Pressure Sensor and b) The Quad-Disc pressure sensor inlet.

Quad-Disc inlets under terrestrial conditions reduce wind effects (dynamic pressure) on pressure measurements to 1% to 0.01%, depending on the Reynolds number of the flow (worse at high Reynolds number). On Mars, the Reynolds number will be about 2 orders of magnitude smaller than on Earth, so the Quad-disc should reduce wind dynamic pressure effects to on the of order 0.0001% (i.e., <1mPa for 1000 Pa ambient pressure). However experimental studies have not been able to empirically confirm this level of performance due to the very difficult nature of such a measurement.
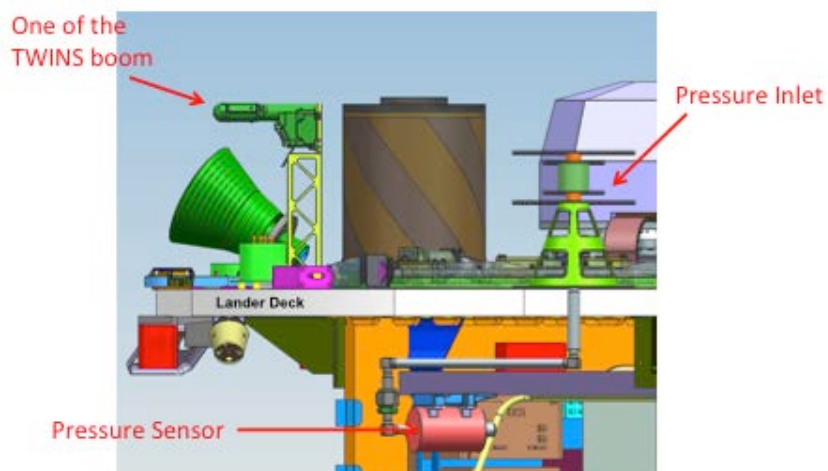
Figure 4.2.3.1-2: Location of PS and TWINS on the lander deck.
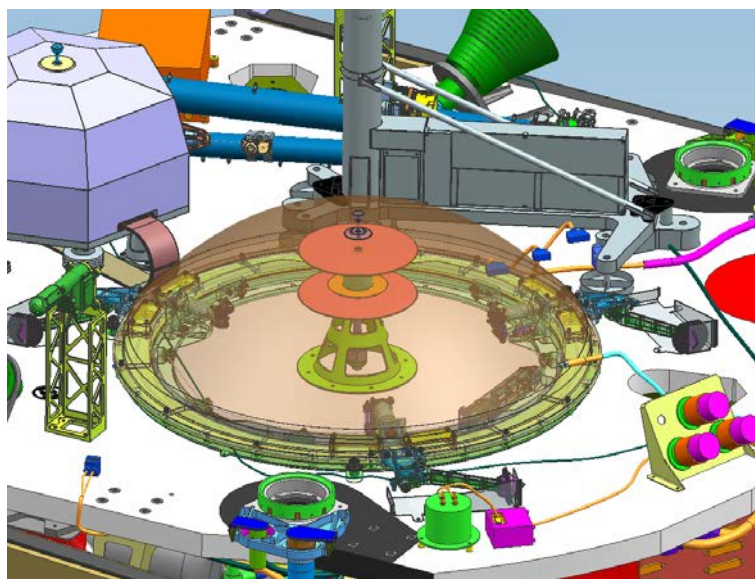
Figure 4.2.3.1-3: Showing the pre-deployment configuration with the WTS covering the pressure-inlet sensor.

4.2.3.2   Science Objectives
The pressure sensor's main purpose on InSight is to supply high-frequency, high-precision pressure measurements for use in decorrelating atmospheric pressure-induced noise from the SEIS measurements. It will also be used to pursue atmospheric science objectives. For example, as the fastest-response, highest-sensitivity continuously sampling pressure sensor ever sent to the surface of Mars, it is expected to contribute in dust devil, bolide, gravity wave and infrasound searches, and perhaps in other ways not anticipated.

4.2.3.3   Instrumentation

The sensor itself is designed to produce valid output between pressures of about 560 Pa and 1000 Pa, which are expected to be the extreme pressures that will be experienced at the InSight landing site (based on VL1 and MSL data and MOLA altitudes of the landing ellipse). The actual calibration is temperature dependent so the ultimate range possible for the instrument will depend on the thermal environment experienced. The sensor is specifically designed to minimize noise, with a typical RMS of about 10 mPa on any particular reading. The instrument's noise spectrum meets the design requirement of:

$$\frac{0.01}{(f/0.1)^{2/3}} \ \ \mathrm{Pa\ Hz^{-1/2}}$$

for 0.01 < f < 0.1 Hz and 0.01 Pa Hz$^{-1/2}$ for 0.1 < f < 1 Hz.

Placing the transducer within the body of the lander allows it to remain in a relatively controlled thermal environment, minimizing temperature effects corrupting the pressure measurement. Nevertheless, the pressure sensor also includes a temperature sensor near the sensor's active element. This is required for accurate calibration of the sensor voltage readings to actual ambient environmental pressures.

The inlet tubing between the atmosphere and the pressure sensor itself produces a response time (or alternatively a cutoff frequency) for the instrument. For perturbations shorter than this time, the sensor's response will be reduced. The cutoff frequency due to the inlet plumbing of the pressure sensor is roughly 6 Hz. There is also a first-order electrical low pass filter on the sensor output with a cutoff frequency of about 3 Hz. The sensor is read by an Analog to Digital Converter on the PAE at 500 Hz, which is then averaged down to a 20 Hz data stream. The two cutoff frequencies in the system provide adequate anti-aliasing filtering for the 10 Hz Nyquist frequency of the fundamental data rate of the pressure sensor.

4.2.3.4   Instrument Operation

The pressure sensor is designed to operate constantly throughout the mission, only being turned off in case of low power availability. Because the pressure decorrelation is crucial to interpreting the seismic signals, pressure data is needed at all times of the mission. The native sampling rate on board the lander is 20 Hz, although downlink budgets preclude returning all of this data to Earth. Instead, on-board processing will filter and downsample this to a lower sampling rate continuous data stream, as well as other processed versions of the full signal to indicate energy in the pressure signal at frequencies above the continuously downlinked sampling rate. For the nominal downlink case (~38 Mbits/Sol), the pressure sensor will return continuous data downsampled to 2Hz, and its temperature sensor will be downsampled to 0.2 Hz. Onboard processing will also produce the RMS of a high-pass version of the pressure signal above 1 Hz, which will be downsampled to 0.5Hz. This latter signal is expected to be indicative of high frequency pressure variations above that resolved in the continuous pressure data, to focus attention for downlink of the full sampling rate data in an "event". There will be a certain amount of the downlink budget allocated to "events" which will be special times in the mission where anomalous signals are detected in the pressure (or seismic or wind or magnetic) data sets, and full temporal resolution data sets are desired. In this case, the full 20 Hz data set from the pressure sensor (or a downsampled version of it) can be downlinked for a short period (~30 minutes/sol).

In the case of extremely small available downlink, the so-called Direct-To-Earth (DTE) case, only about 0.9Mbit/Sol is expected to be available. In this case, the continuous data will be much more severely downsampled (down to 0.1Hz for Pressure and 0.01Hz for the temperature of the pressure sensor). An on board computation will be performed of the average of the RMS of a high-pass version of the pressure signal (above 1 Hz), as well as the maximum of that RMS, both downsampled to 0.001 Hz. Finally, to aid in detecting events like dust devils, an additional on board computation will be done of the average and maximum of the RMS of a bandpass version of the pressure signal (between 0.025 Hz and 1 Hz), downsampled to 0.001 Hz. All of these computed signals will be in the continuous data stream, to aid in selecting events in this low data volume case.

4.2.3.5   Calibration

There are no means of calibrating the PS after launch or at the surface of Mars. Because the sensor does not respond below pressures of about 560 Pa, the vacuum of deep space during cruise will not be useful for calibration. The pressure sensor was calibrated using a Mars atmosphere simulation test

chamber at JPL. This chamber was capable of modulating the pressure in the chamber up to frequencies approaching 1Hz. The PS transfer function was flat up to 1Hz, but theoretical predictions will have to be used to estimate the transfer function between 1Hz and the Nyquist frequency of 10Hz.

4.2.4 InSight Flux Gate (IFG)

4.2.4.1   Introduction

The IFG is a three-axis fluxgate magnetometer manufactured by UCLA, located beneath the lander platform on the main lander body (see Figure 4.2.1-1). It will measure the magnetic field vector in addition to the temperature of the sensor. The magnetic field measured by IFG consists of contributions from naturally occurring sources (Mars' fields) and magnetic fields generated by the lander.   The main purpose of the IFG is to enable removal of the effects of the local magnetic fields (irrespective of their origin) on the SEIS recordings.

4.2.4.2   Science Objectives

The IFG's prime function is to provide magnetic field data for decorrelation of the SEIS signals and will run continuously, recording data at a sufficiently high rate to aid SEIS investigations (see section 4.1.6). It will also contribute to InSight science by providing the first surface measurements of Mars' magnetic field. As such it will provide a record of the time-varying Martian magnetic field in the vicinity of the lander. IFG data are expected to contribute to understanding of the ionosphere including its coupling to the neutral atmosphere and the interaction with the solar wind, and on the interior structure of Mars. Naturally occurring sources include contributions from the ionosphere, crustal fields and possibly induced fields. The magnetic field from crustal magnetization provides indirect information on crustal properties such as magnetic mineralogy and thermal structure (e.g., Purucker, 2000; Arkani-Hamed, 2002a,b; Langlais et al., 2004; Morschhauser et al., 2014). Induced magnetic fields, if observed and characterized, can constrain interior electrical conductivity (Verhoeven et al., 2005). Data from Mars Global Surveyor (MGS) and MAVEN characterize the external magnetic field above and within the ionosphere. At MGS mapping orbit altitudes, above the ionosphere, the power spectrum falls off as 1/f for periods of 1 to 300 seconds (Mittelholz et al., 2014). It is uncertain whether this variability propagates to the ground.   For example, aerobraking orbits on Venus Express and on MGS all show weaker magnetic field variations below the ionosphere than within the ionosphere. The science objectives can leverage and are complementary to MAVEN science.

4.2.4.3   Instrumentation

The fluxgate magnetometer consists of two units, a sensor mounted under the deck on the side facing the SEIS deployment and an electronics unit housed with the Auxiliary Payload Electronics on the upper deck. The electronics board is 14 x 10 x 1.4 cm and weighs 101 g. The sensor measures 7.5 x 7.4 x 5.2 cm and weighs 171 g. These are connected by a harness of 2.5 m length of mass 286 g. Figure 4.3.4.3-1 shows the sensor with its pigtail and the electronics unit that powers the sensors, measures the magnetic field and transmits these values to the spacecraft telemetry system.
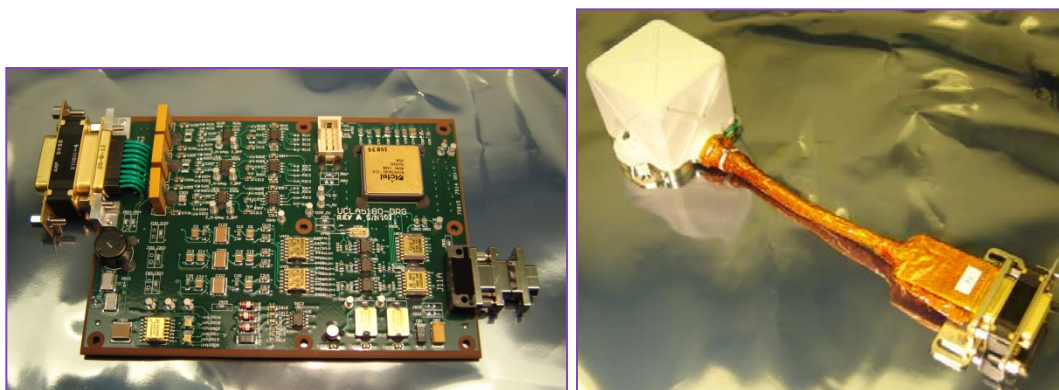

Figure 4.2.4.3-1: (Left) the IFG electronics and (Right) the IFG sensor inside its dust cover
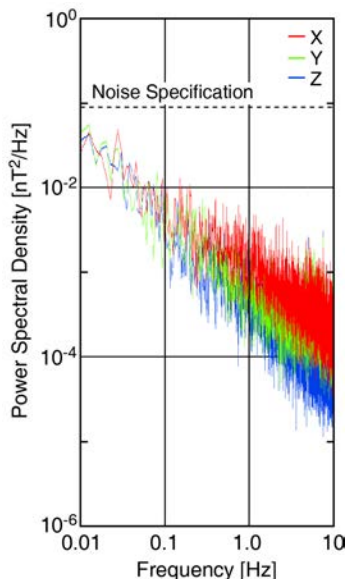
Figure 4.2.4.3-2: Noise in each axis as a function of frequency for the IFG instrument. X-axis noise is in red, y-axis in green, and z-axis in blue.

The IFG is designed to operate constantly throughout the mission, only being turned off in case of low power availability. The IFG sensor is sampled with the IFG electronics using a sigma-delta modulator for high-resolution analog-to-digital conversion (ADC). The sigma-delta ADC produces an 8.192 MHz, 1-bit, pulse density modulated bit stream to the Field Programmable Gate Array (FPGA). In the FPGA, the data stream goes through a Cascaded Integrator–Comb (CIC) filter, Correlation filter, and an Integrator to generate current field strength. This then goes through a block average that takes 400 samples to produce the final 24-bit, 20Hz output. This output is stored for later possible playback.

Typically during realtime transmission, on-board processing will filter and downsample this to a lower sampling rate continuous data stream, and provide a measure of energy in the magnetic field at frequencies above the continuously downlinked sampling rate. For the nominal downlink case (~38 Mbits/sol), the IFG sensor will return continuous data downsampled to 0.2Hz, and its temperature sensor will be downsampled to 0.02 Hz. Onboard processing will produce the total power in the three components of the magnetic signal above 0.1 Hz, which will be downsampled. This is expected to be indicative of high frequency magnetic variations above that resolved in the continuous pressure data, to allow identification of time intervals of magnetic events for which downlink of the full sampling rate data is desired. For magnetic events, the full 20 Hz data set from the IFG (or a downsampled version of it) can be downlinked for a short time interval (~30 minutes/sol).

4.2.4.4 Calibration

The magnetic field of the lander is unknown at the time of writing of the PIP, but will be characterized prior to launch via a series of tests that will provide information on the fields produced by time-varying power sources on the lander and the static field of the lander. It is anticipated that a major activity after deployment will be further characterization of the lander fields to enable separation of the naturally occurring Martian signals from those produced by InSight operations. Variation in gain and zero levels with temperature has been measured in the environmental chamber at UCLA and the instrument noise level and transfer function have also been measured.

4.3 Heat Flow and Physical Properties Probe (HP^3)

4.3.1 Introduction

The purpose of the HP^3 instrument is to determine geothermal heat flow at the landing site (Spohn et al., 2014), which is interpreted in terms of the global heat budget (Grott and Breuer, 2010, Dehant et al., 2012, Plesa et al., 2015). This measurement is augmented by a determination of the surface brightness

temperature using the HP³ radiometer (RAD) to determine the forcing function for the subsurface temperatures. To measure heat flow, a self-hammering mole will emplace a suite of temperature sensors and heaters (the TEM sensor suite) into the subsurface. The progress of the mole is monitored by the tether length monitor (TLM), which measures the length of tether being paid out, and the static tilt meter (STATIL), which determines the inclination of the mole with respect to vertical.
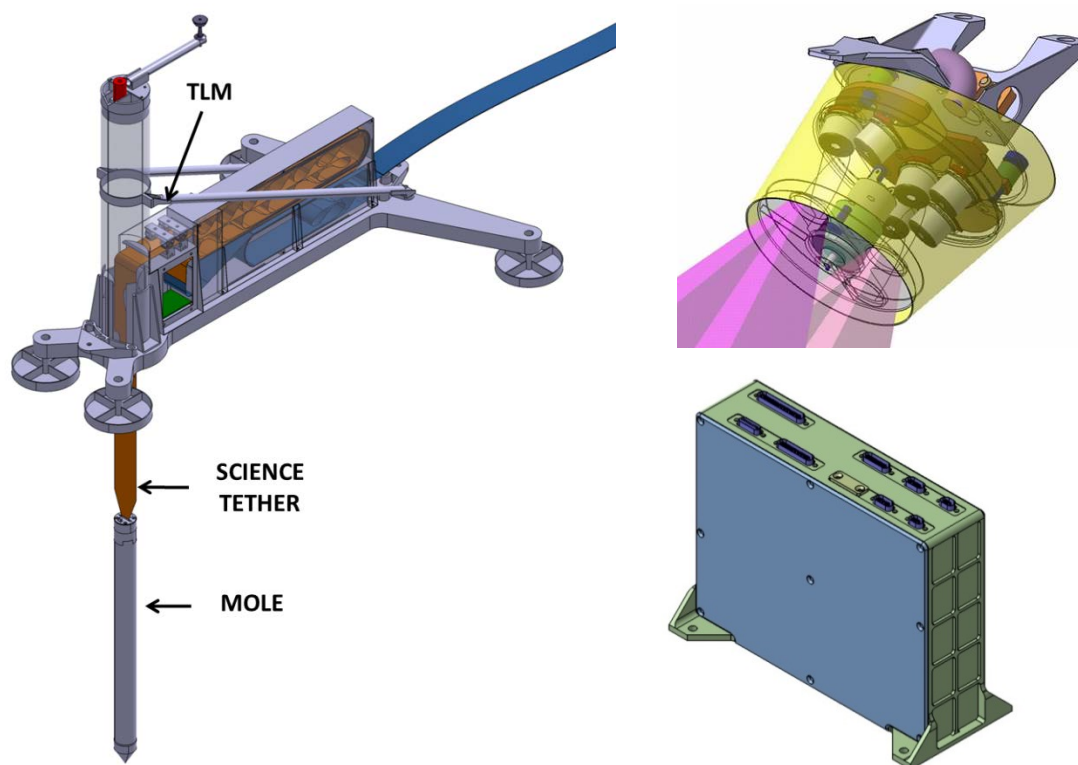

Figure 4.3.1-1: Left: HP³ Deployed Elements including the Mole, Science Tether, and Tether Length Monitor (TLM). Top Right: Radiometer, mounted under the lander deck, indicating the location of the six thermopile sensors and their respective fields of view. A/D conversion is done in the radiometer sensor head. Bottom Right: Backend electronics housing the circuitry for temperature (TEM) and tilt (STATIL) measurements.

The instrument consists of the following functional subunits:
- *Back End Electronics* (BEE), located in the lander warm electronics box
- *Engineering Tether*, electrical connection between the Support System and the BEE
- *Support System* (including TLM, the science tether, and the mole), which will be deployed onto the surface
- *Science Tether* (TEM-P), which will be emplaced into the ground by the mole
- *Mole* (including TEM-A and STATIL)
- *Radiometer* (RAD), which is mounted under the lander deck

The main hardware elements are shown in Figure 4.3.1-1, where the deployed elements of HP³ (Mole, TLM, and Science Tether) are shown in the left panel, whereas the lander mounted elements (RAD and BEE) are shown in the right panel.

A functional block diagram of the instrument is shown Figure 4.3.1-2, where science sensors are indicated in yellow. TEM-A thermal conductivity sensors as well as TEM-A temperature sensors are operated from the BEE, routing the signals through the engineering and science tethers. In this way, thermal disturbance of the regolith is kept at a minimum while operating these subsystems. The same approach is followed for the STATIL and TLM systems, where analog to digital conversion is also

performed by the BEE. On the other hand, the radiometer does have A/D conversion electronics integrated in the sensor head, having a purely digital interface to the BEE.
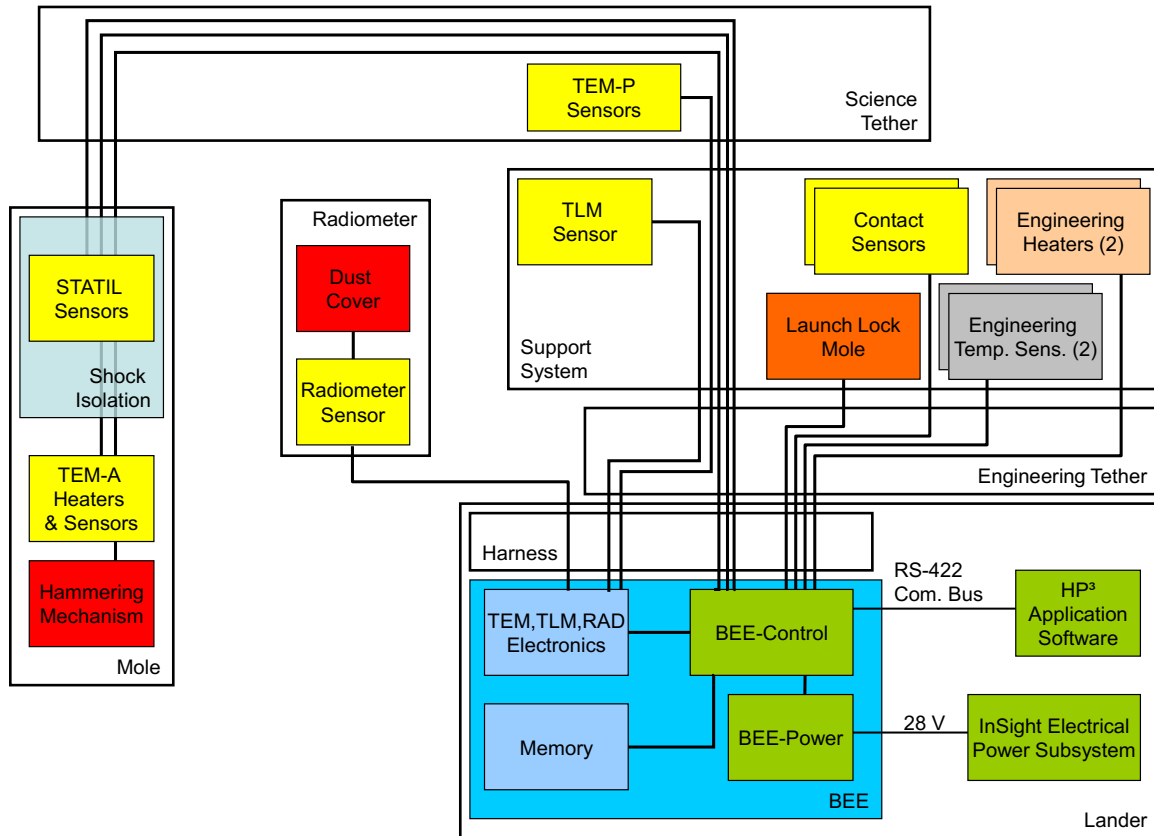

Figure 4.3.1-2: Functional block diagram of the HP^3 instrument indicating the lander mounted BEE, the engineering tether connecting the BEE to the deployed elements, the support system, the science tether, and the mole. Sensors are indicated in yellow, whereas mechanisms are indicated in red. Software and power interfaces are indicated in green.

4.3.2 Science Objectives

4.3.2.1 Heat Flow Determination

The level 1 science objective of the HP^3 experiment is a determination of the surface heat flow *F* at the landing site with an uncertainty of better than ±5 mW m^{-2} (see Grott et al., 2015). Heat flow, or to be more precise the heat flux density, is generally assumed to be one-dimensional from a planet as first approximation, and is given by the 1-D form of Fourier's Law (e.g. Grott et al., 2007, Kömle et al., 2011) where the negative sign is commonly omitted for convenience:

$$F = k \frac{\partial T}{\partial z}$$

Here, *k* is the regolith thermal conductivity, *T* is temperature, and *z* is depth. HP^3 measures temperature *T* using the TEM-P PT100 resistance temperature detectors (100 Ω at 0°C platinum resistance temperature sensors), depth *z* using the inclinations determined by STATIL and length determined by TLM, and thermal conductivity *k* using a the TEM-A temperature sensors and heaters (e.g., Kömle et al., 2011).

4.3.2.2 Surface Brightness Determination

The HP^3 Radiometer (RAD) will measure the surface brightness temperature of the Martian regolith inside its field of view with an uncertainty of better than 4 K. From these measurements, the shape of the forcing function for subsurface temperature fluctuations shall be determined. In addition, measurements

of surface brightness temperatures will allow for a determination of the surface thermal inertia at the landing site.

4.3.3 Detectors

4.3.3.1 Science Tether Temperature Measurements

HP^3 measures the subsurface temperature gradient using PT100 sensors mounted on the science tether. The distribution of temperature sensors along the tether varies with length as shown in Figure 4.3.3.1-1. Sensors are stacked more closely towards the mole to increase the number of sensors unaffected by the annual temperature wave. At the same time, sensors near the surface can be utilized to determine the thermal diffusivity of the regolith from an analysis of the attenuation of the annual temperature wave as a function of depth.
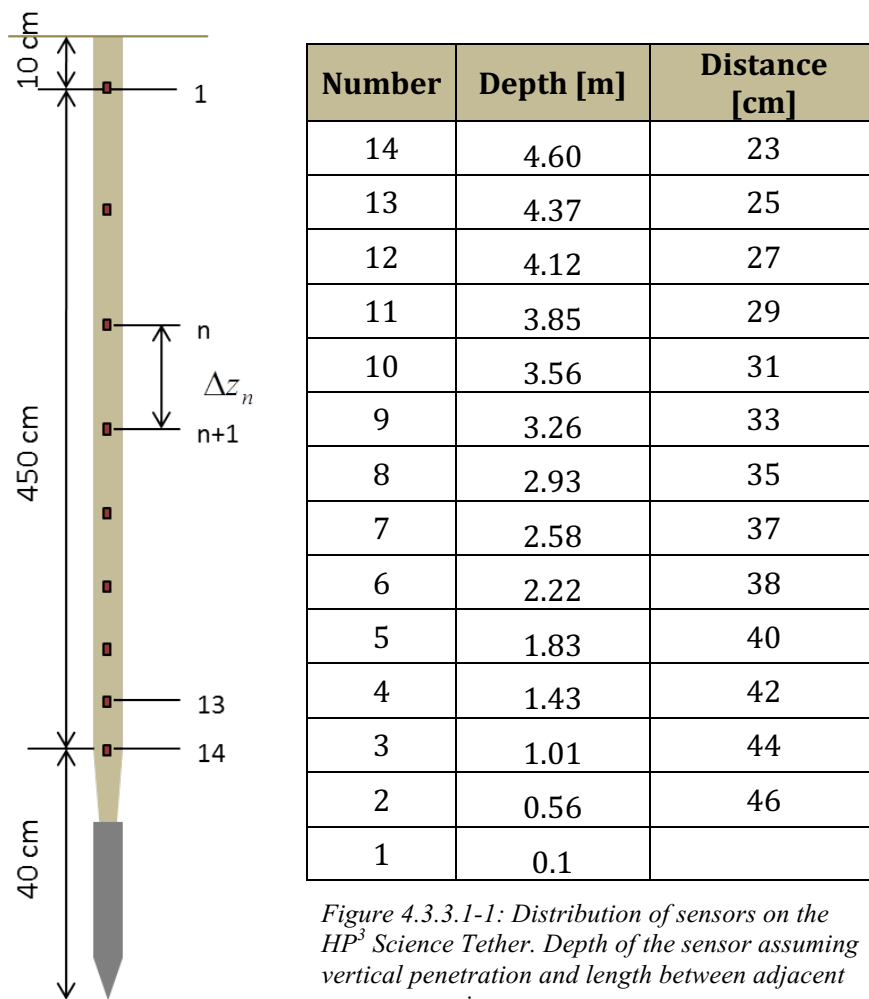
Number	Depth [m]	Distance [cm]
14	4.60	23
13	4.37	25
12	4.12	27
11	3.85	29
10	3.56	31
9	3.26	33
8	2.93	35
7	2.58	37
6	2.22	38
5	1.83	40
4	1.43	42
3	1.01	44
2	0.56	46
1	0.1	

Figure 4.3.3.1-1: Distribution of sensors on the HP^3 Science Tether. Depth of the sensor assuming vertical penetration and length between adjacent sensors are given.

4.3.3.2 Tether Length Measurement

The length of extracted tether is determined by optical sampling of position codes on the science tether by the tether length measurement system (TLM) operated always during Mole release and Mole operation.

4.3.3.3 Mole Tilt Measurement

The STATIL subsystem uses two Dual-Axis Accelerometers to determine the attitude of the HP³ mole in reference to the planetary gravity vector. It is used together with the TLM to determine the path and depth of the mole in the Martian subsurface. Signal output is a voltage that is proportional to the angle of

the mole vs. the gravity vector. The accelerometers are mounted on two PCBs in the rear of the mole that are attached to a sled made of stainless steel. In nominal working position the longitudinal axis of the sled is equal to the hammering axis of the mole.

The shape of the sled and mounting orientation of the sensors has been designed such that the sensors yield maximum signal. Therefore the sensor PCBs are almost perpendicular to the hammering axis. For redundancy two sensors have been used. The accelerometers that form each pair are mounted at 45° to each other; each pair of accelerometers has an 80° tilt from the mole axis to provide the highest sensitivity measurement position within the range of the deployment angle of HP³.

The selected STATIL sensors are dual-axis ADXL203 accelerometers built by Analog Devices. These are high precision, low power, complete dual-axis accelerometers with signal conditioned voltage outputs, all on a single, monolithic IC. The STATIL subsystem is connected to the HP^3 BEE via the Science Tether, the Support Structure and the Engineering Tether. To decrease the influence of electronics noise, a low-pass filter is implemented in the BEE. One filter is used for every analogue STATIL signal and voltages are converted using 24-bit analog-to-digital converters. The BEE is able to trigger on STATIL signatures caused by hammer strokes. The trigger level is adjustable.

4.3.4 Thermal Conductivity Measurement

HP^3 measures thermal conductivity by using the mole as a modified line heat source. This approach consists of injecting a known amount of heat into the probe and measuring the probe's self-heating curve.
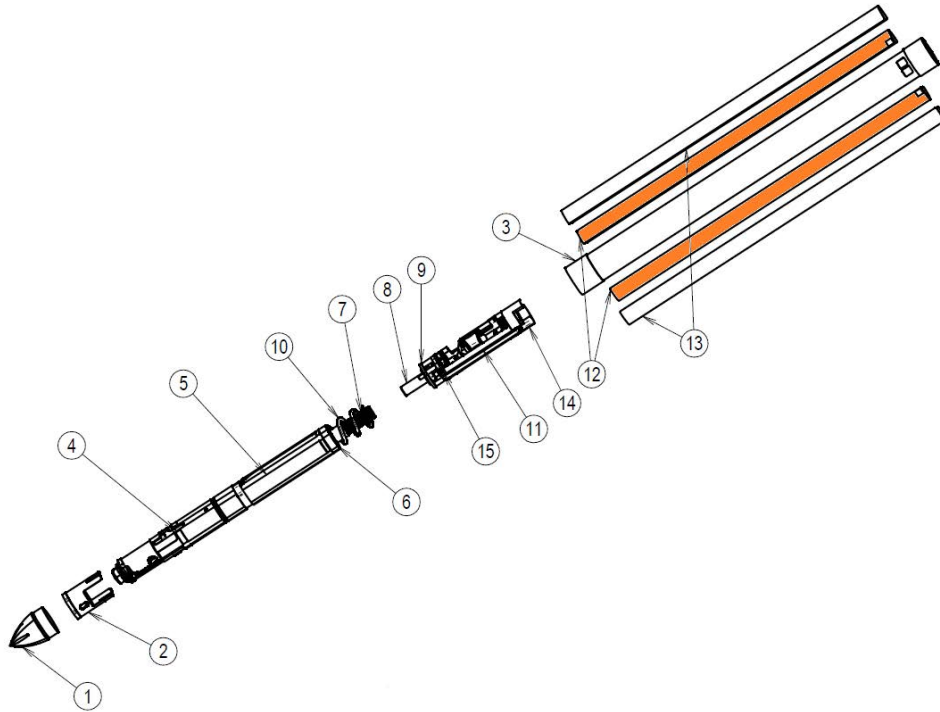
Figure 4.3.4-1: Expanded view of the mole, indicating the TEM-A heating foils (12) in orange. The foils are glued to the mole outer casing (3) and protected against abrasion by the TEM-A covers (13). Other parts refer to the hammering mechanism and STATIL assembly.

For a finite length cylinder such as the mole, the heating curve takes the form

$$\Delta T = C_1 \ln(t) + C_2$$

where *t* is time, and the constant C_1 is primarily a function of heating power and regolith thermal conductivity, while C_2 is a function of the probe's heat capacity and the contact conductance between probe and regolith. Therefore, thermal conductivity can be determined from

$$C_1(k, Q) = \frac{\partial \Delta T}{\partial \ln(t)}$$

by direct numerical simulations if the heating power is known. The TEM-A heaters are Kapton based copper heaters that are glued to the outer casing of the mole and protected against abrasion by aluminum covers. Due to the large temperature coefficient of resistance of copper, the heaters simultaneously act as temperature sensors, and the TEM-A electronics inside the BEE measures the heating power Q as well as the resistance of the heaters to determine the self-heating curve as a function of heating power.
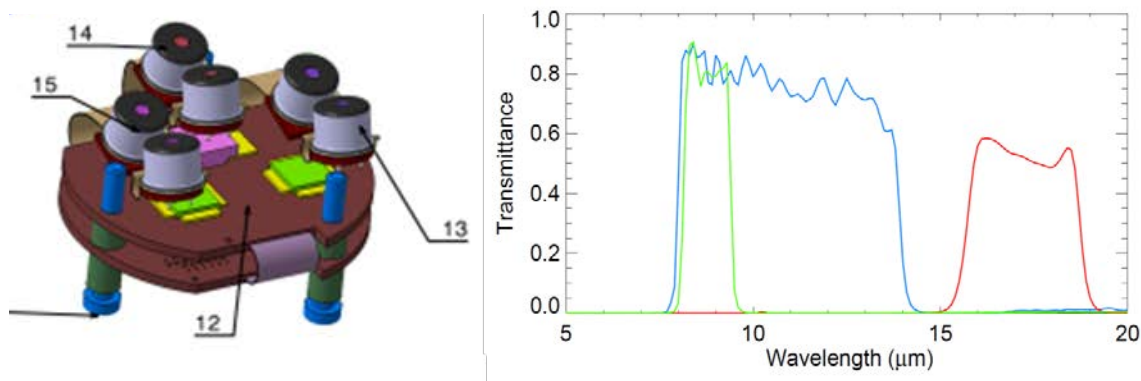
4.3.5 Radiometer (RAD)

Figure 4.3.5-1: Left: PCB and sensor assembly of the RAD. Six thermopile sensors (13, 14, and 15) are accommodated, and each filter wavelength is used with 2 sensors. Right: Transmittance of the three spectral filters multiplied with the spectral absorbance of the thermopiles. Blue: 8-14 µm bandpass, green: 7.8-9.6 µm bandpass , red: 16-19 bandpass.

The radiometer measures surface brightness temperatures using TS 72 thermopile sensors from the Institute of Photonic Technology, Jena, Germany (see http://www.ipht-jena.de/fileadmin/user_upload/redaktion/pdf/Datenblaetter/TS-72-2011-10-28.pdf). The sensors consist of an IR filter and absorbing surface, which is in radiative equilibrium with the target surface in the instrument's field of view. The temperature of the absorbing surface is determined using Bi0.87Sb0.13/Sb (Bismuth-Antimony) thermopairs with an electro-motive force of EMF = 135 µV/K. The absorber area is 0.2 mm2. The generated thermal voltage measures the temperature difference between the junctions of the thermocouples, which in turn is a measure for the net radiative flow of heat between absorber and target.

Sensors are mounted such that 3 thermopiles cover two fields of view each. PT100 sensors mounted inside the sensor housing measure the cold junction temperature. Therefore, a total of 12 signals are recorded: 6 thermopile voltages corresponding to 3 bandpass filters in two fields of view each, and 6 corresponding cold-junction temperatures measured by PT100 sensors.

The fields of view (FOV) are geometrically limited by the sensorhead apertures to 20°. In addition to that a calibration target obscures a part of this 20° circular FOV view. Its temperature provides part of the thermopile signal and is measured by another PT100 sensor. As in the Remote Sensing Mast Ground Temperature Sensor (REMS-GTS0) radiometer on MSL, a calibration target is partially in the FOV. The FOV is in effect reduced by 30% in solid angle. The temperature of the calibration target is controlled by a heater and PT100 temperature sensors.

The sensors and optical apertures are mounted to the lander such that the three sensors have their boresights pointed downward at 55° relative to the lander deck plane (FOV1), and the other three sensors at 25° relative to the lander deck plane. Figure 4.3.5-2 shows the location of the footprints for the nominal case, when the lander deck is not tilted relative to the surface and the solar panels oriented east-west and the instrument deployment workspace to the south. The azimuth of the RAD FOVs is in this case 20° west of north.
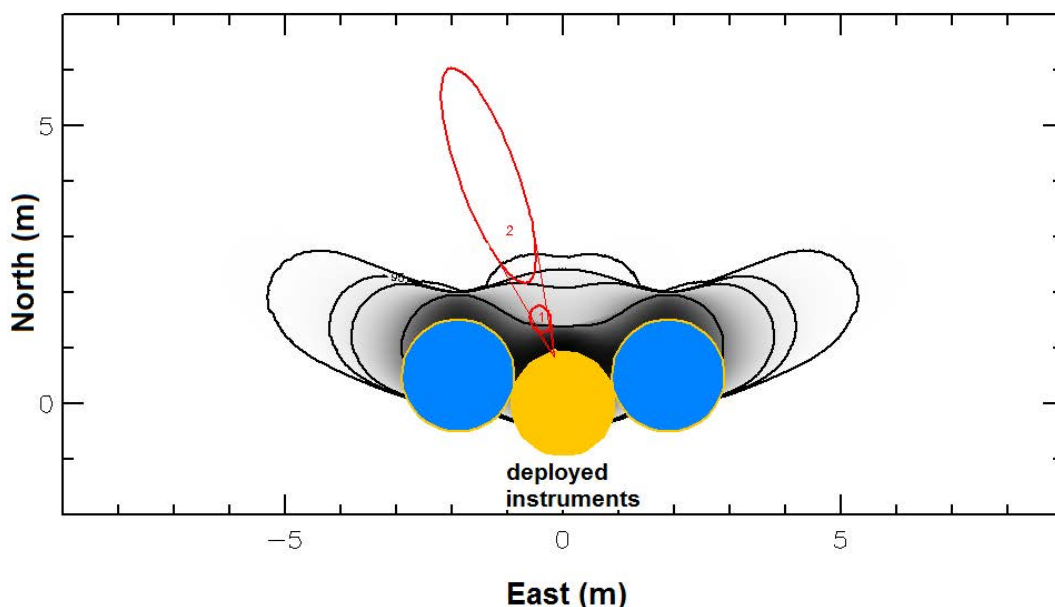
Figure 4.3.5-2: Location of nominal RAD footprints relative to the lander (yellow: deck, blue: solar panels) and its shadow during the landing season plotted as relative loss of daily insolation in grey. The isolines from the outer to inner correspond to 99%, 95%, 90% and 50% of the direct insolation without the lander. The HP^3 mole and SEIS will be deployed south of the lander. The radiometer points to the north. The calibration target further limits the FOVs of the radiometer towards nadir and horizon relative to the figure.

4.3.6 Science Tether Temperature Measurements

TEM-P measures temperatures using 14 PT100 temperature sensors, which are distributed over the entire length of the Tether. Sensors are read by the HP^3 BEE by sourcing current and measuring the voltage drop over the sensor elements in a 4-wire (Kelvin Method) configuration. Two redundant measurement circuits are used. PT100 sensors are alternately routed to one out of two ADCs, such that all even numbered PT100 are measured by one ADC and all odd numbered sensors by a second ADC.

The ADC is operated at an oversampling rate of 4.8 kHz, and values are averaged in a field programmable gate array to one sample. Typically, 600 samples are taken per channel, the first 88 of which are discarded to avoid transient effects after switching of a multiplexer channel. The 512 remaining samples are then again averaged to one value. Sampling all channels of the ADC then takes 2s, and this measurement includes the nominal and offset voltages.

4.3.7 Instrument Operation

4.3.7.1 HP^3 Operations

During deployment, SEIS will be deployed from the lander deck to the surface, followed by its wind and thermal shield, followed by HP^3 (see Section 5.2). The instruments will be deployed on the south side of the lander. If the terrain within the deployment zone permits, HP^3 will be deployed 1 m from SEIS and up to 2 m from the lander. The rock or slope distribution within the landing zone could cause a departure from this nominal configuration.

After deployment of the instrument onto the surface of Mars by the InSight robotic arm, operations of the HP^3 instrument is split into two main mission phases:

1. The penetration phase
2. The monitoring phase

During the penetration phase, the HP^3 mole will hammer itself into the subsurface, trailing behind the science tether, which is equipped with temperature sensors to measure the thermal gradient. At intervals

of 50 cm, hammering will be interrupted, and the heat introduced into the regolith will be allowed to dissipate for a period of at least 2 days. After this time, a TEM-A measurement will be performed, and the thermal conductivity of the regolith will be determined. Heating times for the TEM-A measurement will be up to 24 h to sample a volume of regolith away from the mole. After the conductivity measurement, hammering will be resumed until the next stop. In this way, a profile of thermal conductivity at the landing site will be compiled. During the penetration phase, 10 stops and measurements are planned. The timeline for this mission phase is schematically illustrated in Figure 4.3.7.1-1.

Progress of the mole is continuously monitored by the STATIL tilt meters and TLM, which measures the length of paid out science tether. Taken together, this information uniquely determines the mole path and depth, from which the depth of individual temperature sensors can be derived.

After reaching the final depth, which is limited to 5 m by the length of the tether, but might be smaller depending on the penetration performance of the mole, HP^3 enters the monitoring phase. During this mission phase, HP^3 takes periodic temperature measurements using the sensors on the tether. Readings are to be taken during 5 min every hour, and values are averaged to yield a sampling of the subsurface temperature field every hour to the end of mission.
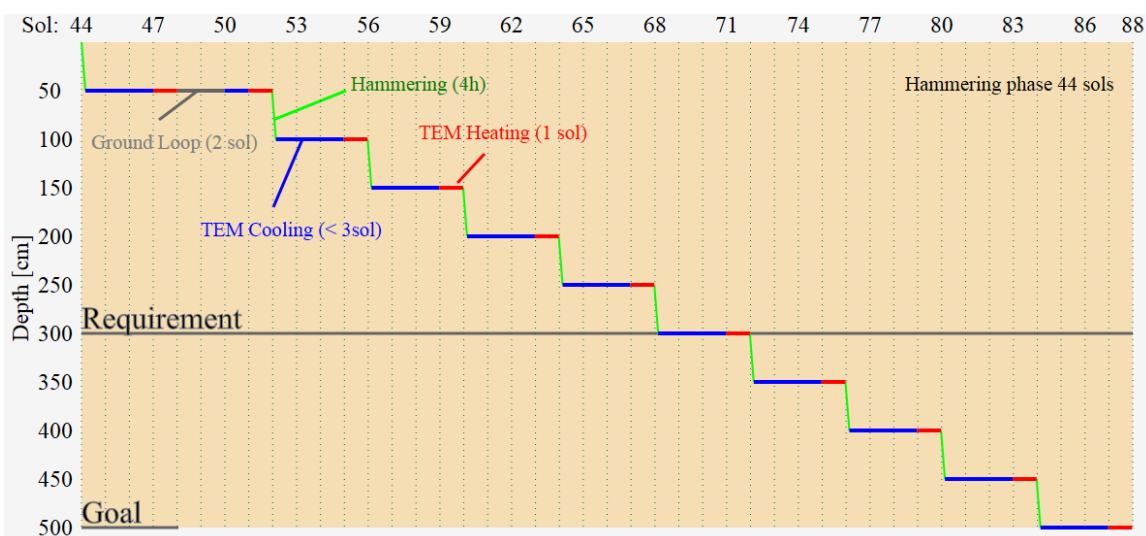

Figure 4.3.7.1-1: Operations of the HP^3 instrument after deployment. Phases of hammering, cooldown, and thermal conductivity measurements (TEM-A) are indicated.

4.3.7.2   RAD Operations

The radiometer typically operates in one of four modes, which determine the timing of measurements and temperature of the instrument.

1. The 'Hourly' mode acquires 24 measurements per sol, each 20 samples over 5 min. This mode is run for at least one sol within each interval of 29 sols.
2. The 'Standard' mode acquires 4 measurements per sol, each 20 samples acquired over 5 min. This mode is run continuously unless there is another mode or the radiometer has to remain off due to power/energy constraints.
3. The 'Single' mode is equivalent to a single observation of the standard mode. After entering the mode the radiometer warms up to one of the calibration points, equilibrates for 1 hour and then acquires 20 samples over 5 min. Timing of telecommand execution, and telecommands to adjust the sampling rate (up to 0.5 Hz), equilibration duration and measurement duration are available to allow for flexible observations of events that are expected to occur at certain times of the day, such as eclipses and shadows moving into the FOV.
4. Calibration mode acquires 6 measurements in 6 h, each with 100 samples, while changing the calibration target temperature.

Modes 1 and 2 run continuously until commanded to idle. In these modes the measurements are within a few minutes synchronized with local true solar time. For standard mode the four measurements are planned for approximately 2 am, 5 am, 2 pm, and 5 pm local time. It is possible to measure at other specified times of the day using the 'Single' mode (see above).

The radiometer sensor head is temperature stabilized using heaters, and as thermopile sensitivity is a function of temperature the instrument is operated at pre-launch calibrated setpoints. As no cooling is performed, the radiometer temperature must be above the ambient temperature for efficient cooling to the environment. To reduce energy consumption and measurement uncertainty the radiometer temperature control is adjusted to the diurnal cycle. There is one setpoint for night (T_{night} = -35°C) and one for day (T_{day} = -5°C). A third temperature setpoint (T_{hot} = 25°C) is used instead of T_{day} if the environment is unexpectedly warm.

The switch from the night to the day/hot day setpoint occurs at approximately 9 am local true solar time in the hourly mode, and between the am and pm measurements in the standard mode. The switch from day to night temperature setpoint occurs at approximately 7 pm local true solar time in the hourly mode and between the pm and the am measurements in the hourly mode. In the single and calibration mode one of the three temperature setpoints is selected upon entering the mode.

The temperature of the calibration target/dust cover is stabilized at the same temperature as the sensorhead body for the 'Hourly', 'Standard' and 'Single ' modes. During the 'Calibration' mode the target temperature is varied relative to the sensorhead body.

4.3.8 Calibration

4.3.8.1   Science Tether Temperature Sensor Calibration

HP[3] temperature sensors are calibrated using a comparison calibration approach, in which the science tether, including the PT100 sensors, is exposed to a controlled temperature environment, whose temperature is simultaneously monitored by a calibrated reference sensor. All measurements are executed using a 4-wire (Kelvin) resistance measurement.

The error budget for the calibration takes into account contributions from the measurement electronics, as well as contributions from the thermal setup. Major factors controlling the error budget are the homogeneity and stability of the calibration bath, the calibration uncertainty of the reference thermometers, as well as the fitting residuals with respect to the Callendar-van Dusen equation. Contributions from the electronics are generally small. In total, the 1-sigma confidence interval for the calibration uncertainty of the HP[3] PT100 sensors is 12 mK.

4.3.8.2   Tether Length Measurement Calibration

The TLM measures relative and absolute tether length codes and does not need to be calibrated.

4.3.8.3   Mole Tilt Measurement Calibration

For calibration, the STATIL accelerometers are mounted flat on a 3D rotation table. The rotation table is then rotated in 0.5° increments along the gravity vector to determine the sensor characteristics and the min and max output of the accelerometers for the different axes. Values are recorded using the HP[3] BEE. The calibration is performed before STATIL assembly and integration into the HP³ mole. An in-flight calibration is not possible. The main goal of the calibration of the STATIL subsystem is to measure the minimum and maximum output voltage of each axis of each accelerometer under 1 g conditions.

4.3.8.4   Thermal Conductivity Sensor Temperature Calibration

The calibration procedure for the resistance vs. temperature calibration of the TEM-A foils follows the same reasoning as that of the science tether PT100 sensors and uses similar hardware. TEM-A foils are connected to the data logger using a 4-wire (Kelvin) measurement configuration. Calibration data is corrected for offset and gain. In total, the 1-σ confidence interval for the calibration uncertainty is 30 mK.

4.3.8.5   Estimated Total Heat Flow Uncertainty

As stated above, heat flow, F, is a function of thermal conductivity, k, and thermal gradient, $\partial T/\partial z$, and is given by:

$$F = k\frac{\partial T}{\partial z} = k\frac{\theta}{L}$$

The thermal gradient is determined from a measurement of the temperature difference between different sensors, θ, and their vertical separation, L. Thermal conductivity is determined from a line-heat source method by providing a known power to the probe and measuring the temperature rise. It is given by:

$$k = \frac{q}{4\pi m C_1}$$

where q is the heating power per unit length provided to the mole, which is given by:

$$q = \frac{RI^2}{l_{Mole}}$$

Here, R is the resistance of the heating foils, I the heating current, and l_{Mole} is the length of the mole. The logarithmic temperature rise m of the probe is given by:

$$m = \frac{dT}{C_1 d\ln(t)}$$

A thermal mole model adapts the ideal line-heat source method to the mole geometry, and is verified by tests, which provide the scaling for C_1 given by $\Delta T = C_1 \ln(t) + C_2$. In total, the measurement induced heat flow uncertainty is then given by:

$$\left(\frac{\Delta F}{F}\right)_{meas} = \sqrt{\left(\frac{\Delta m}{m}\right)^2 + \left(\frac{\Delta q}{q}\right)^2 + \left(\frac{\Delta \theta}{\theta}\right)^2 + \left(\frac{\Delta L}{L}\right)^2}$$

In addition to the measurement errors themselves, heat introduced into the regolith by the HP[3] experiment influences the retrieved heat flow. The three sources of HP[3] induced errors are:

1. Mole induced heat influences the thermal conductivity measurement by influencing m
2. Mole induced heat influences the thermal gradient measurement by influencing dT between sensors
3. Short duration (less than 1 Martian year) measurements add uncertainty to the determination of the average annual temperature at each sensor.

Gaussian error propagation for these errors then results in the final error budget:

$$\left(\frac{\Delta F}{F}\right)_{tot} = \sqrt{\left(\frac{\Delta F}{F}\right)_{meas}^2 + \left(\frac{\Delta F}{F}\right)_{cond}^2 + \left(\frac{\Delta F}{F}\right)_{grad}^2 + \left(\frac{\Delta F}{F}\right)_{dur}^2}$$

In total, for a nominal heat flow at the landing site of 20 mW/m^2, the error budget given in Table 4.3.8.5-1 is obtained, and a total error of 3.3 mW/m^2 is estimated.

Table 4.3.8.5-1: Error budget for a nominal planetary heat flow of 20 mW/m^2.

Error Source	Term	Dist.	1-σ Value	Cont.
Slope uncertainty TEM-A	$\Delta m/m$	norm.	2.5 %	2.5%
Heat input uncertainty TEM-A	$\Delta q/q$	norm.	0.1 %	0.1 %
Temperature difference uncertainty	$\Delta\theta/\theta$	norm.	5.3 %	5.3 %
Depth difference uncertainty	$\Delta L/L$	norm.	1 %	1 %
Heat input effect on TEM-A	$\Delta F/F_{cond}$	squ.	4.5 %	4.5/√3 %
Heat input effect on TEM-P	$\Delta F/F_{grad}$	squ.	2 %	2/√3 %
Annual wave error	$\Delta F/F_{dur}$	norm.	15 %	15 %
Total				**16.4 %**
Total [mW/m²]				**3.3**

4.3.8.6 Radiometer Calibration

The radiometer undergoes radiometric and geometric calibration prior to integration into the lander. The radiometric calibration was carried out under an atmosphere of 8 mbar Ar. As a calibration target, a cavity blackbody, type BB100 (Sapritzky et al., 2003) was used. The blackbody is temperature stabilized at temperatures of T_{BB} = 150K to 300K with an accuracy and homogeneity of ~50 mK. The blackbody cavity is open to the pressure vessel and the instrument is mounted to view into the cavity. The radiometer was

mounted inside a thermal shroud that was temperature controlled within the temperature range of expected Mars environment temperatures of $T_{shroud} =$ 150 K to 300 K.

The radiometer will be calibrated after landing to check for sensor drift. The inflight calibration consists of two measurement sequences, one of which will be executed during the night at the instruments nighttime setpoint (T_{night} = -35°C) and the other during the day (T_{hot} = +25°C). For each setpoint, the temperature of the calibration target will be varied to six setpoints. From these data, the sensitivity of the individual thermopile sensors will be derived.

4.4 Instrument Deployment System (IDS)

4.4.1 Introduction

The function of the IDS is to place the instruments safely on the surface of Mars. The IDS (Figure 4.4.1-1) consists of four main components. The Instrument Deployment Arm (IDA) is responsible for placing the instrument packages on the surface and provides pointing for the Instrument Deployment Camera (IDC). The IDC is mounted on the arm and is used to image the work area in stereo for deployment planning and secondary geologic science of the area surrounding the Lander. The Instrument Context Camera (ICC) provides a wide-angle view of the entire workspace and provides a degraded functional back up to the IDC. The ICC is mounted at the bottom of the Lander's deck, right underneath the base of the IDA. The last component is the IDS control software.
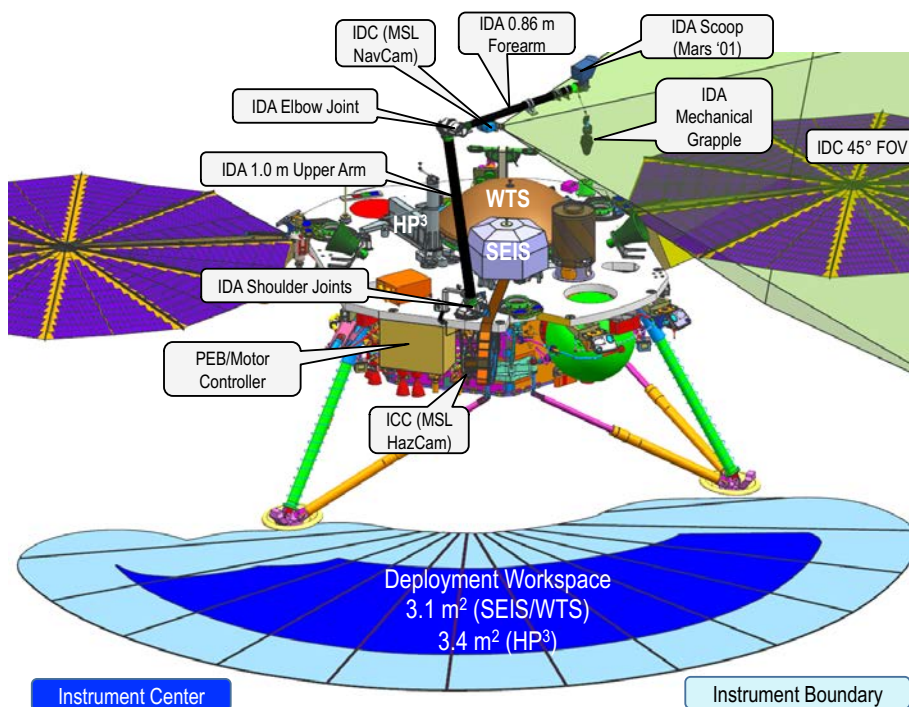
Figure 4.4.1-1: IDS before Instrument Deployment.

4.4.2 Instrument Deployment Arm (IDA)

The IDA is the flight arm from the original Mars '01 lander. The arm has been refurbished and rebuilt by JPL with some components replaced and delivered to LMA for integration onto the Lander. The various components of the IDA in deployed and stowed state are illustrated in Figures 4.4.2-1 and 4.4.2-2, respectively. The arm has been upgraded to include a mechanical grapple that will be used to pick up and deploy and place the instrument components. It preserves the scoop of the original Mars'01 arm with some modifications.

The IDA has four degrees of freedom (DoF). It can capture and retain deployable elements, including under loss of power, until placement on the surface is confirmed. It can lift a mass up to 9.5 kg and deploy

elements to the surface with the Lander deck tilted up to 15 degrees with respect to gravity. The maximum deployment torque occurs when SEIS (9.5 kg) is placed at the farthest reach of SEIS/WTS workspace (179 cm from the IDA base). The IDA actuators performance (motor plus drive train) was characterized, leading to torque ratings at 20° C of about 26 (max continuous) and 46 (max peak) N-m for the azimuth joint, 91 and 146 N-m for the elevation joint, 53 and 86 N-m for the elbow joint, and 10 and 15 N-m for the wrist joint. The Grapple is in the field of view of the IDC during capture and disengagement from deployable elements.
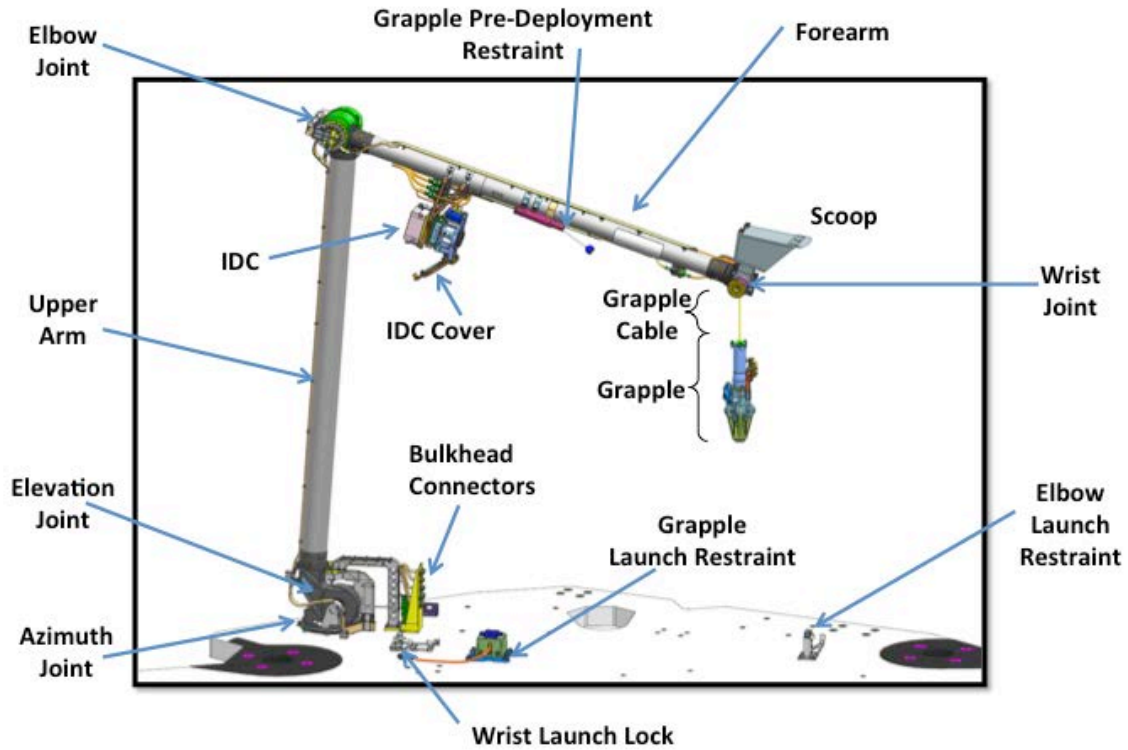
Figure 4.4.2-1: Deployed IDS Configuration Overview.
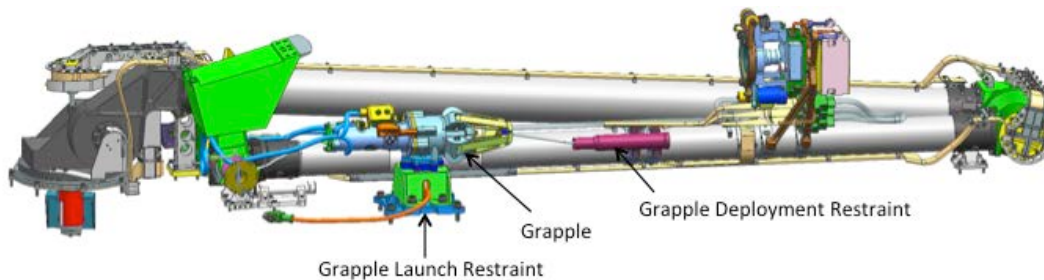
Figure 4.4.2-2: IDA and grapple stowed.

The grapple design is displayed in Figure 4.4.2-3. It hangs from the IDA such that its central axis is within ±1 degree with respect to the gravity vector. The grapple can engage the grapple hook on each deployable element (Figure 4.4.2-4) with up to 15 degrees misalignment and up to 15 mm of positioning error. Its minimum load capacity of 143.2 N when not powered and with its finger closed over a grapple hook. The grapple can be re-stowed against the arm after instrument deployment, which would remove the deployed grapple from the images acquired by the IDC.
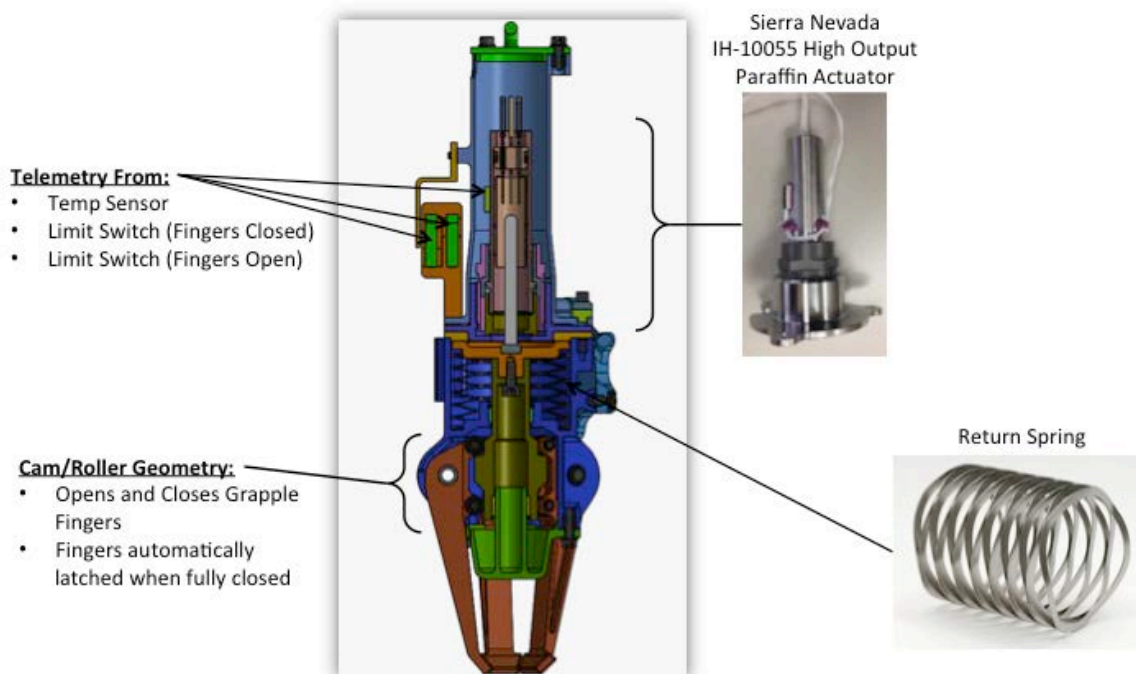
Figure 4.4.2-3: Grapple design.

The grapple is manipulated by the IDA such that it can engage, pick up, and deploy SEIS, WTS, and HP^3 to the Mars surface. The arm deploys the SEIS sensor head, WTS and HP^3 with a surface touchdown velocity of no more than 2.5 cm/sec. The IDA positions the grapple with an absolute error of less than or equal to 0.015 m and determines the IDC imaging baseline to within 0.0028 m. The IDS has the necessary information to localize deployable elements on the surface to within sub-mm accuracy via fiducials on the deployed elements imaged using the IDC stereo pairs. The coordinate frame of the IDS is illustrated in Figure 4.4.2-5.

Figure 4.4.2-4: Image obtained in JPL's IDS testbed of the grapple about to grab the WTS.

Figure 4.4.2-5: (Top) Spacecraft coordinate frame and (bottom) IDA or workspace coordinate frame.

The arm is controlled by software developed by JPL and delivered to LMA. The payload electronics box (PEB) houses the IDA motor controller and camera electronics. The IDA flight software is inherited from Phoenix. It provides the following capabilities: interface with external entities, including Lander Sequencer and IDA MC; motion control of the IDA; expanding high-level IDA commands i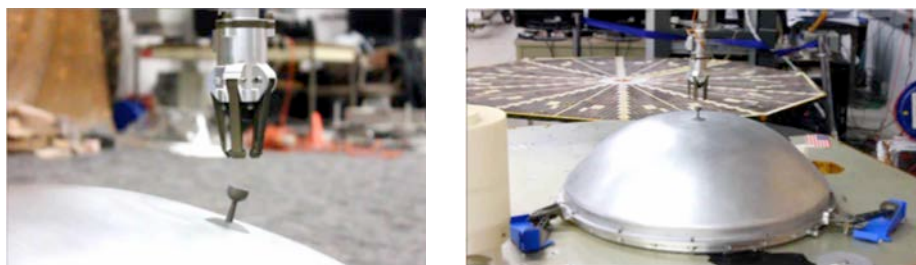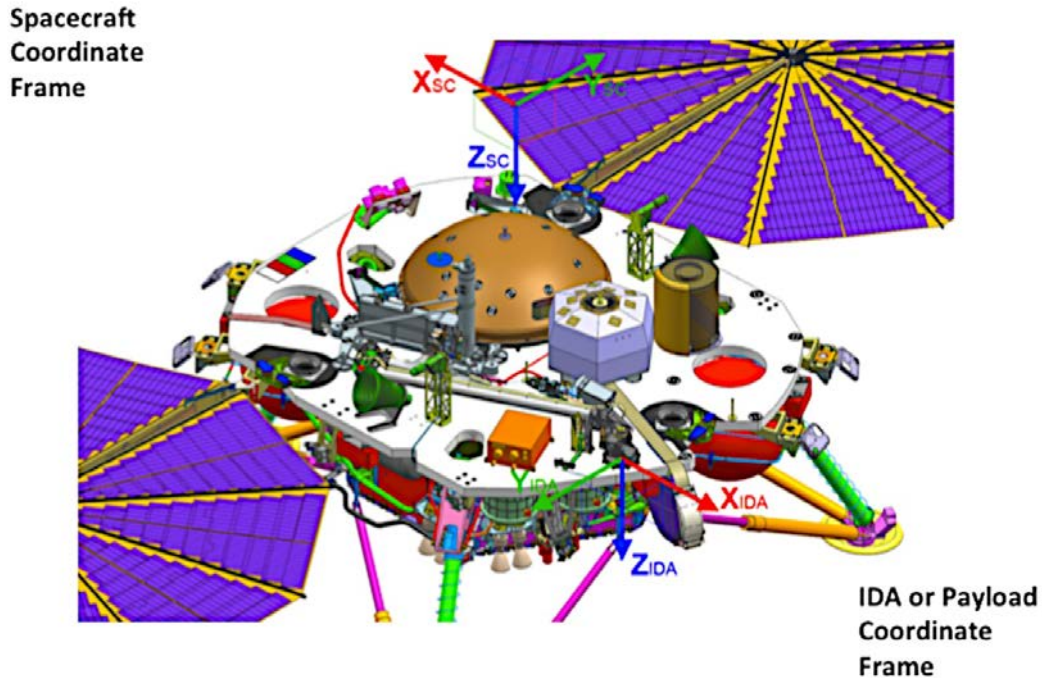nto low-level IDA-commands; fault sensing, recovery, and safing; prevention of collisions with the lander and lander-based instruments; provide visibility of IDA state in telemetry. The motor Controller is an inherited electronics assembly designed to control the four joint IDA and resides in its own enclosure, PEB, attached to PAE and resides in the spacecraft thermal enclosure.

Although the IDA is equipped with a scoop, soil mechanics studies with the IDA (and IDA ground contact) are not in the baseline plan and proposals based solely on this are not appropriate.

4.4.3 Instrument Context Camera (ICC)

The ICC is a wide-angle color camera that is hard-mounted to the lander (see Figure 4.4.1-1). The primary purpose of the ICC is to provide contextual views of the entire deployment area during all phases of instrument deployment (see Figure 4.4.3-1). The ICC will acquire the first image of the workspace on Sol 0 and will continue to monitor the workspace throughout the pre-and post-deployment stages of the mission. The ICC will also provide a backup means of imaging the atmosphere for dust optical depth determinations to assist in power predictions. The ICC is a flight spare MSL Hazcam with an upgraded Bayer color filter array detector. Table 4.4.3-1 lists the main characteristics of the ICC.

Table 4.4.3-1: ICC and IDC camera parameters.

Parameter	ICC Value	IDC Value
Horizontal Field of View (degrees)	124	45
Vertical Field of View (degrees)	124	45
Diagonal Field of View (degrees)	180	67
Pixel Field of View at image center (mrad/pixel)	2.1	0.82
Focal Length (mm)	5.58	14.67
f/number	15	12

| Readout Style	Frame transfer
Imaging area (pixels)	1024 × 1024
Pixel size (microns)	12 × 12
Gain (electrons/DN)	50
Full well capacity (electrons)	170,000
Digitization (bits/pixel)	12
System readout noise (electrons)	25

Figure 4.4.3-1. ICC image from the InSight testbed. The lander footpad can be seen in the lower right.

4.4.4 Instrument Deployment Camera (IDC)

The IDC is a narrow-angle color camera that is mounted on the forearm segment of the Instrument Deployment Arm (see Figure 4.4.2-1). The main purposes of the IDC are to provide detailed stereo views of the deployment area and to verify arm interactions with the instrument hardware (e.g., grapple, lifting, and placement). The IDC will also acquire images of the sky; these images will be used to determine the dust optical depth in the Martian atmosphere as a primary input to solar panel power modeling. The IDC is a flight spare MSL Navcam. Like the ICC, the IDC has been upgraded with a Bayer color filter array detector. Table 4.4.3-1 lists the main characteristics of the IDC.

After arm deployment, the IDC will image the lander feet, solar panels, payload deck, and deck fiducial targets (see Figure 4.4.4-1). The IDC will then be used to image the entire workspace in stereo at varying spatial resolutions; these images will be used to generate three-dimensional Digital Terrain Models (DTMs) of the deployment workspace (see Figure 4.4.4-2). Once the instrument placement sites are chosen, the IDC will image each site at a higher spatial resolution. During instrument deployment, IDC confirmation images will be acquired of the pre-grapple positions, grapple engagements, lifts, placements, and release of the instruments. A final IDC stereo pair will document the actual placement of the instruments. IDC stereo imaging of the SEIS instrument head assembly after placement and disengagement will also be used to determine its orientation (azimuth) on the surface. Although not

required for instrument placement, the IDC will likely be used to acquire a 360-degree panorama of the landing site as well as other images of the surface and atmosphere.
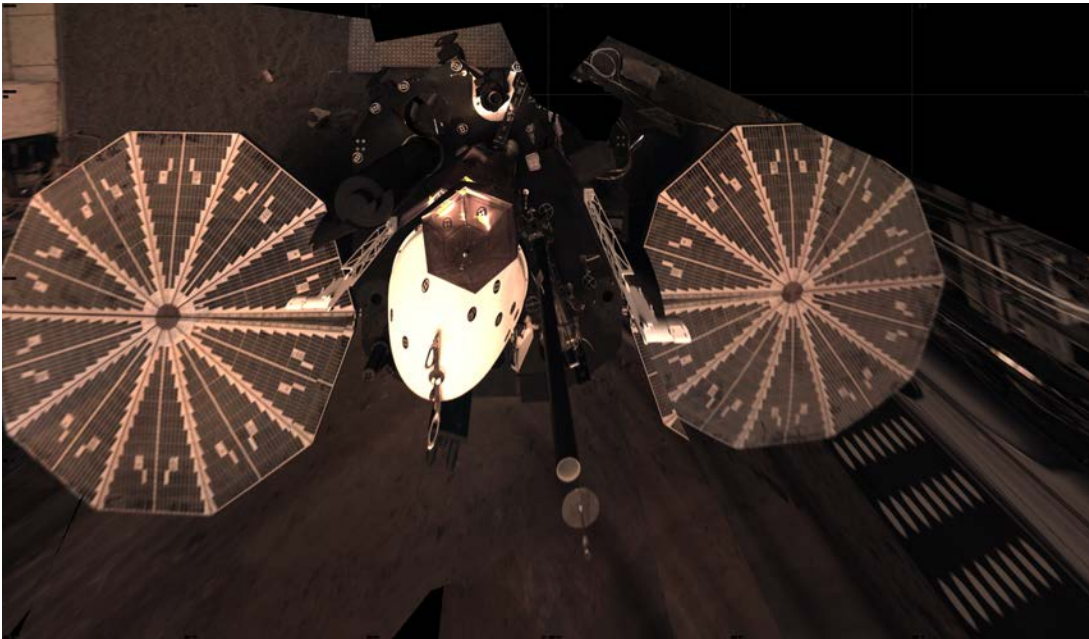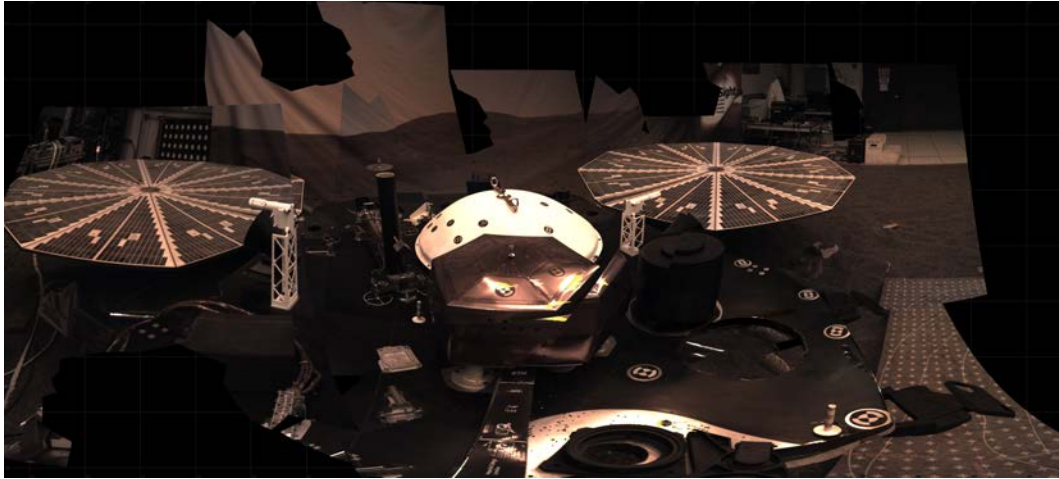
Figure 4.4.4-1: (Upper) Lander horizontal IDC mosaic and (Lower) Lander vertical IDC mosaic
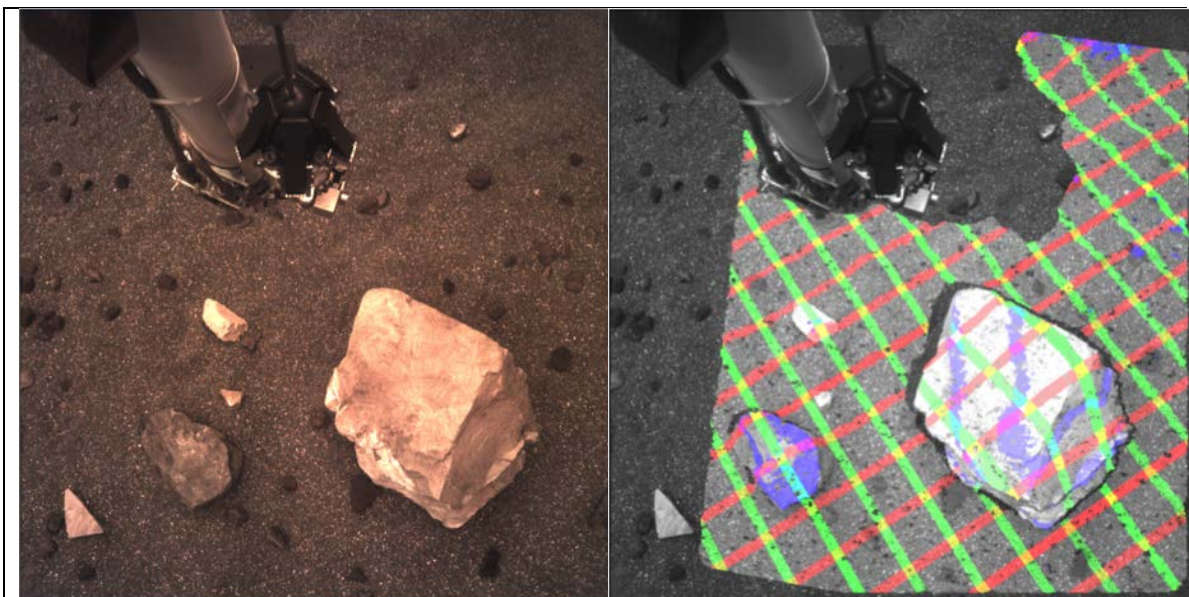
Figure 4.4.4-2. IDC image acquired in the Insight testbed (left). Corresponding 3-dimensional terrain shown as X (green), Y (red), and Z (purple) contours (right).

For more information on the IDC (Navcam) and ICC (Hazcam) hardware, see Maki et al. 2003 and Maki et al. 2012. Additional information on the MER/MSL camera hardware can be found in Bell et al. 2003 and Herkenhoff et al. 2003.

4.4.5 IDS Science

Although the IDS primary function is instrument deployment, a variety of scientific investigations can be carried out using the arm and/or cameras (see for example Arvidson et al. 2009 for experiments conducted with the arm on the Phoenix mission). Observation of the sky to derive atmospheric tau is one task that benefits both science and engineering through its affect on solar power. Additional investigations will be considered if they do not jeopardize instrument deployment and if resources such as power, downlink, and operations staff are available. For this reason, investigations based only on use of the arm, such as for soil mechanics, or imaging beyond the deployment phase (with the exception of tau measurements, which would not require arm movement) are not likely to be successful.

4.5 Rotation and Interior Structure Experiment (RISE)

4.5.1 Introduction

InSight's Rotation and Interior Structure Experiment (RISE) uses the Lander's X-band radio system in combination with tracking stations of the NASA Deep Space Network to estimate the precession and nutation of Mars in order to provide constraints on the Martian interior structure. The Martian axis of rotation precesses and nutates due to external torques, primarily due to the Sun. The precession rate is a key indicator of the density of the Martian core, while the nutation is sensitive to the state of the core; a fluid core results in a larger nutation amplitude. The Martian precession rate has been estimated earlier from Doppler data taken from the Viking and Mars Pathfinder landers (Folkner et al. 1997a) and from the Mars Exploration Rover (Kuchynka et al. 2014). InSight will provide an improved precession rate and the first detection of the nutation amplitudes by providing observations over one Martian year.

The RISE measurements are the two-way Doppler shift measured at the DSN stations of a radio signal sent by the DSN to InSight where the signal is detected and a coherent signal re-transmitted back to the DSN. Nominally, measurements will be made during one 1-hour tracking pass per week during the Instrument Deployment Phase and four 1-hour tracking passes per week during the Science Monitoring Phase.

4.5.2 Science Objectives

The RISE objective are to determine the Martian rate of precession, which is proportional to the polar moment of inertia of Mars, and the amplitude of the semi-annual nutation, which is a function of the polar moment of inertia of the core and the free-core nutation (FCN) rate (Folkner et al. 1997b; Le Maistre et al. 2012). The total and core polar moments of inertia in turn provide constraints on the density, state, and size of the core (Rivoldini et al. 2011).

The RISE measurements are also sensitive to changes in the Martian spin rate, that are driven primarily by seasonal redistribution of CO_2 between the atmosphere and the ice caps. These seasonal changes have been detected previously and compared with models (e.g. Konopliv et al. 2011). InSight will be more sensitive to these effects than previous missions. The changes in rotation rate will be determined during the planned data analysis to determine precession and nutation, but are not specific science objectives for InSight.

4.5.3 Instrumentation

As discussed above (Section 3.3), the InSight lander includes an X-band radio system for communication direct-to-Earth. The X-band radio system includes one Small Deep-Space Transponder (SDST), a Solid-State Power Amplifier (SSPA), and two fixed (non-steerable) Medium-Gain Antennas (MGA). The primary purpose of the X-band radio system is for two-way Doppler measurements for RISE, but also serves as a backup to the primary UHF data transmission to the MRO and Odyssey orbiters.

Two-way Doppler measurements are made at the DSN tracking station. The tracking station transmits an uplink signal to Mars at ~7.2 GHz. The uplink signal is received by one of the MGAs. A switch is used to select the appropriate MGA for a given tracking pass based on the time of the pass. The received signal is routed to the SDST that detects the signal and generates a return signal at ~8.4 GHZ that is coherent with the received signal. (The return signal frequency is 880/749 times the uplink frequency.) The signal output to the SDST is amplified by the SSPA and downlinked back to the DSN station. The DSN station measures the frequency of the downlink signal relative to the station clock used to generate the uplink frequency. The resulting Doppler measurement is delivered to the science operations team.

The two fixed MGAs limit the times of day on Mars that Doppler measurements can be made to times that Earth can be viewed within the 40° beamwidth of one of the MGAs. The landing system is designed for a known orientation, with the center of the beam pattern of one MGA pointed 15.5° south of east and the other MGA pointed 6° north of west, both with elevation of 30°. These directions are chosen to have view of Earth at low elevation as seen from the lander, when the sensitivity of the Doppler measurements to direction of the Martian spin axis is largest. Figure 4.5.3-1 shows the arrangement of the antenna patterns.

A landing error could cause a change in the rotation of the lander about the vertical (azimuth error) of up to 5°. A clockwise rotation as seen from above reduces the number of days that Earth is in view from either antenna, which gives somewhat worse results for RISE, while a counter-clockwise rotation gives better view periods. A tilt in the north or south direction causes negligible change in viewing geometry but can cause reduction in electric power available. A tilt in the east or west direction affects the minimum elevation Earth can be viewed.
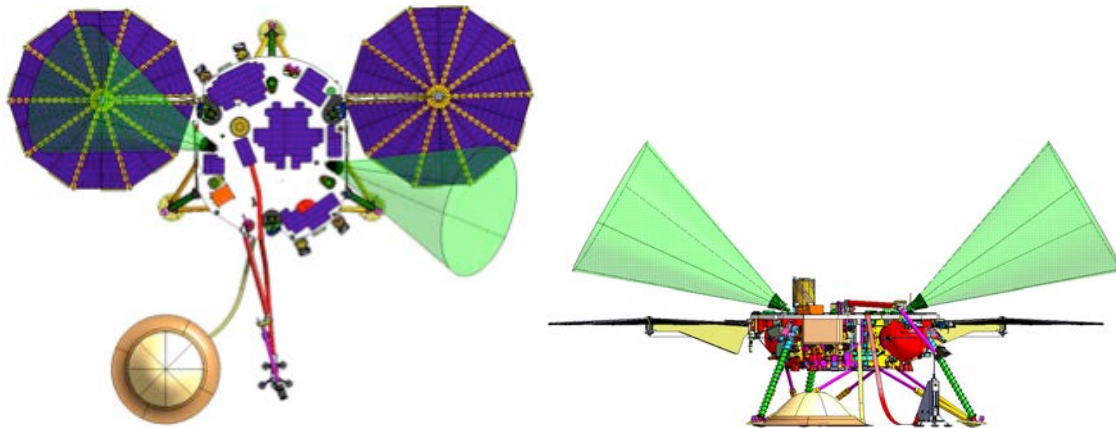
Figure 4.5.3-1: Left: View of lander deployed with solar panels aligned with the east-west axis and the SEIS and HP³ instruments deployed to the south (bottom of figure). The beam patterns of the two MGAs are shown, one pointed 15.5° south of due east, the other pointed 6° north of due west. Right: Lander viewed from the south showing the elevation of the MGA beam patterns centered at 30° in elevation.

The Doppler measurement accuracy for RISE will be limited primarily by fluctuations in the number of electrons between Earth and Mars (solar plasma). Figure 4.5.3-2 shows the Doppler measurement noise from fluctuations in solar plasma and Earth troposphere as a function of elongation from the Sun (Asmar et al. 2005). Other sources of measurement noise come from fluctuations in the Earth troposphere (also indicated in Figure 4), from thermal noise in the SDST and DSN receivers, and fluctuations in the phase-lock loop on the SDST. Given the signal-to-noise ratio for worst-case expected uplink and downlink, the thermal noise contribution is expected to be negligible. The phase-locking noise forthe SDST transponder has been measured and shown to be well below the noise from troposphere fluctuations.

Figure 4.5.3-2: Doppler measurement noise from fluctuations in solar plasma and Earth troposphere as a function of elongation from the Sun (From Asmar et al. 2005).

4.5.4 Operation

Nominally, RISE measurements will be made during one 1-hour tracking pass per week during the Instrument Deployment Phase and fou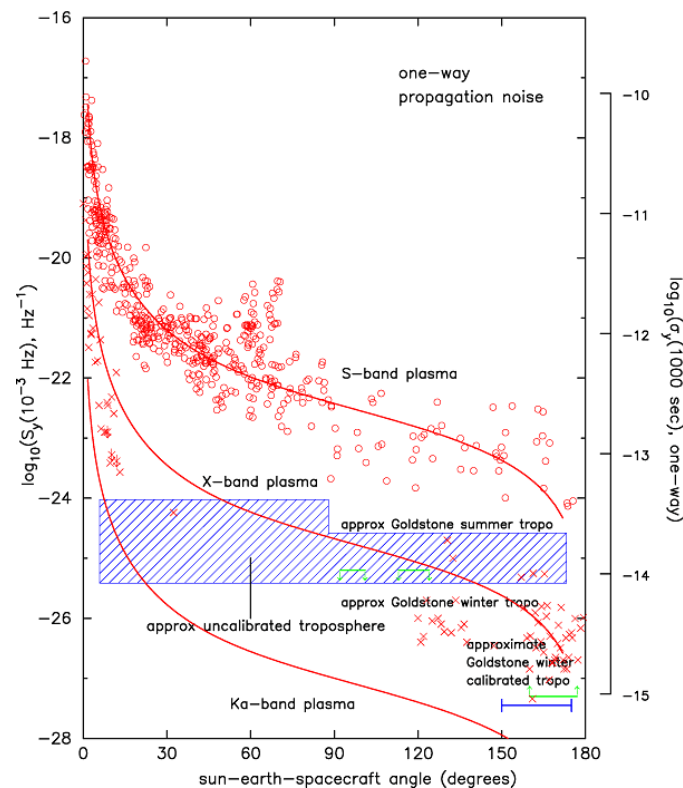r 1-hour tracking passes per week during the Science Monitoring Phase. The tracking pass duration is limited partly by the antenna pattern of the MGAs and partly by the available power and battery energy available on the lander. Dust storms may result in a reduced number of tracks or shorter tracking passes. Simulations show that science return is improved for tracks with elevation of Earth as viewed from the lander as low as possible and when tracking passes alternate between the east-directed MGA and the west-directed MGA. The tracking schedule will be negotiated between the project and the DSN, and adjusted depending on landing errors, dust storms, power availability, and DSN antenna availability.

4.5.5 Calibration

The Doppler measurement noise depends primarily on fluctuations in solar plasma, but also on Earth troposphere and ionosphere fluctuations. The DSN provides estimates of the troposphere and ionosphere during tracking passes based on analysis of GPS signals. These estimates are made available as calibration files to the science teams. On some tracking passes, especially when Mars is near opposition and the solar plasma noise is relatively small, water vapor radiometer data from Advanced Water Vapor Radiometers (AWVR) located at the Goldstone and Madrid DSN sites may be available to provide calibration data at shorter time scales. When available, AWVR calibration data will also be provided to the science team.

5 Mission Planning

The following sections describe the phases of the InSight mission, from launch through the end of surface operations. The timeline and primary activities are summarized for each phase.

5.1 Launch, Cruise, Approach, and EDL Phases

The current baseline launch window for InSight extends from March 4 to March 26, 2016. For a launch on any date during this window, Entry, Descent, and Landing (EDL) will occur September 28, 2016. Cruise operations concentrate on monitoring the health and performance of the flight systems and navigating the spacecraft to Mars. Spacecraft engineering subsystems checkouts, calibration activities, and instrument payload aliveness checkouts are performed early during cruise operations. Other than the checkouts/calibrations 24 days post-launch, all payloads are off during this phase.

During the cruise to Mars, the spacecraft will perform Trajectory Correction Maneuvers (TCMs). The last 60 days before landing compromise the approach phase, involving additional trajectory correction maneuvers. Entry, descent, and landing activities occur within ~10 minutes prior to landing on Mars. InSight uses a heatshield, parachute, and thruster-controlled lander descent stage to reach the surface. Immediately after touchdown, the lander configures itself for landed operations including deploying both solar arrays and taking an image using the ICC.

5.2 Deployment

Instrument deployment begins when the solar arrays are deployed and the lander is in a safe and communicative state. Instrument deployment operations take approximately 42 to 60 sols and cover assessment of the landed workspace, determination of instrument deployment sites, deployment of the instruments (HP^3 and SEIS, including the WTS), and the release of the HP^3 mole. Figure 5.2-1 provides an overview of all the activities required for successful deployment of the instruments. During this phase, the lander, its surrounding environment, and the workspace are characterized, the payload elements are checked out, weekly RISE measurements are acquired, and the critical data collected on Sol 0—the landing sol—are relayed to Earth. After the Science Team has selected suitable deployment sites within the workspace, the IDA places the SEIS (and covering WTS) and HP^3 instruments on the surface of Mars. At that point instrument calibration and science data collection commences and the HP^3 mole is released for penetration activity.
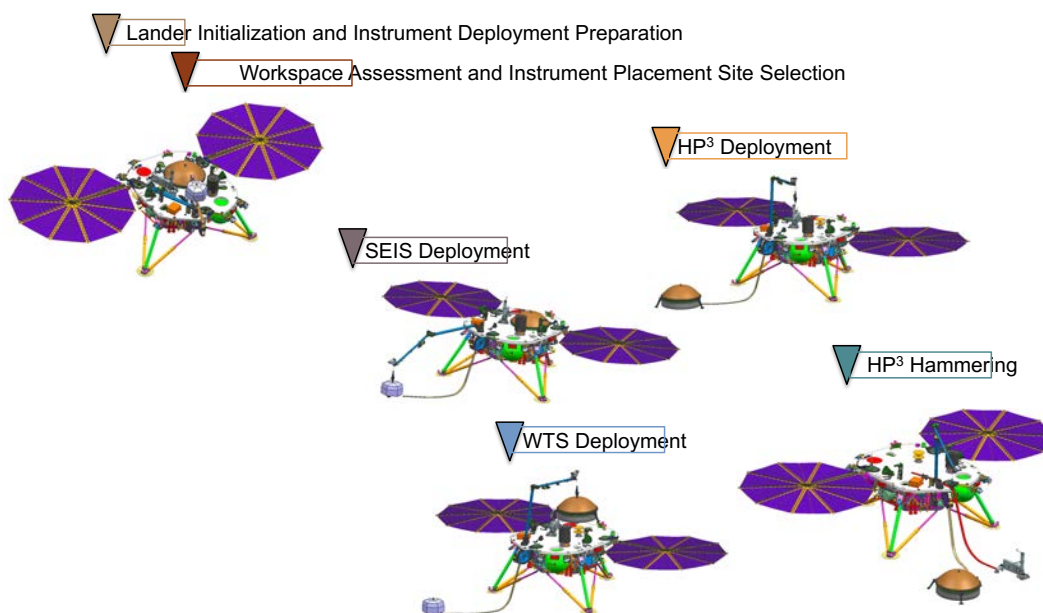
Figure 5.2-1: Overview of required activities and timeline for Instrument Deployment.

The selection of the instrument deployment sites will be governed by the Instrument Site Selection Working Group (ISSWG) and consist of four main phases:
1) Initial qualitative assessment of the workspace
2) Systematic mapping of the workspace
3) Quantitative assessment of four prospective sites
4) Certification of two prospective sites

Analysis data products utilized in this assessment include: 4 mm Digital Elevation Maps (DEMs), maps of the slope, roughness, surface normal, and tilt, terrain and soil maps with soil physical properties assessment, rock map with size-frequency distribution and shadow map, SEIS noise map, HP^3 thermal map, instrument tether routing, and mole penetrability assessment.

Due to the nature of the deployment timeframe, a rapid analysis of lander and payload telemetry is performed to assess the health and safety of the engineering subsystems and the status of instrument deployment activities. During this phase, InSight personnel will be co-located at JPL and work on a modified Earth-time schedule in which the start of the shift on Earth will track Mars time, sliding forward from 6 AM until it reaches 1 PM. After this point, the downlink from Mars arrives too late in the day on Earth to allow commands to be generated before a reasonable end of shift (a 10-hour shift is planned for deployment). Operations will be nominally planned daily with two floating days off per week. Due to the intensive and highly scripted nature of the deployment phase, limited, if any, time is expected to be available for ancillary science to be added during this phase. Operational support for the IDA is only planned for the deployment timeframe. Any IDA operation after the deployment phase is on a best efforts basis.

5.3 Science Monitoring

The science monitoring operations begin after the instruments have been placed on the surface. During this phase, SEIS monitoring starts and the HP^3 mole penetrates to its final depth. During the science monitoring operations, SEIS and HP^3 are in nominal data collection mode and gather science data autonomously and continuously and store this data in the instruments' nonvolatile memory. The lander nominally provides continuous power to SEIS and HP^3 throughout this phase, collects data from the instruments during every full wake up, and relays the data to Earth, usually twice per sol. The lander

powers on the RISE X-band communications system for one-hour an average of four times per week during which Doppler-tone monitoring sessions with the DSN are performed. The radiometer (part of HP^3) is commanded to take four 1-hour measurements during each sol for five minutes duration each, and every L_s ~ 15°, an hourly radiometer measurement campaign is undertaken lasting one entire sol with one measurement per hour for five minutes duration in each instance. The active TWINS' boom is swapped several times per sol to account for changing wind direction.

Since the lander is solar powered, the life of the lander is driven by Mars' diurnal cycle. Lander communications are determined by when orbiter overflights allow for UHF relay, typically twice per day at 3 AM and 6 PM LMST. The lander spends the majority of the science monitoring operations asleep. On a typical sol, the lander wakes up every three hours to check the battery state of charge, to run FSW diagnostics and fault-protection checks, and to collect housekeeping data. During two of the daily wake cycles the lander stays awake for an additional time to process science data and relay the data to an orbiter asset. Although science data are relayed back to Earth twice per sol, commands are relayed to the lander only once per week. A representative sol from the science monitoring operations is depicted in Figure 5.3-1.

Science monitoring operations are simple and routine. No ground-in-the-loop is required under nominal conditions. The flight team works on Earth time, and only during the nominal 8-hr prime shift. All operations teams reside at their respective institutions, and the SEIS and HP^3 IOTs work standard shifts for the time zone of their institutions. Operations are performed using a strategic process/timeline with sequences for the lander uplinked a week at a time. The rapid turnaround process supported during instrument deployment will no longer be used, although anomaly resolution will continue to be supported in that manner. Seismic and APSS event data selection by the instrument and science teams will be performed. Operations processes and interfaces will accommodate time differences for nominal operations between the different institutions supporting Science Monitoring operations.
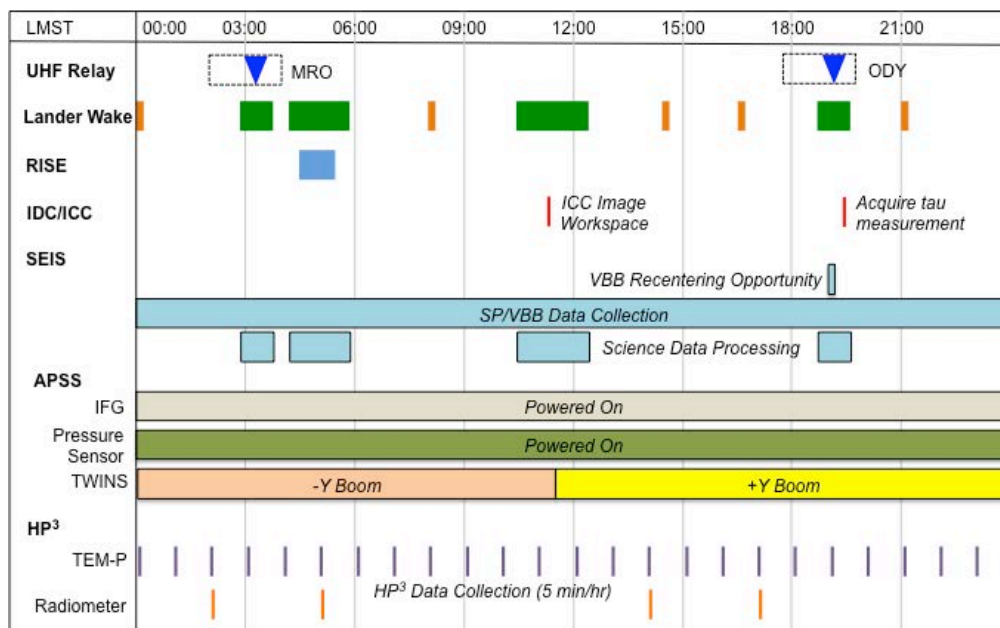
Figure 5.3-1: Sample lander activities during a nominal science monitoring sol.

6 Mission Operations After Landing

InSight has a distributed Mission Operations System (MOS) with international participation (Figure 6-1). InSight instrument and science operations and mission management are coordinated by JPL. The Spacecraft Team from the Mission Support Area located at Denver, CO performs spacecraft operations. Instrument operations are performed by the instruments' respective institutions (SEIS and APSS by CNES

and IPGP in France, HP^3 by DLR in Germany, and IDS and RISE by JPL in the USA). Operations decision-making authority resides at JPL.
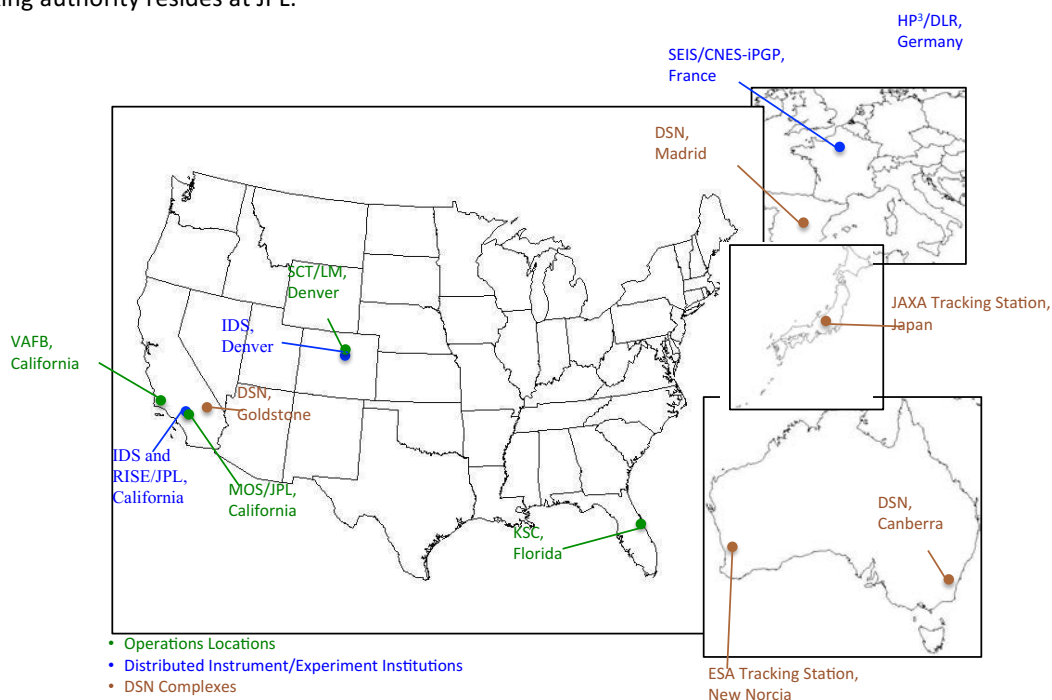
Figure 6-1: InSight—a distributed operations mission.

Instrument deployment is conducted via a tactical (day-to-day) ground operations process. After successful completion of these activities the instruments are ready for nominal surface operations and no further tactical operations are planned. InSight science monitoring operations are simple and routine and require minimum interaction from the flight team (ground-in-the-loop). Science monitoring operations are performed on a strategic (weekly) basis, although flight system and ground system anomaly response always remains tactical.

The Science System Engineer (SSE), in coordination with the PI and the Deputy PI, leads the science planning function. The PI and the Deputy PI lead the Science Team and coordinate the following operations functions: science data analysis, science data products generation, and science data distribution to the science community and archive to the Planetary Data System (PDS).

6.1 Team Structure

Although the Science Team is not part of the MOS, this team plays a major role in Mission Operations and is included here for completeness. The Science Team members, recognized leaders in their respective fields, together provide the breadth and depth of terrestrial and planetary-science expertise, and planetary-mission experience needed for the success of the InSight mission. Most team members have specific payload implementation roles in terms of instrument design, development, and/or scientific oversight, and software development for data analysis. Others participate in science investigation planning during development and lead data-analysis tasks during operations. All Science Team members participate in interpreting science results and Education and Public Outreach (E/PO) functions, and are committed to publishing the science results in peer-reviewed journals and broadly disseminating the data to the scientific community.

During science planning, the following functions are performed by the Science Team:
- Support the planning and integration of science activities led by the Science System Engineer
- Allocate resources (activity timing, power, data volume) to each instrument, if required
- Resolve resource allocation conflicts, if required

- Support the documentation of the results of the science planning and integration functions in a Science Activity Plan by the Science System Engineer (SSE), if required

During the science data management process, the Science Team performs the following functions:

- Process instrument/science data to higher-level (Level-2+) science data products
- Generate higher-level science data products
- Generate PDS labels and volumes for all science data products
- Process science data for use across different science disciplines, if needed
- Store and manage science data for the duration of the mission
- Make science and ancillary data (products) accessible to all science users
- Transfer science data products to the Planetary Data System (PDS)
- Participate in PDS peer reviews and lien resolution process
- Support event readiness reviews, as needed

The science planning function is also shared with the SSE. The SSE will lead the science planning function in coordination with the Instrument Operation Teams (IOTs) and the Science Team. The PI/Deputy PI will approve/disapprove the plan prior to its implementation.

The instrument operations function is performed by the IOTs. The IOTs are staffed by the instrument institutions and are remotely located at their corresponding institutions. Each IOT is responsible for the overall health and safety of their instrument. A summary of the functions performed by the IOTs during operations is as follows:

Instrument operations:

- Analysis and assessment of the health, safety, and trending of the instrument and associated status reporting
- Analysis, prediction and assessment of the performance of the instrument
- Analysis and prediction of instrument resource usage
- Maintenance of instrument telemetry alarms
- Assessment and resolution of instrument anomalies
- Maintenance of team operations procedures and contingency plans
- Maintenance of instrument operations software tools
- Support event readiness reviews, as needed

The IOTs also participate in the instrument/science activity planning and command generation as follows:

- Participation in the planning of the instrument activities through the Science Team
- Generation, verification (constraint checking), and validation of instrument commands and sequences
- Generation, verification (constraint checking), and validation of instrument FSW uploads, as needed
- Validation of the final sequence products via manual review

The IOTs also participate in science data processing:

- Process Level-1a science data (calibrated data)
- Process Level-1b science data (resampled data)

6.2 Science Operations

The mechanism for generating and prioritizing lander and instrument activities in support of science operations after lander on Mars will be through initiation by the science theme groups and deliberation in the Science Operations Working Group (SOWG) meetings. Each theme group will be composed of team members representing multiple instruments, working together to analyze scientific results and propose science activity plans that address their group's science objectives. In the SOWG meeting, members will present and advocate for their science activity plan. The SOWG chair will lead the SOWG to a consensus on a plan that meets the resource constraints and the Long Term Planner (LTP) strategic direction. The LTP is responsible for maintaining a list of goal science activities in a clear priority order.

Because the payloads are nominally powered off during the cruise and EDL phases, the science planning process is only required for surface operations. Operations during the instrument deployment timeframe have been preplanned with all the lander, instrument, and ground activities. These activities will be tested and practiced several times prior to execution on Mars. Therefore, minimum additional science planning will be utilized during this phase. The plan will be updated as needed based on situations encountered. Ancillary science activities not required as part of the deployment process may be inserted into the plan, resources permitting and with agreement of the SOWG chair and Mission Manager, provided there is no impact to the instrument deployment timeline. During this timeframe, there are fewer science team tagup meetings to coordinate opportunistic science. Team members interested in requesting ancillary science opportunities should coordinate with the respective science group lead, SOWG chair, and Long Term Planner (LTP). During the deployment phase, the IDS team will be fully staffed, possibly enabling arm science.

Since the activities to be performed during the science monitoring phase are simple and repetitive, it is expected that planning during this timeframe will be minimal. The science system engineer in coordination with the PI and the Deputy PI leads science monitoring planning. The PI or the Deputy PI, in consultation with the Science Team, the Project Manager, and the Mission Manager, makes decisions that are related to science planning. This includes the approval of the final science monitoring activity plan. During the science monitoring phase, event selection requests for SEIS and APSS will be finalized at an event selection meeting designed to fit within a data resource budget. The event selection meeting will be led by the InSIght or SEIS PI to coordinate science team priorities in event selection. Early in science monitoring the IDS team may still be available, but not baselined, in which case science requiring the arm would be possible. Once the IDS team is no longer available on the mission, the IDA will likely be left in a single, final pose to enable regular imaging of the workspace, night sky, and atmosphere for tau measurements. A summary of science operations planning meetings during the science monitoring phase is provided in Table 6.2-1.

Table 6.2-1: Science Operations Meetings During the Science Monitoring Phase. With the exception of the Long-Term Science Meeting (held monthly), all meetings are weekly, following the Insight uplink cadence.

Meeting	Nominal Time	Description
Strategic Science Meeting	Thursdays, 08:00 Pacific	During the Science Monitoring Phase, this meeting provides the Science Team a look-ahead at the upcoming week's plan (just as the current week's sequences are being finalized). The meeting is led by the Long Term Planner, with the goal of establishing the Science Team's inputs to the upcoming activity plan.
Long-term Science Meeting	Thursdays, 09:00 Pacific (Monthly)	During science monitoring, a monthly tagup led by the Long Term Planner, to coordinate longer-term science objectives amongst the Science Team..
Science Operations Working Group (SOWG) Meeting	Mondays, 08:00 Pacific	This multi-team meeting, led by the SOWG Chair, will integrate recent requests from the Science Team, Instrument Teams, and Spacecraft teams, to augment the upcoming activity plan. Where necessary, clear prioritization will be established between competing activities. Science Team attendance is not required, apart from the SOWG Chair and Long Term Planner. The Science Planner will subsequently review and edit the activity plan based on feedback from this meeting, delivering a plan that maximizes science return while meeting all engineering constraints.
Activity Plan Approval Meeting (APAM)	Tuesdays, 08:00 Pacific	The APAM meeting provides review of the activity plan prior to beginning activity sequence development. The SOWG chair will participate in this meeting to approve the plan for the Science Team. The final APAM plan includes a model of power and data resources for all instrument activities, and releases a data allocation for SEIS/APSS event selection.

Event Selection Meeting	Wednesdays, 07:00 Pacific	Throughout the preceding week, Science Team members will have submitted event requests, based on their analysis of the APSS and SEIS continuous decimated data. This weekly meeting will finalize which of these detailed event data will be selected from the on-board buffer for downlink in the current plan. The SOWG chair will participate in this meeting to understand event priorities. Other Science Team members will also join the discussion. Immediately following this meeting, the sequences to perform the agreed upon event selection are autonomously generated and delivered by the SEIS team.

6.3 Pre-landing Training and Operational Readiness Tests

Surface Operational Readiness Tests (ORTs) will be more beneficial to science team training than EDL ORTs, but EDL ORTs can be used to fulfill the required training.   The following test schedule is preliminary and subject to change:

    Nominal Approach and EDL – September 2015
    Nominal Launch and TCM-1 – November 2015
    Launch Abort / Recycle – December 2015
    Anomalous Launch – January 2016
  * Surface Nominal Deployment – January 2016
    Anomalous Approach and EDL – May 2016
  * Surface Anomalous Deployment and Nominal Science Monitoring – June 2016
    Nominal Approach and EDL – July 2016
  * Surface Nominal Deployment and Science Monitoring – August 2016
  Those marked with an asterisk (*) are most relevant for science operations training.

7 Description of Appendices

Appendix A consists of the InSight Archive Generation, Validation, and Transfer Plan, which documents the current plan for what products will be archived in the Planetary Data System (PDS). Appendix B is the InSight Science Team 'Rules of the Road', which describes the data access, sharing, release, and publication policies.

8 References

Ahern, T et. al., Standard for the Exchange of Earthquake Data, *SEED format version 2.4, on line at www.fdsn.org/**seed**_manual/**SEED**Manual_V2.4.pdf*, 2012.

Anderson D.L., Miller W.F., Latham G.V., et al., Seismology on Mars, *J. Geophys. Res.*, 82, 4524–4546, 1977.

Arvidson, R. E. and 21 other authors, Results from the Mars Phoenix Lander robotic arm experiment, J. Geoph. Res., 114(E00E02), doi:10.1029/2009JE003408, 2009.

Arkani-Hamed, J., Magnetization of the Martian crust, *J. Geophys. Res.*, *107*(E5), 5032, 2002a.

Arkani-Hamed, J., An improved 50-degree spherical harmonic model of the magnetic field of Mars derived from both high-altitude and low-altitude data, *J. Geophys. Res.*, *107*(E10), 5083, 2002b.

Asmar, S. W., Armstrong, J. W., Iess, L., and Tortora, P., Spacecraft Doppler tracking: Noise budget and accuracy achievable in precision radio science observations, *Radio Science*, 40, RS2001, 2005.

Beauduin, R., P. Lognonné, J.P. Montagner, S.Cacho, J.F. Karczewski and M. Morand, The effect of the atmospheric pressure changes on seismic signals or how to improve the quality of a station, *Bull. Seism. Soc. Am.*, 86, 1760-1769, 1996.

Bell, J. F., et al., Mars exploration rover Athena panoramic camera (Pancam) investigation, *J. Geophys. Res.: Planets (1991–2012)*, 108.E12, 2003.

Bloom, C., Golombek, M., Warner, N., and Wigton, N., Size frequency distribution and ejection velocity of Corinto crater secondaries in Elysium Planitia (expanded abstract): Eighth International Conference on Mars, Pasadena, CA, July 14-18, 2014, Abstract #1289, Lunar and Planetary Institute, Houston, 2014.

Catling, D.C., et al., A lava sea in the northern plains of Mars: Circumpolar Hesperian oceans reconsidered, 42nd Lunar and Planetary Science Conference, Abstract #2529, Lunar and Planetary Institute, Houston, 2011.

Catling D.C., et al., Does the Vastitas Borealis formation contain oceanic or volcanic deposits? Third Conference on Early Mars, Lake Tahoe, NV, May 21-25, 2012, Abstract #7031, Lunar and Planetary Institute, Houston, 2012.

Chenet, H., Lognonné, P., Wieczorek, M and H.Mizutani, Lateral variations of Lunar crustal thickness from Apollo seismic dataset, *Earth Planet Sci. Let.*, 243, 1-14, , 2006.

Cooper, M.R., Kovach, R.L.. Lunar near-surface structure. *Rev. Geophys. Space Phys.*, 12, 291–308. 1974.

Dainty, A.M. et al., Seismic scattering and shallow structure of the Moon in Oceanus Procellarum. Moon 9, 11–29, 1974.

Dal Moro, G., Joint analysis of Rayleigh-wave dispersion and HVSR of lunar seismic data from the Apollo 14 and 16 sites, *Icarus*, 254, 338–349, 2015.

Davis P.M., Meteoroid impacts as seismic sources on Mars, *Icarus*, 105, 469–478, 1993.

Dehant, V.; B.W. Banerdt, P. Lognonné, M. Grott, S. Asmar, J. Biele, D. Breuer, F. Forget, R. Jaumann, C. Johnson, M. Knapmeyer, B. Langlais, M. LeFeuvre, D. Mimoun, A. Mocquet, P. Read, A. Rivoldini, O. Romberg, G. Schubert, S. Smrekar, T. Spohn, P. Tortora, S. Ulamec, S. Vennerstroem, Future Mars geophysical observatories for understanding its internal structure, rotation, and evolution, *Planetary and Space Science*, 68(1), 123-145, 2012.

Folkner, W. M., Yoder, C. F., Yuan, D. N., Standish, E. M., Preston, R. A., Interior structure and seasonal mass redistribution of Mars from radio tracking of Mars Pathfinder, *Science*, 278 1749-1752, 1997.

Folkner, W. M., Kahn, R. D., Preston, R. A., Yoder, C. F., Standish, E. M., Williams, J. G., Edwards, C. D., Hellings, R. W., Eubanks, T. M., Bills, B. G., Mars dynamics from Earth-based tracking of the Mars Pathfinder lander, *J. of Geophys. Res.*, 102, 4057-4064, 1997.

Forbriger, T., R.Widmer-Schnidrig, E.Wielandt, M. Hayman and N. Ackerley, Magnetic field background variations can limit the resolution of seismic broad-band sensors, *Geophys. J. Int.*, 183, 303–312, 2010.

Gagnepain-Beyneix, J., P.Lognonné, H.Chenet, T.Spohn, Seismic models of the Moon and their constraints on the mantle temperature and mineralogy, *Phys. Earth Planet. Int.*, 159, 140-166, 2006.

Garcia, Gagnepain-Beyneix, J., Chevrot, S., Lognonné, P., Very Preliminary Reference Moon Model, *Phys. Earth. Planet. Int.*, 188, 96-113, 2011.

Golombek M.P., Banerdt W.B., Tanaka K.L., and Tralli D.M., A prediction of Mars seismicity from surface faulting. *Science*, 258, 979–981, 1992.

Golombek, M. P., et al., Geology of the Gusev cratered plains from the Spirit rover traverse, *J. Geophys. Res. Planets*, 110, E02S07, 2006.

Golombek, M. P., Haldemann, A. F. C., Simpson, R. A., Fergason, R. L., Putzig, N. E., Arvidson, R. E., Bell III, J. F., and Mellon, M. T., 2008, Martian surface properties from joint analysis of orbital, Earth-based, and surface observations: Chapter 21 in, The Martian Surface: Composition, Mineralogy and Physical Properties, J. F. Bell III editor, Cambridge University Press, p. 468-497.

Golombek, M., Warner, N., Schwartz, C., and Green, J., Surface characteristics of prospective InSight landing sites in Elysium Planitia (expanded abstract) : 44th Lunar and Planetary Science, Abstract #1696, Lunar and Planetary Institute, Houston, 2013a.

Golombek, M., Redmond, L., Gengl, H., Schwartz, C., Warner, N., Banerdt, B., and Smrekar, S., Selection of the InSight landing site: Constraints, plans, and progress (expanded abstract) : 44th Lunar and Planetary Science, Abstract #1691, Lunar and Planetary Institute, Houston, 2013b.

Golombek, M., Warner, N., Wigton, N., Bloom, C., Schwartz, C., Kannan, S., Kipp, D., Huertas, A., and Banerdt, B., Final four landing sites for the InSight geophysical lander (expanded abstract) : 45th Lunar and Planetary Science, Abstract #1499, Lunar and Planetary Institute, Houston, 2014b.

Grott, M., J. Helbert and R. Nadalini, The thermal structure of Martian soil and the measurability of the planetary heat flow, *J. Geophys. Res.*, 112, E09004, 2007.

Grott, M. and D. Breuer, On the spatial variability of the Martian elastic lithosphere thickness: Evidence for Mantle plumes?, *J. Geophys. Res.*, 115, E03005, 2010.

Grott, M.; A.C. Plesa, I. Daubar, M. Siegler, T. Spohn, S. Smrekar, and the HP3 instrument team, Retrieving the Martian Planetary Heat Flow from Measurements at Shallow Depth (Poster), 46th Lunar and Planetary Science Conference (LPSC), 16.-20 March 2015, The Woodlands, Texas, USA, 2015.

Gudkova, T., Lognonné, P. , Gagnepain-Beyneix, J., Seismic source inversion for Large impacts detected by the Apollo seismometers, *Icarus*, 211, 1049-1065, 2011.

Gudkova, T., P. Lognonné, K. Miljković and J.Gagnepain-Beyneix , Impact cutoff frequency –momentum scaling law inverted from Apollo seismic data, 427, 57-65, *Earth. Planet. Sci. Let.*, 2015.

Herkenhoff, K. E., et al., Athena microscopic imager investigation, *J. Geophys. Res. Planets* (1991–2012), 108, E12, 2003.

Horvath, P. et al., Lunar near-surface shear wave velocities at the Apollo Landing Sites as inferred from spectral amplitude ratios, *J. Geophys. Res*., 85, 6572–6578, 1980.

Khan A., Mosegaard K., and Rasmussen K.L., A new seismic velocity model for the Moon from a Monte Carlo inversion of the Apollo lunar seismic data, *Geophys. Res. Let.*, 27, 1591–1594, 2000.

Khan A. and Mosegaard K., An inquiry into the lunar interior – A non linear inversion of the Apollo seismic data, *J. Geophys. Res.,* 2002.

Khan A., Connolly J.A.D., Maclennan J., and Mosegaard K., Joint inversion of seismic and gravity data for lunar composition and thermal state. *Geophys. J. Int.*, 168, 243–258, 2007.

Knapmeyer M., Oberts J., Hauber E., Wählisch M., Deuchler C., and Wagner R., Working models for spatial distribution and level of Mars' seismicity, *J. Geophys. Res.*, 111, E11006, 2006.

Kömle, N.I., Hütter, E.S., Macher, W., Kaufmann, E., Kargl, G., Knollenberg, J., Grott, M., Spohn, T., Wawrzaszek, R., Banaszkiewicz, M., Seweryn, K., and Hagermann, A., In situ methods for measuring thermal properties and heat flux on planetary bodies, *Planetary and Space Science*, 59(8), 639-660, 2011.

Konopliv, A. S., Asmar, S. W., Folkner, W. M., Karatekin, O., Nunes, D. C., Smrekar, S. E., Yoder, C. F., Zuber, M. T., Mars high resolution gravity fields from MRO, Mars seasonal gravity, and other dynamical parameters, *Icarus*, 211, 401-428, 2011.

Kuchynka, P., Folkner, W. M., Konopliv, A. S., Parker, T. J., Park, R. S., Le Maistre, S., Dehant, V., New constraint on Mars rotation determined from radiometric tracking of the Opportunity Mars Exploration Rover, *Icarus*, 229, 340-347, 2014.

Langlais, B., Purucker, M.E., and Mandea, M., Crustal magnetic field of Mars, *J. Geophys. Res.*, *109*, E02008, 2004.

Le Maistre, S., Rosenblatt P., Rivoldini, A., Dehat, V., Marty, J.-C., Karatekin, O., Lander radio science experiment with a direct link between Mars and Earth, *Planetary and Space Science*, 102, 105-132, 2012.

Lognonné, P. and Johnson, C., Planetary Seismology, in <u>Treatise in Geophysics, 10, Planets and Moons</u>, G.

Shubert editor, chapter 4, 69-122, Elsevier, 2007.

Lognonné, P. and Johnson, C. L., Planetary Seismology, in <u>Treatise in Geophysics, 2nd edition, 10, Planets and Moons</u>, G. Shubert editor, chapter 4, 65-120, Elsevier, 2015.

Lognonné, P., Zharkov, V.N., Karczewski, J.F., Romanowicz, B., Menvielle, M., Poupinet, G., Brient, B., Cavoit, C., Desautez, A., Dole, B., Franqueville, D., Gagnepain-Beyneix, J., Richard, H., Schibler, P., Striebig, N., The Seismic Optimism Experiment, *Planetary Space Sciences*, 46, *739-747*, 1998.

Lognonné, P., Gagnepain-Beyneix, J., and Chenet, H., A new seismic model of the Moon: implication in terms of structure, formation and evolution, *Earth Plan. Sci. Let.*, 6637, 1-18, 2003.

Lognonné, P., Le Feuvre, M., Johnson, C. L., and Weber, R. C., Moon meteoritic seismic hum: steady state prediction, *J. Geophys. Res*., 114, E12003, 2009.

Lorenz, R.D., Planetary *seismology*—Expectations for lander and wind noise with application to Venus, *Planetary and Space* Science, 62:1, 86-96, 2012.

Maki, J. N., et al., Mars exploration rover engineering cameras, *J. Geophys. Res. Planets (1991–2012)*, 108, E12, 2003.

Maki, J., et al., The Mars science laboratory engineering cameras, *Space science reviews*, 170.1-4, 77-93, 2012.

Mittelholz, A., Johnson, C. L., Langlais, B., Large-scale geometry and temporal variability of the Martian external magnetic field, Abstract GP51B-3721, presented at 2014 Fall Meeting, American Geophysical Union, San Francisco, Calif., 15-19 December, 2014.

Morschhauser, A., Lesur, V., Grott, M., A spherical harmonic model of the lithospheric magnetic field of Mars, *J. Geophys. Res.*, 119, 6, 1162-1188, 2014.

Mueller, K. and Golombek, M. P., Compressional structures on Mars, *Annual Rev. Earth Planet. Sci.*, 32, 435–464, 2004.

Nakamura, Y., Dorman, J., Duennebier, F., Lammlein, D., and Latham, G., Shallow lunar structure determined from the passive seismic experiment, *Moon*, 13, 57–66. 1975.

Nakamura, Y. and Anderson, D.L., Martian wind activity detected by a seismometer at Viking lander 2 site, *Geophys. Res. Lett*., 6, 499–502, 1979.

Nakamura, Y., Latham, G.V., Dorman, J., Harris, J., Passive Seismic Experiment Long-Period Event Catalog, Final Version, 1969 day 202-1977 day 273, 314 pp., Galveston Geophysics Laboratory Contribution No. 491, University of Texas, Austin, 1981.

Nakamura, Y., Seismic velocity structure of the lunar mantle, *J . Geophys. Res*., 88, 677–686, 1983.

Panning, M.P., Beucler, E., Drilleau, Mocquet, Lognonné, P., Banerdt, W.B., Verifying single-station seismic approaches using Earth-based data: Preparation for data return from the InSight mission to Mars, *Icarus*, 230-242, 248, 2015.

Phillips, R. J., Expected rates of Marsquakes, in Scientific Rationale and Requirements for a Global Seismic Network on Mars, LPI Tech. Rep.91– 02 LPI/TR-91– 02, pp. 35– 38, Lunar and Planet. Inst., Houston, 1991.

Pivarunas, A., Warner, N. H., and Golombek, M.P., Onset diameter of rocky ejecta craters in western Elysium Planitia, Mars: Constraints for regolith thickness at the InSight landing site (expanded abstract): 46th Lunar and Planetary Science, Abstract #1129, Lunar and Planetary Institute, Houston, 2015.

Plesa, A.-C., Tosi, N., Grott, M. and Breuer, D., Thermal evolution and Urey ratio of Mars, *J. Geophys. Res. Planets*, 120, Issue 5, 995–1010, 2015.

Purucker, M. E., et al., An altitude-normalized magnetic map of Mars and its interpretation, *Geophys. Res. Lett.*, 27, 2449-2552, 2000.

Rivoldini, A., Van Hoolst, T., Verhoeven, O., Mocquet, A., Dehant, V., Geodesy constraints on the interior structure and composition of Mars**, *Icarus*, 213, Issue 2, 451-472, 2011.

Sapritsky, V.I., et al., Temperature: Its Measurement and Control in Science and Industry, vol. 7, 619-624 2003.

Sorrells G.G., A preliminary investigation into the relationship between long period seismic noise and local fluctuations in the atmospheric pressure field, *Geophys. J. Royal Astro. Soc.*, 26, 71–82, 1971.

Spohn, T., Grott, M., Smrekar, S., Krause, C., Hudson, T.L., and the HP3 instrument team, Measuring the Martian Heat Flow using the Heat Flow and Physical Properties Package (HP3) (poster), In 45th LPSC 2014, 17-21 March 2014, The Woodlands, Texas, 2014.

Tanaka, K., et al., Geologic map of Mars, *U. S. Geol. Surv. Sci. Invest.*, Map 3292, 2014.

Teanby, N.A., Wookey, J., Seismic detection of meteorite impacts on Mars, *Phys. Earth Planet. Int.*, 186, 70–80, 2011.

Teanby**, N.A., Predicted detection rates of regional-scale meteorite impacts on Mars with the InSight short-period seismometer, *Icarus*, 256, 49–62, 2015.

Van Hoolst, T., Dehant, V., Roosbeek, F., and Lognonné, P., Tidally induced surface displacements, external potential variations, and gravity variations on Mars, *Icarus*, 161, 281-296, 2003.

Verhoeven, O., Rivoldini, A., Vacher, P., Mocquet, A., Choblet, G., Menvielle, M., Dehant, V., Van Hoolst, T., Sleewaegen, J., Barriot, J.-P., Lognonné, P., Planetary interiors structure inferred from electromagnetic, geodetic and seismic network science I: Forward problem an the case of Mars, *J.Geophys. Res*., 110, 2005.

Verhoeven, O., Rivoldini, A., Vacher, P., Mocquet, A., Choblet, G., Menvielle, M., Dehant, V., Van Hoolst, T., Sleewaegen, J., Barriot, J.- P., Lognonné, P., Interior structure of terrestrial planets: modeling Mars' mantle and its electromagnetic, geodetic and seismic properties, *J. Geophys. Res.*, 110, E04009, 2005.

Vinnick L., Chenet, H., Gagnepain-Beyneix, J., and Lognonné, P., First seismic receiver functions on the Moon, *Geophys. Res. Lett*, 28, 3031-3034, 2001.

Warner, N. H., Golombek, M. P., Bloom, C., Wigton, N., and Schwartz, C., Regolith thickness in western Elysium Planitia: Constraints for the InSight mission (expanded abstract): 45th Lunar and Planetary Science, Abstract #2217, Lunar and Planetary Institute, Houston, 2014.

Weber, R., Lin, P.Y., Garnero, E., William, Q., and Lognonné, P., Seismic detection of the Lunar Core, *Science*, 331, 309-312, 2011.

Wigton, N.R., Warner, N., and Golombek, M., Terrain mapping of the InSight landing region: Western Elysium Planitia, Mars (expanded abstract): 45th Lunar and Planetary Science, Abstract #1234, Lunar and Planetary Institute, Houston, 2014.

Zürn, W. and Widmer, R., On noise reduction in vertical seismic records below 2 mHz using local barometric pressure, *Geophys. Res. Lett.*, 22(24), 3537–3540, 1995.

9 List of Acronyms

ADC	Analog to Digital Converter
APSS	Auxiliary Payload Sensor Suite
APAM	Activity Plan Approval Meeting
BEE	Back End Electronics
CIC	Cascaded Integrator–Comb
DFE	Direct-from-Earth
DTE	Direct-to-Earth
EDL	Entry, Descent, and Landing
FIR	Finite Impulse Response
FPGA	Field Programmable Gate Array
FSW	Flight Software
HP^3	Heat Flow and Physical Properties Package
ICC	Instrument Context Camera
IDA	Instrument Deployment Arm
IDC	Instrument Deployment Camera
IDS	Instrument Deployment System
IFG	InSight Fluxgate Magnetometer
IOT	Instrument Operation Team
ISSWG	Instrument Site Selection Working Group
LTP	Long Term Planner
LVL	Leveling System
MGA	Medium Gain Antenna
MOS	Mission Operations System
MRO	Mars Reconnaissance Orbiter
MSL	Mars Science Laboratory
ORT	Operational Readiness Test
PAE	Payload Auxiliary Electronics
PDS	Planetary Data System
PS	Pressure Sensor
RAD	Radiometer
RISE	Rotation and Interior Structure Experiment
SA	Sensor Assembly
SDST	Small Deep-Space Transponder
SEED	Standard for the Exchange of Earthquake Data
SEIS	Seismic Experiment for Interior Structure
SOWG	Science Operations Working Group
SP	Short-Period Seismometer
sps	Samples per second
SSE	Science System Engineer
SSPA	Solid-State Power Amplifier
STATIL	Static Tilt Meter
TCM	Trajectory Correction Maneuver
TEM-A	Thermal Excitation Measurement – Active
TEM-P	Thermal Excitation Measurement – Passive
TLM	Tether Length Monitor
TWINS	Temperature and Wind Sensor
UHF	Ultrahigh Frequency
VBB	Very Broad Band Oblique Seismometer
WTS	Wind and Thermal Shield

InSight

PIP 4.3 Archive Generation, Validation, and Transfer Plan

Initial Release

Note: Printed copies of this document may not be relied upon for official purposes. The current version is in the Product Data Management System: https://pdms.jpl.nasa.gov.

September, 2015

JPL D-75289

NASA Structure Management (NSM) #: 448550

Discovery Program

This document is based on the template
04.02_Science_Data_Mgmt_&_Archive_Plan_070123_notrax.doc.

Prepared by: Suzanne Smrekar, Sue LaVoie, Amy Culver and Susan Slavney

Signature Page (signatures have been obtained electronically)

Prepared by:

_____   _____
Suzanne Smrekar, InSight Deputy Principal Investigator   Date

_____   _____
Sue LaVoie, Co-I, PDS Imaging Node   Date

_____   _____
Amy Culver, PDS Imaging Node   Date

Approved by:

_____   _____
W. Bruce Banerdt, InSight Principal Investigator   Date

_____   _____
Suzanne Smrekar, InSight Deputy Principal Investigator   Date

_____   _____
Stacy Weinstein-Weiss, Insight Mission System Manager   Date

_____   _____
Robert Fogel, InSight Program Scientist   Date

_____   _____
Thomas Morgan, Planetary Data System Program Manager   Date

Concurred by:

_____   _____
Philippe Lognonné, SEIS PI   Date

_____   _____
Justin Maki, IDC/ICC   Date

_____   _____
Tilman Spohn, HP^3 PI   Date

_____   _____
Don Banfield, APSS Team   Date

_____   _____
Sami Asmar, RISE   Date

_____   _____
Chris Russell, IFG Lead   Date

_____   _____
Julie Rogez-Castillo, IDA   Date

_____   _____
José Antonio Rodriguez-Manfredi, TWINS PI   Date

.

.

**This page is intentionally left blank
for pasting in the electronic approval/signature screen
from PDMS.**

.

Change Log

Date	Sections Changed	Reason for Change	Revision
07/09/13	All	New document.	Initial Release
4/10/13	1.2, 1.3, 2.7, 3.4	Geoscope is now under the umbrella of the IPGP Data Center	
9/23/15	Signature page	Julie Rogez-Castillo now responsible for IDA data archiving so replaces Ashitey Trebi-Ollennu	2nd release
9/23/15	2.4	Add a paragraph describing our intent to archive spacecraft engineering data. The exact data to be archived will be specified after teams can assess what data is useful during Mars operations.	2nd release

.

Table of Contents

Table of Figures

Table of Tables

1 Introduction

1.1 Purpose

This plan provides for the timely generation, validation, and transfer of raw and reduced data products acquired by the Interior Exploration Using Seismic Investigations, Geodesy, and Heat Transport (InSight) project to the Planetary Data System (PDS) in complete, well-documented, permanent archives (archival data products).

1.2 Scope

This plan covers the policies and procedures for the specific generation, validation, and transfer to the PDS of archival data products, and expectations for access and distribution of those data products. The plan will specify the distribution and archiving of raw and reduced data sets, along with pertinent accompanying information to be acquired or derived during the InSight project. In addition to being archived in the Planetary Data System (PDS), Seismic Experiment for Interior Structure (SEIS) data will be delivered both to the Institut de Physique du Globe de Paris (IPGP) Data Center and Incorporated Research Institutions for Seismology (IRIS) for archiving and public distribution. The reason for delivery paths outside of PDS is that the global seismic community uses data in a standardized format, Standard for the Exchange of Earthquake Data (SEED), which is available for public access via IPGP and IRIS. We include a high level discussion of these additional deliveries for completeness. Specific aspects addressed in this plan are:

- Generation of high-level project, spacecraft, and instrument documentation; instrument calibration reports; and documentation of algorithms and/or software used to produce reduced data records.
- Reduction of science packet data in the spacecraft telemetry to raw data, calibrated data, and finally to derived data products. These will have associated documentation that records when and where the data were acquired and for what purpose.
- Generation of SPICE archives used to support mission operations and analysis and labeling of science data products.
- Generation and validation of archives containing InSight science and engineering data, software, algorithms, documentation, and ancillary information.
- Delivery of validated InSight archives to the PDS.
- Delivery of copies of validated InSight SEIS archives to the IRIS and IPGP data centers.

1.3 Organization

This plan begins with overviews of the InSight project, PDS, and IRIS and IPGP data centers, followed by a summary of roles and responsibilities for organizations and personnel associated with generation, validation, transfer, and distribution of InSight archival data. The document then discusses in detail the types of data products to be produced and archived to PDS during the InSight project. The document ends with a description of the InSight PDS archiving process, including data flow and delivery schedule.

.

1.4 Applicable and Reference Documents

1.4.1 Applicable Documents and Constraints

This plan is responsive to the following Discovery Program and InSight documents:

1.   Discovery Program Plan, DISC-PLAN-001B, Rev. B, Sep. 16, 2008.
2.   InSight Concept Study Report, in response to Discovery AO NNH10ZDA007O, March 19, 2012.
3.   InSight Project Plan, Initial Release, JPL D-75275, May 22, 2013.
4.   InSight Mission Plan, Initial Release, JPL D-75260, April 4, 2014.

This plan is consistent with the principles delineated in the following National Academy of Sciences reports:

1.   Data Management and Computation, Volume 1, Issues and Recommendations, 1982, National Academy Press, 167 pp.
2.   Issues and Recommendations Associated with Distributed Computation and Data Management Systems for the Space Sciences, 1986, National Academy Press, 111 pp.
3.   Ensuring the integrity, accessibility, and stewardship of research data in the digital age, 2009, Committee on Science, Engineering, and Public Policy, National Academies Press, http://www.nap.edu/catalog.php?record_id=12615.

This plan is also consistent with the following Planetary Data System documents:

1.   Data Providers' Handbook, Archiving Guide to the PDS4 Data Standards, Jan. 31, 2012, Version 0.3.6.
2.   Planetary Data System Standards Reference, version 1.2.0, March 27, 2014.
3.   PDS4 Data Dictionary, Abridged, version 1.2.0.1, March 28, 2014.

InSight will strive to be consistent any future versions.

This plan requires the generation of the following project documents:

1.   Interface Control Documents (ICD) specifying relationships between the InSight project, instrument science teams, and PDS nodes (finalized in Phase B).
2.   Data Product and Archive Bundle Software Interface Specification (SIS) for all standard products (draft at beginning of Phase C, final at beginning of Phase D).

Finally, this plan is consistent with the following:

1.   The InSight Level-1 requirements.
2.   The contracts negotiated between the InSight project, the Principal Investigator (PI), and Co-Investigators (Co-Is) in which archival data, software, algorithms, and documentation are explicitly defined as deliverables.
3.   ITAR rules for release of information will be followed. Specifically, scientific and technical information, such as documents and presentations, will be reviewed under JPL

.

procedures prior to being published, released external to the NASA, or to foreign persons outside of the project.

2   InSight Archive Generation, Validation, and Transfer to the PDS

2.1   The Project

InSight will be launched in March 2016 and will place a geophysical lander on Mars on September 28, 2016, to study its deep interior. The Surface Phase consists of Deployment and Penetration, and Science Monitoring. It ends after one Mars year plus approximately 40 sols. The project timeline is shown in Figure 2-1.

The science payload comprises two instruments: the Seismic Experiment for Interior Structure (SEIS) and the Heat-Flow and Physical Properties Probe (HP^3). In addition, the Rotation and Interior Structure Experiment (RISE) will use the spacecraft's X-band communication system to provide precise measurements of planetary rotation. SEIS and HP^3 will be placed on the surface with an Instrument Deployment System (IDS) comprising an Instrument Deployment Arm (IDA), Instrument Deployment Camera (IDC), and Instrument Context Camera (ICC). There are also several supporting instruments. The Auxiliary Payload Sensor Subsystem (APSS) includes a pressure sensor, the InSight Flux Gate (IFG) magnetometer, and Temperature and Wind for InSight (TWINS) sensors. The SEIS team will use environmental data collected by APSS to reduce and analyze their data. Within the project, the IFG is considered part of the APSS. For the purposes of data archiving, the IFG data are listed separately as they will be delivered by the magnetometer lead, Chris Russell, to the PDS Planetary Plasma Interactions node. The wind, temperature, and pressure data will be delivered to the PDS Atmospheres node. The radiometer (RAD) data will be used to measure surface temperature and estimate thermal properties, and to support the HP^3 team data analysis. Table 2-1 summarizes the InSight payload and supporting instrumentation.

The JPL Advanced Multimission Operations System (AMMOS)/ Multimission Image Processing Laboratory (MIPL) processes raw InSight data and produces PDS4 raw data products for TWINS, the pressure sensor, IDA, and higher-level products for the ICC and IDC. MIPL will deliver CCSDS telemetry packets to the SEIS and HP3 teams, and SFDU telemetry packets to the IFG team. MIPL will generate PDS4-compatible, documented products for use by the instrument science teams and delivery to the PDS and distribution to the science community and public. All PDS4 products will contain PDS4 XML labels.

In addition, SEIS products delivered to PDS, IRIS and the IPGP Data Center will be in mini-SEED format and have SEED headers. The use of this international standard makes the products immediately accessible to the international research community and facilitates their use. The PDS archive for SEIS will contain two versions of each data product, one in SEED format and one in a standard PDS table format.
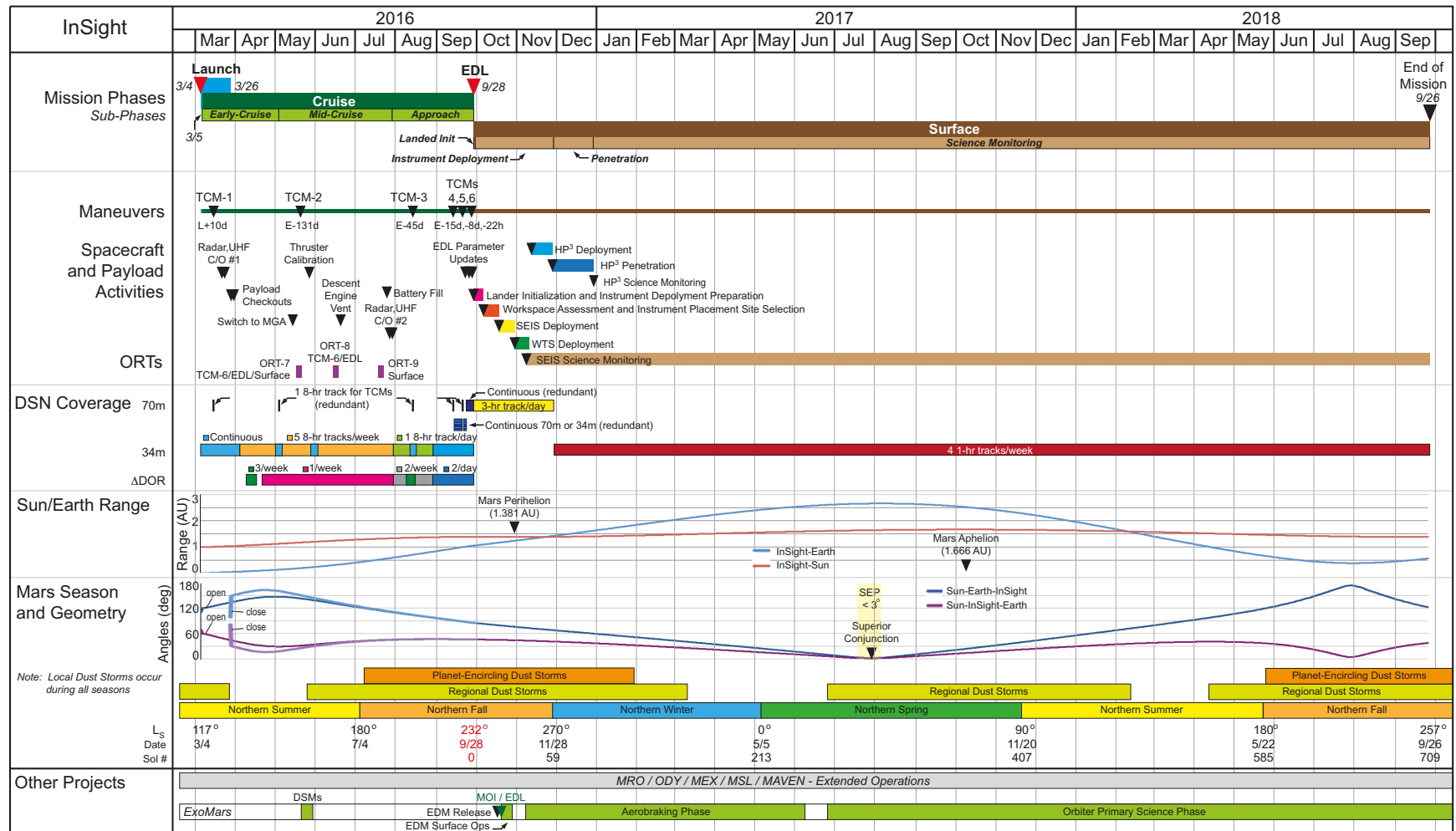
Figure 2-1: InSight project timeline.

.

Table 2-1: InSight payload and supporting instrumentation.

Payload Element/Investigation	Description	Instrument PIs and Leaders
Seismic Experiment for Investigating the Subsurface (SEIS)	Two three-axis seismometers, one Short-Period (SP), one Very-Broad-Band (VBB), to measure seismic waves traveling through the interior	PI: Philippe Lognonné (IPGP)
Rotation and Interior Structure Experiment (RISE)	Radiometric geodesy, to determine precession & nutation of the Martian rotation axis	Lead: William Folkner (JPL)
Heat-Flow and Physical Properties Probe (HP^3)	Subsurface heat probe, to measure the heat flux from the interior; also provides surface brightness temperature from the radiometer (RAD)	PI: Tilman Spohn (DLR)
Instrument Deployment System (IDS)	Arm (IDA): Deploys the SEIS and HP^3 to the surface; 2 Cameras (ICC/IDC): Support SEIS and HP^3 deployment	Leads: ICC/IDC: Justin Maki (JPL) and IDA: Ashitey Trebi-Ollennu (JPL)
Auxiliary Payload Sensor Subsystem (APSS)	Two booms, arrayed with wind and temperature sensors (TWINS) plus a single pressure sensor to monitor environmental conditions in support of SEIS	TWINS PI: José Antonio Rodriguez-Manfredi (CAB); Pressure sensor lead: Don Banfield, (Cornell Univ.)
InSight Flux Gate (IFG)	Triaxial magnetometer to measure variations in the magnetic field from the martian ionosphere or the lander in support of SEIS; considered by the project to be part of APSS.	Lead: Chris Russell (UCLA)

2.2 Data Flow

InSight data products are generated in a data-driven automated fashion during project operations using well-understood, multiproject capabilities. Each data product will be described in a data product software interface specification (SIS) document. PDS4 definitions of processing levels for science data products are found in Table 2-2.

**Table 2-2: Definitions of processing levels for science data sets.**

Processing Level	Description
Telemetry	An encoded byte stream used to transfer data from one or more instruments to temporary storage where the raw instrument data will be extracted.
Raw	Original data from an instrument. If compression, reformatting, packetization, or other translation has been applied to facilitate data transmission or storage, those processes will be reversed so that the archived data are in a PDS approved archive format.
Partially Processed	Data that have been processed beyond the raw stage but which have not yet reached calibrated status.
Calibrated	Data converted to physical units, which makes values independent of the instrument.
Derived	Results that have been distilled from one or more calibrated data products (for example, maps, gravity or magnetic fields, or ring particle size distributions). Supplementary data, such as calibration tables or tables of viewing geometry, used to interpret observational data should also be classified as 'derived' data if not easily matched to one of the other three categories.

PDS and its data providers have used both the CODMAC and NASA systems to describe data processing levels, sometimes in the same data set; this has led to confusion. In developing PDS4, PDS has determined that a simpler system, relying on only a few categories, is sufficient. PDS adopted the above terms for broadly classifying archival data according to processing level. When making such classification, data providers (in consultation with the cognizant PDS node) will select the most appropriate term and give a detailed description of the processing in accompanying documentation.

In addition to calibrated data products, higher-level, derived data products will be generated by instrument science teams. Each derived data product will be described in a SIS. Those derived data products that are completed and validated in time for a scheduled release to PDS may be delivered along with the standard products. PDS will continue to accept derived data products after the end of the project as long as they are documented and validated according to PDS standards.

Figure 2-2 shows the flow of science data products from the InSight downlink through project operations and instrument science team operations to their ultimate delivery to the PDS. Downlink telemetry is received at Project Operations at JPL. MIPL generates PDS4 raw data for TWINS, the pressure sensor, IDA, ICC, IDC, and the full set of data products for the IDC and ICC. InSight instrument science teams generate all data products derived from the raw data for SEIS, RISE, and HP[3]. All products will be generated under the cognizance of the relevant InSight instrument science teams and validated by those teams. Within the SEIS team, Renee Weber and the Marshall Flight Center Archive Assembly Team will be responsible for taking data from the IPGP Data Center in mini-SEED format, adding PDS labels, and delivering to PDS. Higher level SEIS data products will follow the same path to PDS. The Project Science Group (PSG) will make products available to science team members and the public. SEIS data will also be available to the public via the IRIS and IPGP data centers.
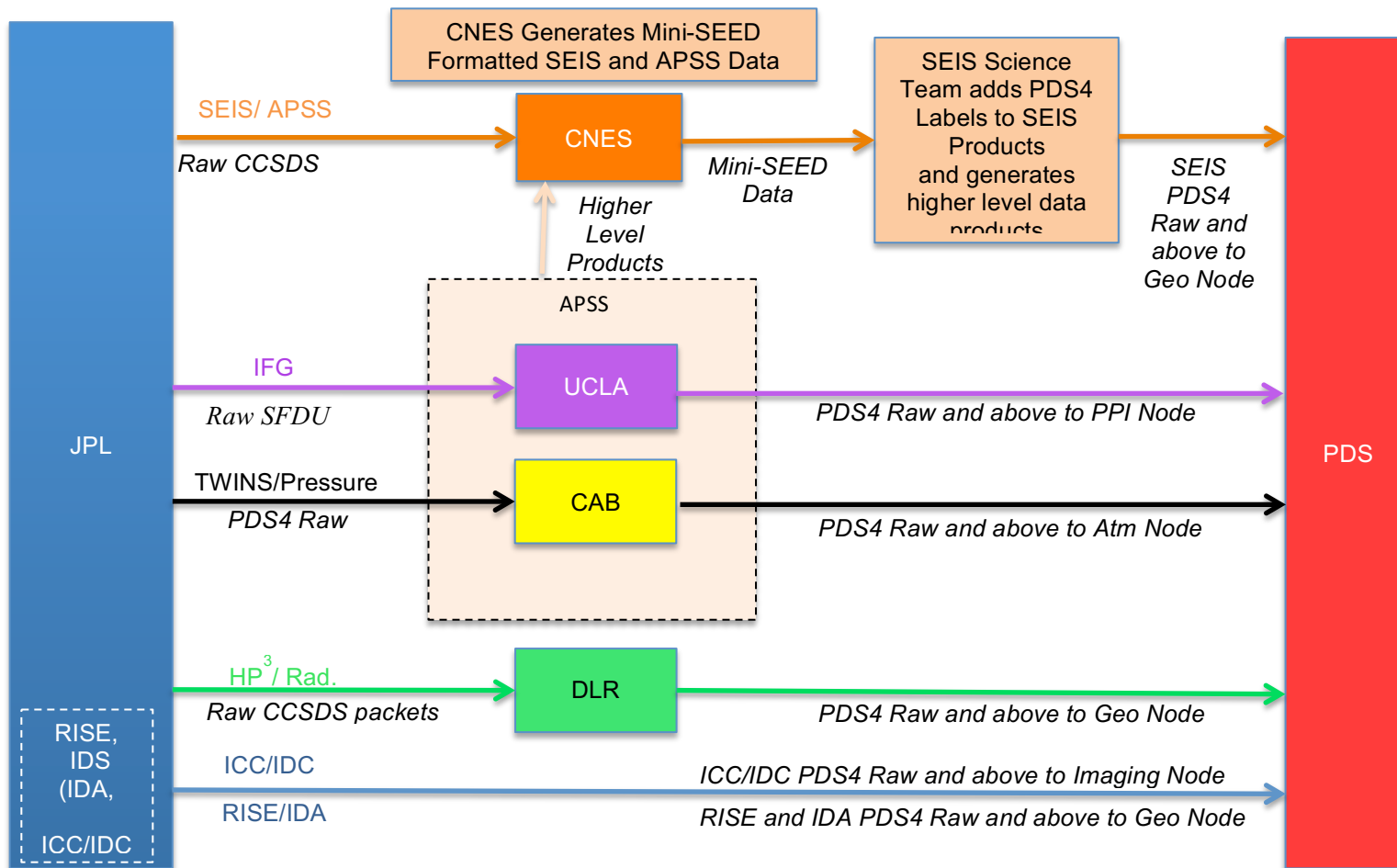
Figure 2-2: Data flow.

Complete archive bundles including data products, documentation, and ancillary materials are assembled, validated under InSight project auspices, and then delivered to the designated PDS nodes. PDS personnel will work closely with instrument science team members to ensure a smooth transfer. Table 2-3 lists the elements that comprise the InSight archives, and Table 2-4 provides a detailed list of all the data sets and their producers. All InSight archive collections will be assembled according to designs specified in archive bundle SIS documents.

Table 2-3: Components of InSight archives.

Component	Contents	Supplier
SPICE Archives	SPICE kernels	NAIF
Instrument Data Collections	• Raw data products • Calibrated data products • Derived data products	MIPL & instrument science teams
Supporting Materials	• Ground calibration data files (safed—PDS archive format compliance not required) • High-level project, spacecraft, instrument, data set, software, and personnel descriptions for the PDS catalog • Data product SIS documents • Archive bundle SIS documents • Processing descriptions, algorithms, and software (to use in understanding reduced data product generation) • Instrument calibration plans and reports and associated data needed to understand Level-1 product generation • Verification and validation (V&V) reports • Characterization, calibration, cataloging (CCC) reports • Notes that describe uplink and downlink results	Instrument science teams
Engineering Archives	• SIS documents • Uplink/command sequences and notebook entries • Telemetry data	InSight project

Table 2-4: List of InSight data products to be archived.

Instrument —Sensor	Processing Level	Product/Data Set	Volume (Mbit)	Data Set Producer	Archive Producer	1st Release Date & Frequency	PDS Curator
SEIS—All	n/a	Calibration and Installation Report	10	SEIS Team	SEIS Team	Landing –1 m	Geo
SEIS—All	n/a	Ground calibration files	800	SEIS Team	SEIS Team	Landing –1 m	Geo
SEIS—VBB	Raw	Raw velocity	17,500	SEIS Team	SEIS Team	Start Monitoring Phase +3 m; quarterly	Geo
SEIS—VBB	Calibrated	Calibrated continuous and event data	22,500	SEIS Team	SEIS Team	Start Monitoring Phase +4 m; quarterly	Geo
SEIS—VBB	Derived	Instrument transfer function model for tide output	10	SEIS Team	SEIS Team	EOM +5 m	Geo
SEIS—SP	Raw	Raw velocity, temperature	8,500	SEIS Team	SEIS Team	Start Monitoring Phase +3 m; quarterly	Geo
SEIS—SP	Calibrated	Calibrated continuous and event data	11,000	SEIS Team	SEIS Team	Start Monitoring Phase +4 m; quarterly	Geo
SEIS-All	Derived	Geophysical structure and seismic velocities catalog, seismic source catalog	10	SEIS Team	SEIS Team	EOM +5 m	Geo

.

Instrument —Sensor	Processing Level	Product/Data Set	Volume (Mbit)	Data Set Producer	Archive Producer	1st Release Date & Frequency	PDS Curator
APSS-TWINS & PS	n/a	Calibration report	10	APSS Team	APSS Team	Landing –1 m	Atm
APSS-TWINS & PS	n/a	Ground calibration files	0.1	APSS Team	APSS Team	Landing –1 m	Atm
APSS-TWINS & PS	Raw	Raw pressure, temperature, wind speed	7,600	MIPL	APSS Team	Start Monitoring Phase +3 m; quarterly	Atm
APSS-TWINS & PS	Calibrated	Calibrated time series of pressure, temperature, wind speed	11,400	APSS Team	APSS Team	Start Monitoring Phase +4 m; quarterly	Atm
SEIS—ENG	Raw	Housekeeping, temperature	1200	MIPL	SEIS Team	Start Monitoring Phase +3 m; quarterly	Atm & Geo
SEIS—ENG	Calibrated	Housekeeping, temperature	1500	SEIS Team	SEIS Team	Start Monitoring Phase +4 m; quarterly	Atm & Geo
RISE	Raw	Doppler from DSN Tracking	1600	DSN to RISE Team	RISE Team	Start Monitoring Phase +4 m; quarterly	Geo
RISE	Derived	Rotation vector vs. time	10	RISE Team	RISE Team	EOM +5 m	Geo
RISE	Derived	Total and core moment of inertia (MOI), free core nutation period, core density and radius	1	RISE Team	RISE Team	EOM +5 m	Geo
HP³—All		Calibration report	10	HP³ Team	HP³ Team	Landing –1 m	Geo
HP³—All		Ground calibration files	0.1	HP³ Team	HP³ Team	Landing –1 m	Geo
HP³—STATIL/TLM	Raw	Raw voltages vs. time	100	HP³ Team	HP³ Team	Start Monitoring Phase +3 m; one-time delivery	Geo
HP³—STATIL/TLM	Calibrated	Voltages vs. time	120	HP³ Team	HP³ Team	Start Monitoring Phase +4 m; one-time delivery	Geo
HP³—STATIL/TLM	Derived	Deployed tether length	120	HP³ Team	HP³ Team	9 m; one-time delivery	Geo
HP³—TEM-A	Raw	Raw temperature vs. time	400	HP³ Team	HP³ Team	Start Monitoring Phase +3 m	Geo
HP³—TEM-A	Calibrated	Temperature vs. time	230	HP³ Team	HP³ Team	Start Monitoring Phase +4 m	Geo
HP³—TEM-A	Derived	Conductivity vs. depth	0.1	HP³ Team	HP³ Team	Start Monitoring Phase +6 m	Geo

.

Instrument —Sensor	Processing Level	Product/Data Set	Volume (Mbit)	Data Set Producer	Archive Producer	1st Release Date & Frequency	PDS Curator
HP^3—TEM-P	Raw	Raw temperature vs. time	710	HP^3 Team	HP^3 Team	Start Monitoring Phase +14 m; quarterly	Geo
HP^3—TEM-P	Calibrated	Temperature vs. time	20	HP^3 Team	HP^3 Team	Start Monitoring Phase +15 m; quarterly	Geo
HP^3—RAD	Raw	Raw voltages vs. time	291-1500	HP^3 Team	HP^3 Team	Start Monitoring Phase +3 m; quarterly	Geo
HP^3—RAD	Calibrated	Radiometric temperatures vs. time	56-271	HP^3 Team	HP^3 Team	Start Monitoring Phase +3 m; quarterly	Geo
HP^3—RAD	Derived	Surface temperature vs. time	400	HP^3 Team	HP^3 Team	Start Monitoring Phase +3 m; quarterly	Geo
IDC/ICC	n/a	Calibration report	10	IDC/ICC Team	IDC/ICC Team	Landing –1 m	Img
IDC/ICC	n/a	Ground calibration files	0.1	IDC/ICC Team	IDC/ICC Team	Landing –1 m	Img
IDC/ICC	Raw	Raw images	393	IDC/ICC Team	MIPL	Start Monitoring Phase +3 m; quarterly	Img
IDC/ICC	Calibrated	Calibrated images	2,360	IDC/ICC Team	MIPL	Start Monitoring Phase +4 m; quarterly	Img
IDC/ICC	Derived	DEMs, mosaics, stereo	3,540	IDC/ICC Team	MIPL	Start Monitoring Phase +4 m; quarterly	Img
IDA	Calibrated	Joint angles,	15	MIPL	IDA Team	Start Monitoring Phase +3 m; quarterly	Geo
IDA	Calibrated	Position in spacecraft coordinates	90	IDA Team	IDA Team	9m; one-time delivery	Geo
APSS-IFG	n/a	Calibration and Installation Report	1	MAG Team	MAG Team	Landing –1 m	PPI
APSS-IFG	Raw	Time series of 3 components of magnetic field	2500	MIPL	MAG Team	Start Monitoring Phase +3 m; Quarterly	PPI
APSS-IFG	Calibrated	Calibrated magnetograms	3750	MAG Team	MAG Team	Start Monitoring Phase +3 m; Quarterly	PPI
SPICE	Derived	Derived kernels	1,600	NAIF	NAIF	Start Monitoring Phase +3 m; quarterly	NAIF
TOTAL			**~130 Gb**				

When data products have been posted on the PDS website, they are regarded as publicly available. It is expected that the data will be made available to the public online through the PDS online distribution systems and the Planetary Image Atlas and the Analyst's Notebook. SEIS data will also be available via the IRIS and IPGP data centers.

2.3 Data Volume

For planning purposes, the expected downlinked data volume from InSight is 40 Mb/sol (average) UHF link to MRO, which includes 39 Mb/sol for payload data, of which 38 Mb/sol is for SEIS/APSS. The total downlink for the 708-sol project should be approximately 28.3 Gb. The total volume of science data products (raw, reduced, and derived) is estimated to be ~130 Gb, based on evaluation of project scenarios and the experience of the Phoenix project. These estimates will be refined based on further project scenario development and data product definitions.

2.4 Generation

The InSight project will provide oversight on implementation of this plan and ensure timely generation, validation, and delivery of archives to the PDS. The Navigation and Ancillary Information Facility (NAIF) will generate an archive of all SPICE data.

InSight science operations will be geographically distributed, with a project-controlled operations database that contains telemetry data, SPICE files, and other information needed by the InSight PSG members. The project will implement a system that meets the timeliness requirements associated with operations, analysis, and archiving of data. The system will allow the PSG members to access the data and information and to transfer the files to their home institution facilities.

The raw data, SPICE files, and other required data sets will be used at the home facilities to generate higher-level data products for use by PSG members and for archiving. Data product type definitions are provided in Table 2-2. Each archival product will be defined in a data product SIS document. Instrument data products are but one component of PDS-compliant archives. Other elements are summarized in Table 2-3, including archives to be supplied by the Project Office.

The archives associated with instrument data will be assembled at the home institutions of the instrument PIs or relevant Co-Is. Archives produced by the Project Office, specifically telemetry files, SPICE files, engineering data sets, and any other relevant information, will follow the same procedures that are designated for the science archives.

Most instruments have identified the need for data from the spacecraft to assist in interpreting their data. Examples of the types of data include lander temperature, currents and voltages for better interpreting the thermal environment and fields that could affect the instruments. Although each team has identified possible data of interest, the choice of data to be archived will not be finalized until after nominal operations have begun. The rationale is that the spacecraft generates a large volume of data. It won't be clear what data is actually of value until the teams have gained experience routinely analyzing their data. At that point, which could come as late as the end of the nominal mission, the individual teams will make informed decisions about what engineering data should be included in the archive. Individual instrument teams will be responsible for the archive of these data.

2.5   Data Validation and Peer Reviews

InSight engineering, science, and SPICE archives will be validated before being released to the PDS. Validation is accomplished in two parts: 1) validation for scientific integrity and 2) validation for compliance with PDS standards and data usability. PSG members are expected to conduct validation for scientific integrity in the course of their analysis of the range of data products derived from the raw data. The details of the science validation process are the responsibility of the PI and instrument Co-Is.

Validation for compliance with PDS standards and data usability is also the responsibility of the PI and each instrument PI or Co-I, with help from the PDS node that will receive the data products. The PDS will provide software tools, examples, and advice to help make this part of the validation as efficient as possible. This validation includes a peer review of the design and labeling of data products as laid out in the data product SIS documents, and validation of the PDS4 XML labels using sample data. The review committee will consist of a small group of scientists who represent typical users of the data. The instrument science team and the relevant PDS node will also be represented on the review committee. The review period will last approximately one month and will be conducted mostly by email, culminating in a teleconference, if needed. The result of the review will be a list of liens, or problems, that the team must resolve before the product can pass the review. Another month (or more depending on the nature of the liens) will be allowed for the instrument science team to address the liens. All reviews will be completed and liens resolved before landing on Mars. The goal is to allow the teams enough time to correct any problems before systematic generation of standard products begins. After the start of operations, when generation of products has begun, each individual product will be validated by the instrument team to see that it conforms to the design specified in the SIS. Validation of individual products will be automated as much as possible.

2.6   Data Delivery Schedule

Table 2-5 shows important dates and events in the InSight archive and data release process. Included are dates for completion of required documents, peer review, delivery of ancillary products and software, as well as public and PDS delivery and release dates. The initial release of raw data archive products to the PDS will occur within three months of receipt of raw data from the spacecraft, with calibrated products and SPICE kernels following one month later. Following these initial releases, will be released by the PDS as part of a single release every three months. Public release of preliminary seismic velocity data will occur every two weeks beginning three months after initial receipt of data from the spacecraft.

Table 2-5: InSight archive generation, validation, and release schedule. Note that this table assumes a nominal timeline for the start of data acquisition.

Date	Phase	Event
Aug 2013	B	• Project PDR • Draft Archive Plan complete • Draft Interface Control Document (ICD) complete

.

Date	Phase	Event
Sep 2014	C	• MOS/GDS CDR • Draft data product SIS documents complete • Draft archive bundle SIS documents complete • Final Interface Control Document complete • Archive Plan complete • Science Data Management Plan complete • Peer Review begins
1 Dec 2015	D	• Science Data User Guide complete
15 Dec 2015	D	• Updated Archive Plan complete (if necessary) • Updated Science Data Management Plan complete (if necessary)
Mar 2016	D	• Launch • Final data product SIS documents complete • Final archive bundle SIS documents complete • Peer Review is complete
Aug 2016	E	• Calibration files and calibration reports delivered to PDS • PDS Analyst's Notebook prototype inputs • Utility software programs for working with data products released
Sep 2016	E	• EDL
21 Sep–30 Dec 2016	E	• Surface Operations—Instrument Deployment Subphase, Commissioning and Penetration Subphase • Data product generation • Data product validation
Sep 2016–Sep 2018	E	• Surface Operations—Science Monitoring Subphase (see Figure 2-1) • Data product generation • Data product validation
1 Jan 2017	E	• Nominal start of science monitoring for all instruments (some will have already begun)
13 Mar 2017	E	• Delivery of raw products to PDS 3 weeks before Release 1A (see Table 2-4 for details) • Data acquired from EDL up to start of science monitoring (31 Dec 2016)
3 Apr 2017	E	• **PDS Release 1A**: raw data products and SPICE kernels • Begin 2 week cycle of public release of "uncertified" seismic velocity data and "uncertified" APSS data
10 Apr 2017	E	• Delivery of calibrated products to PDS 3 weeks before Release 1B • Data acquired from EDL up to start of science monitoring (31 Dec 2016)
1 May 2017	E	• **PDS Release 1B**: calibrated data products • For first release only, calibrated data will be released one month later than raw data.
12 Jun 2017	E	• Delivery of raw, calibrated and derived products to PDS 3 weeks before Release 2 • Data acquired 1 Jan 2017 through 31 Mar 2017 (3 months)
3 Jul 2017	E	• **PDS Release 2**: raw, calibrated and derived products and SPICE kernels
11 Sep 2017	E	• Delivery of raw, calibrated and derived products to PDS 3 weeks before Release 3 • Data acquired 1 Apr 2017 through 30 Jun 2017 (3 months) • One-time delivery of HP^3 and IDA derived products to PDS
2 Oct 2017	E	• **PDS Release 3**: raw, calibrated and derived products, SPICE kernels, HP^3 and IDA one-time derived products, released 9 months after start of science monitoring
12 Dec 2017	E	• Delivery of raw, calibrated and derived products to PDS 3 weeks before Release 4 • Data acquired 1 Jul 2017 through 30 Sep 2017 (3 months)
2 Jan 2018	E	• **PDS Release 4**: raw, calibrated and derived products and SPICE kernels

.

Date	Phase	Event
12 Mar 2018	E	• Delivery of raw, calibrated and derived products to PDS 3 weeks before Release 5 • Data acquired 1 Oct 2017 through 31 Dec 2017 (3 months)
2 Apr 2018	E	• **PDS Release 5**: raw, calibrated and derived products and SPICE kernels
11 Jun 2018	E	• Delivery of raw, calibrated and derived products to PDS 3 weeks before Release 6 • Data acquired 1 Jan 2018 through 31 Mar 2018 (3 months)
2 Jul 2018	E	• **PDS Release 6**: raw, calibrated and derived products and SPICE kernels
10 Sep 2018	E	• Delivery of raw, calibrated and derived products to PDS 3 weeks before Release 7 • Data acquired 1 Apr 2018 through 30 Jun 2018 (3 months)
1 Oct 2018	E	• **PDS Release 7**: raw, calibrated and derived products and SPICE kernels
Sep 2018	E	• End of mission operations (EOM)
12 Dec 2018	E	• Delivery of raw, calibrated and derived products to PDS 3 weeks before Release 8 (last of the quarterly deliveries) • Data acquired 1 Jul 2018 through EOM (almost 3 months)
2 Jan 2019	E	• **PDS Release 8**: raw, calibrated and derived products and SPICE kernels
25 Feb 2019	E	• Delivery of final revisions and end-of-mission derived products to PDS about 2.5 weeks before Release 9 • Data acquired throughout mission
15 Mar 2019	E	• **PDS Release 9**: final release of raw, calibrated and derived products from all instruments • Completion of mission closeout

.

2.7 Integrated Archives

The InSight PSG and the general science community will require access to science data archives that are integrated across instruments by time and location, at a minimum. Two complementary PDS systems will provide access to the archives: the Planetary Image Atlas and Analyst's Notebook. In addition, for the researcher familiar with seismic formatting standards and access to standardized processing tools, the IRIS and IPGP Data Centers will provide access to all SEIS data in SEED format (including raw data). SEIS data in SEED format and in standard PDS table format will be available via PDS. In addition to being available in standard formats in PDS, APSS raw data will also be distributed in SEED format, in order to provide to seismologists the complete data set necessary for decorrelation.

The Planetary Image Atlas is a Web-based system for locating and downloading image and other data from planetary projects. It allows cross-instrument and cross-project selection based on various search criteria, browsing of data, and downloading in various formats. The system will be adapted to support InSight data products and can be used both by project personnel and by the general science community. The Planetary Image Atlas is developed, maintained, and operated by the PDS Imaging Node at JPL.

The Analyst's Notebook is a Web-based tool for capturing daily scientific activities and their basis. It will record the goals for specific scientific operations, as well as the reasoning and discussion leading to them. It will help in correlating data products from various InSight instruments based on time, location, observation target, and other criteria. The Notebook will provide detailed views into DAILY LOGS, science working group meeting minutes, operational decisions, results, and access to raw and derived data and instrument calibration information. Using the Notebook, a scientist can virtually replay project events to better understand and select

.

data products of interest.. The Analyst's Notebook will be designed and implemented at PDS Geosciences Node at Washington University, based in part on similar Notebooks built to support analyses of data collected during the Phoenix, and Mars Exploration Rover, and Mars Science Laboratory projects.

Both IRIS and IPGP data centers offer a variety of tools for requesting and viewing processed and calibrated seismograms in SEED format. The SEED headers include key information necessary for seismic analysis (time, sampling rate, ID and station position, pole and zero of transfer functions, calibration information, etc.), and enable the use of numerous analysis and mapping tools available through the data centers and across the community.

3 Roles and Responsibilities

This section summarizes the roles and responsibilities for personnel and organizations involved in InSight archive generation, validation, transfer, and distribution.

3.1 Project Responsibilities

The InSight project has overall responsibility for generation and validation of archives for release to the PDS. The project is also responsible for distribution of data and associated information to InSight personnel.

The Principal Investigator (PI), working with the Deputy Principal Investigator (Deputy PI), provides oversight of the archiving process. They will review data analysis plans to ensure timely and adequate analysis of spacecraft data and delivery of documented, complete data to the PDS. They are responsible for the administrative management of data archive planning and implementation.

The InSight Data Archive Working Group (DAWG) will coordinate the planning of the generation, validation, and release of PDS-compliant archives to the PDS. The DAWG is a subgroup of the InSight PSG. The DAWG Chair is the Deputy PI who will, under the direction of the PI, ensure that archives are planned, validated, and delivered. DAWG membership includes the PI, the Deputy PI, the Project Science Systems Engineer, the instrument Co-Is, representatives from NAIF, and project personnel selected to ensure that raw packets, engineering data sets, and documentation are included in the archives. Representative PDS personnel will be liaison members of the DAWG. During the active project, the DAWG will provide the coordination needed to ensure that archives are assembled, validated, and delivered according to schedule.

MIPL is responsible for generating PDS-compatible raw data products for ICD, ICC, IDA, TWINS, the pressure sensor, and calibrated and derived products for the ICC and IDC, as specified in Table 2-4. The InSight instrument teams are responsible for validating the data products.

The InSight instrument teams are responsible for generating validated, PDS-compatible collections containing raw (except for the MIPL-produced IDC/ICC products), calibrated and derived data for their instruments as specified in Table 2-4. PDS-compatible archives include documentation, algorithms or software for generating derived data products, calibration data and reports, and other supporting materials in addition to science data products.

3.2 PDS Responsibilities

The PDS is the designated point of contact for InSight on archive-related issues. The PDS is also the interface between InSight and the National Space Science Data Center (NSSDC). The PDS will work with the DAWG to ensure that the InSight archives are compatible with PDS standards and formats. Personnel from the PDS Geosciences, Imaging, Atmospheres, Planetary Plasma Interactions (PPI), NAIF, and Engineering nodes will be liaison DAWG members.

The PDS will distribute and maintain InSight archives for the NASA planetary science community once the archives have been delivered by InSight.

The PDS Geosciences Node will provide overall coordination of PDS activities for InSight. The individual nodes will archive InSight data sets as designated in Table 2-4.

Primary responsibility for archiving InSight data will rest with the Geosciences Node. The PDS nodes involved with InSight data archiving will work together to archive data products from all of the InSight science instruments as a set of integrated archives using the PDS online services (e.g., Planetary Atlas and Analyst's Notebook).

The InSight Data Engineer from the Engineering Node will work with the PDS discipline nodes involved with InSight throughout the archive planning, generation, and validation phases.

3.3 NSSDC Responsibilities

The National Space Science Data Center will maintain an archive of InSight data for long-term preservation and for filling large delivery orders to the science community. The PDS will deliver at least one copy of InSight archive bundles to NSSDC. NSSDC may also provide support for distribution of InSight data to the general public, although this is beyond the domain of this plan.

3.4 IRIS and IPGP Data Center Responsibilities

The U.S. IRIS Data Center and the French IPGP Data Center will distribute SEIS raw data, calibrated data and derived data including data products to the international seismic community. Raw and calibrated data will be in SEED format. APSS raw data will also be transferred in SEED format under the responsibility of SEIS. For SEIS Derived data, Eidgenössische Technische Hochschule Zürich (ETHZ) will coordinate the production of the seismic source catalog and IPGP will coordinate the production of the geophysical/seismic velocity catalog and instrument transfer function for tide output. After project completion, each data center will also maintain an archive of InSight data for long-term preservation.

4   Appendices

4.1 Appendix A: Acronyms

AMMOS	Advanced Multimission Operations System
APSS	Auxiliary Payload Sensor Subsystem
Atm	PDS Atmospheres Node
CAB	Centro de Astrobiología
CCC	characterization, calibration, cataloging
CDR	Critical Design Review

.

CNES	Centre National d'Etudes Spatiales (French Space Agency)
CODMAC	Committee on Data Management and Computation
Co-I	Co-Investigator
D	document
DAWG	Data Archive Working Group
DEM	digital elevation model
DLR	Deutsches Zentrum für Luft- und Raumfahrt (German Aerospace Center)
DSN	Deep Space Network
EDL	entry, descent, and landing
EOM	end of mission
ETHZ	Eidgenössische Technische Hochschule Zürich (ETHZ)
GDS	Ground Data System
Geo	PDS Geosciences Node
HK	housekeeping
HP³	Heat-Flow and Physical Properties Probe
ICC	Instrument Context Camera
ICD	Interface Control Document
ID	identification
IDA	Instrument Deployment Arm
IDC	Instrument Deployment Camera
IFG	InSight Flux Gate
Img	PDS Imaging Node
InSight	Interior Exploration Using Seismic Investigations, Geodesy, and Heat Transport
IPGP	Institut de Physique du Globe de Paris
IRIS	Incorporated Research Institutions for Seismology
ITAR	International Traffic in Arms Regulations
JPL	Jet Propulsion Laboratory
Mb	megabit
MIPL	Multimission Image Processing Laboratory
MOI	moment of inertia
MOS	Mission Operations System
MRO	Mars Reconnaissance Orbiter
NAIF	Navigation and Ancillary Information Facility
NASA	National Aeronautics and Space Administration
NSSDC	National Space Science Data Center
PDR	Preliminary Design Review
PDS	Planetary Data System
PDS4	Planetary Data System Standard 4

.

PI	Principal Investigator
PIP	Project Implementation Plan
PPI	PDS Planetary Plasma Interactions Node
PSG	Project Science Group
RAD	radiometer
RISE	Rotation and Interior Structure Experiment
SEED	Standard for the Exchange of Earthquake Data
SEIS	Seismic Experiment for Interior Structure
SIS	Software Interface Specification
sol	martian solar day
SP	Short-Period Seismometer
SFDU	Standard Formatted Data Unit
SPICE	spacecraft ephemeris, planetary/satellite ephemeris and constants, instrument, C-pointing (attitude/orientation) matrix, and event information
STATIL	static tilt meter/sensor
TEM-A	thermal excitation measurement—active
TEM-P	thermal excitation measurement—passive
TLM	tether-length monitor
TWINS	Temperature and Wind for InSight
UCLA	University of California at Los Angeles
UHF	ultrahigh frequency
V&V	verification and validation
VBB	Very Broad Band Oblique Seismometer
XML	Extensible Markup Language